Load Shaping of Thermostatically Controllable Devices by constructing Retail Prices

Vom Promotionsausschuss der
Technischen Universität Hamburg

zur Erlangung des akademischen Grades

Doktor-Ingenieur (Dr.-Ing.)

genehmigte Dissertation

von

Henrik Tobias Lübkert

aus

Hamburg, Deutschland

2020

Date of Oral Examination	February 5th, 2020
Chair of Examination Board	Prof. Dr. Sibylle Schupp Institute for Software Systems Hamburg University of Technology
First Examiner	Prof. Dr. Volker Turau Institute of Telematics Hamburg University of Technology
Second Examiner	Prof. Dr.-Ing. Christian Becker Institute of Electrical Power and Energy Technology Hamburg University of Technology
Digital Object Identifier	doi.org/10.15480/882.2785
ORCID-iD	orcid.org/0000-0001-5125-5191

Acknowledgment

I want to thank my former colleagues and especially my supervisor Prof. Dr. Volker Turau for a great time at the Institute of Telematics. Prof. Turau gave me a lot of valuable feedback on my work. Many ideas originated from fruitful discussions with Dr. Marcus Venzke and Prof. Turau. I learned a lot about Smart Grids from Marcus Venzke, thank you for the detailed conversations.

I am glad to have met many smart and kind people during my time at the institute and want to thank all of them. In particular Dr. Nhat Vinh Vo, for introducing me to the topic of bilevel optimization. Abdolhamid Ghodselahi and Gerry Siegemund for many great coffee talks. Furthermore, it was a pleasure to teach together with Florian Kauer, Florian Meyer, and Andreas Weigel. I will miss the lunch discussions with Christopher Weyer and all other colleagues.

Finally, I want to thank my family, my parents for their support during my years of study, as well as my wife Kim and my daughter Clara for an enjoyable life outside the office and especially for our memorable vacations.

Tobias Lübkert
Lübeck, June 2020

Abstract

In the course of the energy transition the process of balancing power supply and demand becomes more challenging due to the uncertainty of renewable energy sources. Demand Response (DR) mechanisms encourage consumers to change their energy consumption, e.g. through time-varying electricity prices. This dissertation develops a price-based DR mechanism for cost-optimizing thermostatically controlled loads, which induces an aggregated load profile approximating a target schedule. A heuristic algorithm is developed to calculate suitable price signals. Simulations of realistic scenarios are analyzed to validate the functionality.

Table of Contents

Chapter 1

Introduction

The share of renewable energy sources (RES) in the European electrical power grid is increasing significantly, especially in Germany, which accounted for the major part of additional non-hydro RES from 2014–2017 [ES18], leading to a total share of 30 %. The German renewable energy act (Erneuerbare Energien Gesetz, EEG) [dJufV] provides that by the year 2050 a minimum of 80% of the electrical energy is produced by renewable sources in order to counteract the climate change and reduce costs of the economy in a long term. For this purpose conventional power plants relying on fossil fuels need to be replaced. The energy transition shall take place in a continuous process preserving adequate costs and stability of the power grid. Fundings based on the EEG already have accelerated the increased renewable energy share of the energy consumption from 3.6 % in 2000 to 36.2 % in 2017, with wind energy as the most significant source [fSuWFBWH].

A high share of RES is challenging for a stable operation of the power grid. In the electrical power grid, produced and consumed power must be balanced at any time. For this purpose, energy suppliers traditionally schedule the power production to meet the expected demand of their customers. Suppliers have to ensure the availability of electrical energy and may do so by buying the required energy via direct contracts with electricity producers or at the energy exchange [Kon13]. This process becomes problematic when the energy availability highly depends on fluctuating weather conditions. Energy may not be sufficiently available at times of high demand or available energy may be lost when energy generation needs to be reduced at times of low demand. In principle, a surplus of energy can be stored for later shortages, but large scale storage systems are still too expensive in practice. A cost-effective

alternative is adapting the load to the availability [Lin10]. Within the scope of this dissertation, a mechanism is developed which shapes the aggregated load profile of many domestic appliances such that it follows a target schedule, i.e. the energy availability.

Consuming renewable energy when it is produced is not only ecologically but also economically beneficial. The volatility of wind and solar power has a significant impact on the resulting market prices, as the major part of produced renewable energy is traded at the energy exchange at the day-ahead market as a consequence of the EEG-based funding [Gra14]. When the availability of fluctuating energy sources is low, suppliers have to pay higher prices to fulfill the demand of the customers. In contrast, if the energy offered exceeds the demand, prices are low (even negative) and renewable energy remains unused. In case of low prices, EEG fundings pay the difference of a contracted payment for a power plant to the generated market revenue. In the end, the energy price as well as the fundings are payed by the consumers.

The development of a smart grid supports the energy transition from a few centralized large power plants to many distributed generators by increasing grid monitoring and adding two-way communication down to end-consumers [FMXY12]. The smart grid enables several demand side management (DSM) mechanisms for load shaping. A classical mechanism is direct load control (DLC), where aggregators (e.g. utilities) modify the customer's demand by controlling some appliances directly, e.g. turning devices on or off remotely [VZV15]. This technique has been used for several decades and is common praxis today [VZV15]. However, the future smart grid will more likely focus on techniques which leave the user in control over their appliances [EK16, PD11]. Thus, a key concept enabled by the smart grid is demand response (DR), which describes the encouragement of end-consumers to beneficially change their electricity consumption based on time-varying prices or incentive payments [VZV15, DOE06]. In particular, the goals of DR approaches are to shape consumption profiles such that they follow the availability of RES, reduce transmission losses, prevent overloads and improve the profit of power utilities as well as consumers. Furthermore, DR schemes are supposed to consider protecting the privacy and minimizing the discomfort of consumers [VZV15].

Applicable electricity consumers for DR are residential, commercial and industrial consumers. Whereat the residential sector shows the highest potential for DR [Gil16], especially households using electric storage water heaters, space heaters, or large battery storages as well as electric vehicles (EV) play an important role [Gil16, Gä16, GGSW17]. Storage heating appliances show a high potential for DR, which

is comparable to EVs [GGSW17]. A significant part of the total energy demand of German households accounts for water heating with about 14.4 % in 2015 [Umw17]. Domestic electric water heaters (DEWHs) which store hot water are responsible for roughly 9.3 % of the residential electricity consumption [LVVT18] and are found in about 15 % of the households in Germany [SH+07]. DEWHs show a high potential for DR due to the high energy demand and flexibility, as the stored water can be preheated to higher temperatures some time before it is demanded.

Residential customers prefer smart devices that automatically reduce their electricity costs by receiving price information directly from the smart meter instead of adjusting the behavior manually just to save a small part of the electricity bill [Sio11]. Thus, embedded controllers of the appliances need to perform the scheduling of the power consumption while requiring little interaction of the user but still maintain the comfort of use. In order to keep the investment and operational costs down, low-power and low-cost controllers are promising. However, limited computational resources of small controllers require efficient control algorithms.

Algorithms of different complexity can be utilized to control the temperature of the DEWH. Simple approaches select a temperature setpoint relative to the current price [LVT17b]. More complex solutions consider the formulation of an optimization problem based on a thermal model and taking into account the expected water consumption over the day [KHP15]. As generic optimization solvers for linear programs (LPs) or mixed-integer linear programs (MILPs) may be inapplicable for small controllers, application specific heuristics can be developed, which requires understanding the cost-optimal behavior regarding the model.

When many smart devices participate in a DR program and optimize their power consumption schedules based on time-varying prices, two questions arise. First, what should the course of the price function look like to achieve the supplier's objective and second, how can this function be calculated in an efficient way. In particular, the resulting aggregated power consumption shall follow the availability and must be approximately known by the energy supplier a day before. Several pricing schemes are considered in the context of DR. Common schemes are time-of-use (TOU), critical peak pricing (CPP), inclining block rates (IBR), real-time pricing (RTP) and day-ahead RTP (DA-RTP). TOU uses fixed prices for different time periods, e.g. three prices per day. IBR introduces price steps depending on the power level, such that higher power consumption is facing higher prices. With RTP prices are announced periodically some time ahead (e.g. every 15 min) and thus offers more flexibility and is most promising [Bor05] compared to TOU. DA-RTP removes the uncertainty for

customers, as all prices are announced a day head and thus is particularly suitable for DR, as customers may schedule their consumption in advance without the need of forecasting the future prices, which may also simplify the forecast of their expected behavior by the energy supplier.

However, DA-RTP is known to lead to load synchronization resulting in large peaks of the power consumption concentrated at times of minimal prices [ZWYK13]. Such peaks hinder the objective of an aggregated power consumption following the availability and furthermore, it may overload the power grid. Different strategies to avoid this synchronized behavior have been studied. More complex approaches involve message exchanging between consumers [CAS13] or also the supplier [YH17, SFFL14], whereat power consumption schedules are iteratively updated. The model of an energy exchange may be applied on a household level, which then trades energy as prosumers with neighbors or operators [JDDA17]. A less complex approach is using IBR in addition to DA-RTP, which induces each household to distribute their power consumption in order to avoid peak loads [HSW17]. The acceptance of DA-RTP with IBR for households however is questionable, as some common price-insensitive household activities such as cooking, which require high power consumption, would likely become more expensive. Thus, IBR increases the required awareness of the consumer about the pricing scheme and the autonomously resulting smart schedules of other appliances. Furthermore, it is dispensable that each household flattens its power consumption in order to reduce load peaks in the aggregated consumption. Peak loads can also be avoided when individual peak consumptions of households are distributed sufficiently, which is also the case for the traditional power grid today.

This dissertation develops a novel approach to shape the aggregated power consumption profile of many domestic appliances regarding a target schedule (i.e. the power availability of RES) using a DA-RTP scheme. The considered scenario is illustrated in Fig. 1.1. An electricity supplier buys required energy at an energy exchange a day-ahead considering forecasts of RES. The concluded trades build the target schedule for the energy consumption of its customers. The supplier has some knowledge about its customer devices and in particular groups them by their thermostatically controllable loads (TCLs) properties in order to calculate prices. A single price vector is determined and broadcast to all customers a day ahead, once per day.

In order to find the optimal price vector, a bilevel optimization problem is formulated. However, the exact solution method cannot meet the scalability requirements for practicably relevant scenarios. Thus, a heuristic optimization method is developed,

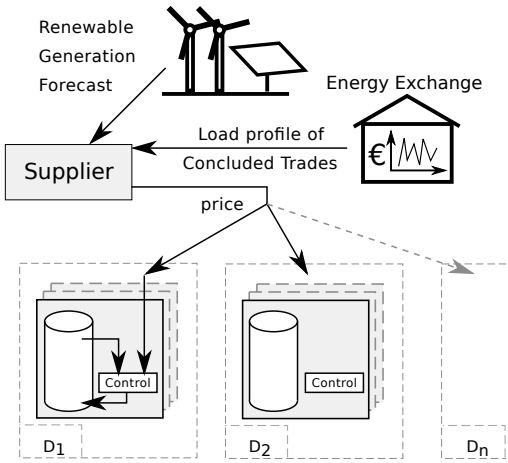

Figure 1.1: System Overview

based on understandings of the cost-optimal behavior of considered appliances. The underlying principle is to consider the variance of domestic appliances over a large set of households. The approach focuses on TCLs and especially DEWHs, which are not only a significant load type for DR, but also particularly suitable to react differently to the same price function. It is shown that the characteristics of these appliances have a sensitive impact on their optimal behavior, due to different energy efficiencies at different temperatures. Furthermore, a more sophisticated understanding of the behavior of DEWHs participating in a DR program is established, which is required for being able to calculate the prices inducing a desired behavior. For this purpose, different DR mechanisms for DEWHs and the impact of physical device parameters on the DR performance are analyzed. For this purpose, many DEWHs are simulated using real hot water usage data. The behavior of the cost-optimal heating schedule is understood in detail, which then allows to construct computationally efficient heuristic optimization methods for DEWHs minimizing their operational costs. Finally, the gained knowledge allows to construct a heuristic algorithm to calculate prices, which induce an aggregated power consumption following a target schedule.

The structure of this dissertation is as follows: Chapter 2 introduces the state of the art of smart grid and demand response mechanisms, explains the principle of bilevel optimization problems and their solution, and explains the thermal model of a DEWH

required for simulation and formulation of an optimization problem. The simulation environment is described Chapter 3. In Chapter 4 a cost-optimizing heuristic is developed by improving an algorithm from literature, the impact of each improvement is analyzed and the resulting algorithm is shown to yield nearly optimal solutions by performing an empirical study. The optimal heating behavior of a DEWH is further understood by the parameter study of Chapter 5, varying physical and optimization parameters. Chapter 6 defines the bilevel optimization problem of finding prices for load shaping and discusses possible solutions. The impact of the resulting prices are analyzed in more detail in Chapter 7. Based on these findings, Chapter 8 develops a heuristic algorithm to construct prices for load shaping of many DEWHs and evaluates the result performance. Chapter 9 concludes this dissertation.

Chapter 2

State of the Art

This chapter first gives an overview of today's electricity network structure, important actors and their role within the network operation. Afterwards, the concepts for developing a smart grid are explained, in particular different approaches for DSM with a focus on the promising class of loads, which is TCLs and especially DEWHs. Formulating optimization problems and developing control methods for DR with TCL requires knowledge of thermal model. Optimizing the aggregated behavior of many self-optimizing appliances can be modeled as bilevel optimization problem, which is explained in Section 2.3.

2.1 Power Grids

The operation of today's cross-border electrical power system is a very complex task. Power generation and consumption must be balanced at any time, as otherwise voltage and frequency will deviate from desired values [Sch09]. Operators of the power system have different responsibilities, which is either generation, transmission or distribution of electrical power. Transmission system operators (TSOs) transport electricity over high voltage power grids (110 – 380 kV) covering large distances. Distribution system operators (DSOs) distribute the energy in smaller regions with medium voltage (6 – 110 kV) and down to the end consumers via low voltage power grids (400 V). Other actors are involved with energy trading or reselling. Suppliers buy energy at the wholesale market and resell it to end customers [Sch09].

Each TSO is responsible for power balancing of a control area covering its power grid. A control area is further divided into several, e.g. 100 – 200, balancing groups

(BGs) [HDS10]. Every feed-in and extraction point is assigned to a single BG. Power plants, energy traders and suppliers must be part of a BG [Sch09]. The BG ensures power balance and has to inform the TSO about planned power flows for the next day with a 15-minute time resolution. The provided information includes feed-in and extraction points, which may involve other BGs as well as control areas. TSOs ensure power balance on a smaller time scale using balancing power. The resulting costs are later distributed over BGs depending on their deviation of planned and actual power flow.

Electrical energy can be procured at the wholesale market with over the counter deals between two partners or at an energy exchange. At the exchange, energy is traded with different delivery periods at different markets. The future market involves trades for delivery in months or years. Spot (day-ahead) markets usually cover the next day with a resolution of hours or days. The Intraday market allows short term trades (30 minutes in advance or 5 minutes within a control area [SPO18]) for the current or next day with a 15 minute resolution and resulting power flows are mostly related to BGs compensating forecast errors [Sch09]. The actual price which has to be paid for traded energy is the market clearing price, which results from the intersection of aggregated bid and offer curves. Each time period (e.g. one hour) has its own clearing price. The most significant spot market for Germany belongs to the European Power Exchange SPOT (EPEX) [Gra14]. The European Electricity Index (ELIX) shows the market prices of all markets combined.

2.2 Smart Grid

Transforming traditional power grids into smart grids is a cost-effective concept to allow a high integration of RES. With increased measurement deployment and two-way information and power flow, the resolution for the control system is increased, in time and space [SACQ19]. Communication down to end-consumers, i.e. using smart meters, not only allows high frequency remote monitoring, but also more detailed electricity tariffs depending on time or load [HDS10].

A promising key feature of the smart grid is DSM, which describes any measure of improving the power system with a focus on the demand side, including energy efficiency programs as well as more complex control approaches [Jor19]. In particular it allows modifying the load in order to counteract fluctuations of power generation with RES, by DR programs, which is a large subset of DSM. Noteworthy DR programs

are DLC, price responsive control (PRC) and transactive control [SACQ19], which are covered in this section.

2.2.1 Demand response

A commonly used definition from the U. S. Department of Energy defines DR as *"a tariff or program established to motivate changes in electric use by end-use customers in response to changes in the price of electricity over time, or to give incentive payments designed to induce lower electricity use at times of high market prices or when grid reliability is jeopardized."* [DOE06]

Thus, DR programs are mainly distinguished by their motivation, which is either incentive- or price-based [VZV15, Jor19]. Related classification aspects are the purpose of a DR program, which is either to contribute to the reliability of the power grid or to act economically based on pricing methods [Sia14, CL12]. Additionally, programs can be classified by whether they contribute to the planning or operating phase [VT16]. Programs contribute to the planning phase by considering power availability forecasts or statistics to schedule the energy consumption of the planning period. Contributing to the operating phase can be done by reacting on frequency changes or deviation (primary control), load shedding (frequency- or voltage-based) or by providing secondary or tertiary control power. Vardakas et al. [VZV15] further consider the control mechanism (centralized or distributed) and the decision variable (task scheduling / energy management).

A classical incentive-based DR program is DLC, where loads are controlled centrally, whereas other programs leave the control at the consumer's side and gives a motivation for voluntarily changing the load or penalize registered consumers which fail to respond to requests. A common price-based DR approach is PRC, where consumers schedule their power consumption individually based on received prices. However, finding prices which induce a reliable aggregated load profile is a challenging task. A more complex alternative is transactive control, which applies market strategies and thus requires two-way communication [SACQ19].

Main objectives of DR programs are reducing total power consumption beneficially for suppliers, grid operators and consumers, avoid expensive power generation for demand peaks, matching demand and power availability (in particular RES), and reduce overload situations of the power grid [VZV15]. As a result, common optimization objectives for DR are minimizing electricity costs, maximizing social welfare,

minimizing aggregated power consumption, or combinations of these. Social welfare is defined as the difference of suppliers profit and procurement costs.

2.2.2 Direct load control

Direct load control with DEWHs was utilized to generate balancing power at least since 1968 [Has80, Oli69]. In the following decade a large testbed containing 200 thousand devices with a total installation power of 700 MW was evaluated at Detroit Edison [Has80]. To reduce costs for generating regulating power, water heaters were switched off during peak hours. The maximum power reduction of about 200 MW was controllable by the operator in 10 %-steps using ripple control to address distinct groups of devices.

In [KAY+04] an independent and a cooperative control mechanism based on frequency measurement for DEWHs and generators are compared to the classical frequency regulation utilizing only generator control. The water heaters are switched on or off based on a local decision requiring no communication or per request using a bi-directional information network. Reducing the peak demand is also possible by lowering the operating voltage of the heating element as shown in [NJPH07]. However, it was shown by simulation, that the effect only is noticeable when the water demand is large compared to the tank capacity or the rated power of the heater is small enough to ensure longer heating periods.

Kondoh, Lu and Hammerstrom [KLH11] proposed a centralized control mechanism to provide positive and negative regulation power. Utilizing a two-way communication infrastructure, the central controller has knowledge of each DEWH on/off state and whether it wants or needs to change it. The aggregated power then is increased or decreased by switching the applicable amount of DEWHs. Simulation results have shown that the customer discomfort has increased, but still remains low. Furthermore, they approximated that 33 thousand water heaters are needed to provide 2 MW regulation power for a whole day.

In [BOA13] the communication requirement is reduced by removing the need to know individual states of appliances. Instead only the aggregated power consumption is measured and the DEWHs perform a switching decision based on a broadcast signal and a random number. Loads are only switchable when the temperature is between the thermostat minimum and maximum. Instead of switching the power of a water heater, the temperature setpoint can be adjusted to vary its power consumption as studied in [DLE+12, XOT11]. The appliances may be controlled by a centralized

signal requiring one-way communication or they can measure the system frequency and contribute to stabilization. For example after a generator outage, the temperature range will be reduced until the frequency reaches and holds an upper threshold.

A centralized control of appliances within multiple households is proposed in [VMLL14] which reduces peak consumption and stabilizes the feeder voltage. After collecting information about the individual priority, flexibility and current satisfaction from all appliances, switching decisions are provided to all loads. The decision also considers the power similarity of each appliance to the average load reduction and the current power consumption compared to the maximum of all households. Consumers receive rebates for shifting energy consumption and contributing to voltage improvement, which is assumed to generate higher benefits compared to reducing energy costs based on hourly tariffs.

Roux et al. [RAB18] proposed a peak demand management method which limits the maximum aggregated load while taking users' comfort into account. The centralized controller creates a prioritized list of DEWHs in order to distribute the available power. Based on historic consumption data, the controller estimates future demand and determines the required energy with the current temperature information.

2.2.3 Pricing schemes

A common alternative DR approach is PRC, in order to protect the privacy of consumers. Instead of controlling appliances remotely, suppliers send price information to customers in order to induce a change in their load. Besides today's available flat or day/night tariffs, the most common pricing schemes in literature are TOU, CPP, RTP and DA-RTP. [VZV15, SACQ19]

Flat pricing is the most simple scheme and common for most contracts today. The price for electricity is constant over time for long periods, e.g. a year. Customers can only reduce their costs by reducing their total energy consumption, i.e. increasing the efficiency of devices. TOU pricing introduces different price periods, e.g. electricity is cheaper during the night than at daytime. There may be more than two periods, e.g. another price at midday. The individual price values are also fixed for a longer time period as for flat pricing. CPP extends TOU by allowing the price of a period to change in case of some event. Consumers are notified a day ahead.

With RTP prices are much more variable and time periods are smaller, as suppliers announce them some time in advance (e.g. 15 minutes). Thus, this scheme requires a continuous information flow from the supplier to all customers in real-time, which

may be limited by smart meter capabilities. As a compromise, DA-RTP allows a high flexibility of prices for each day with different values for small time periods, but the update period is reduced to once per day. This pricing scheme fits good into the planning process of suppliers buying energy at the day-ahead market. Furthermore, customers' appliances may schedule their power consumption with less uncertainty as prices are fixed in advance.

2.2.4 Price-based DR

Early work on price-based DR focuses on the optimal control of appliances under dynamic electricity tariffs assuming some given price signals, e.g. from spot markets. DR optimization problems are often formulated using binary on/off decisions of appliances at different times and thus MILPs are a common choice to describe problems [SACQ19].

To minimize the energy costs for DEWHs considering market prices, Lu and Katipamula [NK05] consider switching off the load during peak price hours or varying the thermostat setpoint as a function of the price. Prices may be estimated by historical data or obtained by a competitive power market requiring a communication network. Furthermore, an optimized strategy is proposed, which schedules a preheating and cooling phase per day to hours with lowest or highest prices respectively. The energy consumption is controlled by setting the thermostat to a maximum within the preheating phase and to a minimum when cooling.

Du and Lu later proposed a heuristic optimization algorithm for DEWHs based on [LCD04] using real-time-pricing (RTP) [DL11]. The costs are minimized while predefined comfort temperatures are observed considering a water consumption forecast. The total heating time is determined based on the forecast and scheduled in the cheapest hours. When the temperature reaches the minimum or maximum, the scheduling starts over at the time when the bound is not violated any more. The temperature schedule then is saturated to the bound in between. To react to deviations of the real-time price and water consumption to their forecast, the schedule is updated on any change. Compared to a conventional thermostat the electricity payment could be reduced by about 20 % using the same temperature constraint.

Other work includes multiple load types to minimize residential energy costs. Mohsenianrad et al. schedule the planned energy consumption of different loads considering RTP [MRLG10]. For larger horizons price forecasting is used. Each load of a household is switched on or off depending on the maximum power of each load

and the total household. The schedule is optimized regarding the waiting time as comfort indicator using linear programming.

Tsui and Chan [TC12] formulate the energy schedule optimization of un-/interruptible, battery-assisted and model-based appliances (e.g. thermostatically controlled) as convex programming problems utilizing RTP. The costs are minimized together with the discomfort of the customer, which is a function of the assumed energy demand. Additionally, the consumption of distributed renewable energy is maximized.

2.2.5 Price responsive control

The problem of the electricity supplier, which is creating DA-RTP prices for customers including demand response systems can be formulated as a bilevel optimization problem or Stackelberg game, where the supplier takes the leader's part and the customers are followers. The principle of bilevel optimization and their solution is described in more detail in Sec.2.3. Here, the supplier wants to influence its customer's consumption with RTP, thus it has to find prices that make its customers shift their consumption as desired. Because customers minimize their electricity costs based on received prices, the resulting consumption impacts the supplier's objective and thus the prices to be selected. Some works consider maximizing the supplier's profit directly as a result from the difference of their income for energy sold and its procurement costs at day-ahead markets [MZ13, ZMPM13, WLM15, KVH17, MZZ+17]. To estimate the resulting procurement costs, forecasts of exchange prices can be considered [ZMPM13]. Alternatively, prices can be expressed as a function of time (e.g. for each hour) and the required energy quantity [MZ13, KVH17, CAS13]. The available power of the supplier may be complemented by additional power sources, e.g. renewable sources [CAS13] or battery storage [WLM15, KVH17]. Furthermore, positive or negative amounts of balancing energy have to be purchased during power flow [ZMPM13, CAS13]. Chang et al. considers this as part of the supplier's objective, e.g. when trades are already concluded [CAS13]. If the available power is known in advance, the problem becomes a load shaping problem, where the aggregated load shall follow a target schedule [LVVT18, HSW17].

Finding the optimal price function to be sent to all customers is a complex task, unless customers' utility functions are convex and differentiable, which allows to analytically determine strategies [YH17]. A simple solution is to use a price that is inverse to the power availability of the supplier. However, this leads to synchronized load peaks and thus high costs for power balancing during the day [CAS13]. To reduce

the peaks, the loads need to distribute their energy consumption. This can be achieved by exchanging messages between customers [CAS13] or with the supplier [YH17, SFFL14, SFFL16]. Such an approach allows iteratively shaping the aggregated consumption profile directly or indirectly by updating the prices [KVH17]. When behavioral knowledge of the customers is given, the bilevel problem can be solved by converting it into a single-level problem [ZMPM13, WLM15, KVH17] or by heuristic optimization such as genetic algorithms [MZ13, MZZ+17].

Load shaping regarding a target schedule becomes simpler when retail prices increase with larger power consumption by using IBR, as considered in [HSW17]. As customers face stepwise increasing costs depending on the power level, they prevent load peaks to reduce costs. Therefore, this approach allows an iterative price adjustment to find a price function inducing the desired load shape.

When maximizing the suppliers profit regarding day-ahead procurement costs, authors often implicitly assume that the exchange price is not influenced by the supplier, which is not true unless the amount is negligibly small and other suppliers follow different strategies. However, in a larger scale, e.g. many suppliers follow the same strategy, expected low exchange prices may become higher in the end. Furthermore, suppliers face additional expenses for power balancing if the actual consumption of their customers does not match the day-ahead contract.

Costs for power balancing is considered by Zugno et al. [ZMPM13], who studied a bilevel price generation considering multiple scenarios for three different customers. Each customer has an inflexible power consumption and optimizes the heating schedule of an underfloor heating system. Prices have to meet predefined maximum, minimum and average values. The heating decisions are limited by an allowed temperature range. The results showed that the profit was increased compared to fixed time-of-use or flat pricing schemes. However, they state that the maximum profit can only be achieved when customers select a particular solution out of several solutions with the same costs.

Meng and Zeng [MZ13] describe a similar Stackelberg game where the supplier maximizes its profit regarding customers minimizing their shiftable, non-shiftable, and curtailable appliances. A genetic algorithm is used to solve the problem. In conclusion both parties benefit financially and the peak to average ratio is reduced. Wei et al. [WLM15] introduce a second operation stage, where the supplier uses an energy storage unit to optimize the energy balance regarding market prices, consumer demand, and the charging efficiency of the storage. The supplier may also use the storage to sell energy at the market. Reduction of load peaks was not considered.

In contrast, Safdarian et al. [SFFL14, SFFL16] propose a decentralized two stage approach, where suppliers forward a price function to their customers that respond with load profiles minimizing their electricity costs. Afterwards, each customer tries to flatten the aggregated load while maintaining minimum costs. The problem is solved iteratively until no customer may further improve the aggregated load. Other work follows a similar approach [CAS13], e.g. using simulated annealing (SA) as solution mehtod [QZHW13].

2.2.6 Transactive Control

The motivation behind transactive control is to combine the strength of DLC and PRC, while avoiding their shortcomings. Thus, the objective is to achieve a reliable aggregated load response and also preserve privacy. A common approach is using market-based coordination [SACQ19].

Samadi et al. [SMRSW12] propose a Vickrey-Clarke-Groves (VCG) mechanism, where consumers truthfully communicate their utility function together with the feasible set of power consumption profiles. A predefined generic utility function is considered to reduce the required information to a single parameter. The central controller maximizes social welfare, which is maximizing all utility functions with minimal procurement costs. Each consumer receives individual payment instead of a single price.

A TCL specific controller is proposed by Li et al. [LZLK16], which sends a bid containing price and average power to the coordinator based on a thermal model. The bid is determined by considering the desired and measured temperature. Temperatures within an allowed interval are mapped to prices, where the average of previous clearing prices is mapped to the desired temperature and the actual bid corresponds to the current temperature. The required energy is calculated by a thermal model. The coordinator then determines the clearing price regarding feeder capacity constraint.

Siano et al. [SS16] consider an extended problem formulation, where the coordinator acts as DSO and considers additional constraints for power balances at several buses, active and reactive power, voltage levels, temperature of wires and transformers, and operative slopes of distributed generators (DGs). In addition to TCLs, also shiftable loads are considered by an extra transactive controller, placing bids depending on earliest starting time and latest ending time for dish washer and washing machine.

Households may also act as prosumers on local markets buying and selling energy from and to neighbors or operators [JDDA17]. Prosumers optimize their bids considering consumption and photovoltaic panel (PV) generation forecasts and decide whether to charge or discharge their battery. After market clearing, the power flow is optimized again considering concluded trades and deciding whether to sell or buy energy to/from suppliers or use the battery.

2.3 Bilevel Optimization

With time varying pricing schemes, both, the suppliers and their customers want to optimize their financial benefits. The interdependency of the decisions of both parties can be modeled as a bilevel optimization problem. Therefore, this section describes bilevel problems in general and discusses their application for demand response in literature.

2.3.1 Problem formulation

The problem formulation of bilevel optimization originates from the Stackelberg game [VS34, vS11] for studying the decision dependencies of market economics [Dem02, DKPVK15]. Bilevel optimization problems consider two decision vectors x and y for two interdependent optimization targets (2.1) and (2.3), where x is the optimal solution of the second problem for a given y.

$$\min_{y} F(x,y) \tag{2.1}$$

$$\text{s. t. } G(x,y) \leq 0 \tag{2.2}$$

$$\min_{x} f(x,y) \tag{2.3}$$

$$\text{s. t. } g(x,y) \leq 0 \tag{2.4}$$

Both problems depend on the solution of the other problem. Thus, it is not possibe to solve one problem first and then the other, as the resulting optimal solution of the second problem may also lead to a different solution of the first problem and vice versa. The interdependency of both problems is resolved by integrating the second optimization problem into the first problem as part of its constraints.

The bilevel program can be formulated according to [Dem02], where the second problem is described by (2.5).

$$\min_{x} \{f(x,y) : g(x,y) \leq 0\} \tag{2.5}$$

This problem is also called *follower's problem* or *lower problem*, as it considers y as given. To incorporate the follower's problem into the constraints of the bilevel problem, let $\Phi(y)$ denote the solution set of problem (2.5) and $x(y)$ some member of $\Phi(y)$. Then, the task of the bilevel problem (2.6), which is also called *leader's problem* or *upper problem*, is to determine the best solution y^* together with $x(y^*) \in \Phi(y^*)$ satisfying constraint $G(x(y), y) \leq 0$ and giving the best possible value for $F(x(y), y)$.

$$\min_{y} \{F(x(y), y) : G(x(y), y) \leq 0, x(y) \in \Phi(y)\} \tag{2.6}$$

There is no fully dominating player in bilevel problems, as for example in economical optimization problems, prices usually do not determine the profit directly, because a change of the price also has an impact on the actual sales volume. Thus, the task of such a bilevel program is to find the best price optimizing a given objective. An example objective is defining toll costs to distribute traffic such that the profit is maximized or specific areas experience less traffic [DKPVK15].

2.3.2 Solving bilevel problems

Solving bilevel optimization problems is a complex task, as these problems are nonconvex optimization problems and the optimization is NP-hard in general. Bilevel problems can be solved with different approaches. A common approach is to convert the problem into an equivalent one-level optimization problem. If the solution in the lower level problem is unique, the bilevel program is stable. Otherwise, the solution of the problem is not unique, but there may exist many local optimal solutions of the lower level problem. [DKPVK15]

The most common approach to formulate an equivalent one-level optimization problem is using the classical Karush-Kuhn-Tucker (KKT) transformation defined by (2.7) – (2.12). The lower level optimization problem is converted into constraints of the upper problem using the KKT conditions. Due to (2.12), the resulting problem describes a mathematical program with complementary constraints. [DKPVK15]

$$F(x,y) \rightarrow \min \tag{2.7}$$
$$G(x) \leq 0 \tag{2.8}$$
$$0 \in \delta_y f(x,y) + \lambda^T \delta_y g(x,y) \tag{2.9}$$
$$\lambda \geq 0 \tag{2.10}$$
$$g(x,y) \leq 0 \tag{2.11}$$
$$\lambda^T g(x,y) = 0 \tag{2.12}$$

Different solution methods can be used to solve such a problem, e.g. by reducing it to a mixed-integer nonlinear problem. This is done by introducing a sufficiently large number Q and use boolean variables z_i in order to achieve that either $\lambda_i = 0$ or $g_i(x,y) = 0$. The constraints (2.10) – (2.12) are then replaced by (2.13) – (2.15). [DKPVK15]

$$0 \leq \lambda_i \leq Q z_i \tag{2.13}$$
$$-Q(1-z_i) \leq g_i(x,y) \leq 0 \tag{2.14}$$
$$z_i \in \{0,1\} \tag{2.15}$$

An alternative solution approach for bilevel problems is using generic heuristic optimization methods, such as particle swarm optimization (PSO), genetic algorithm (GA) or SA. These methods allow to solve the follower's problem directly while only solving the leader's problem heuristically.

2.4 Particle Swarm Optimization

PSO was introduced by Ebhart et al. [KE95, SE98]. The idea of PSO is that many candidate solutions are updated iteratively in the direction of the best known solution within the swarm. Each particle in a swarm of size s has a position vector x and a velocity vector v. In every iteration, the velocities and positions of all particles are

updated according to (2.16) – (2.17).

$$v \leftarrow \omega v + \phi_p r_p (p - x) + \phi_g r_g (g - x) \tag{2.16}$$

$$x \leftarrow x + v \tag{2.17}$$

The velocity update depends on three predefined parameters. The inertia weight ω determines the impact of the current velocity. Whereas, the attraction weights ϕ_p and ϕ_g, together with random values $r_p \in [0,1]$ and $r_g \in [0,1]$, specify the impact of the best known positions p and g accordingly. Here, p is the best known position of the particle and g the best position known within the whole swarm.

2.5 Thermal Model

In general, many different types of DEWHs exist, which differ not only in size but also in the type and number of the heating elements [KW98]. This work focuses on a common type for medium sized tanks, which are either mounted to the wall or stand on the ground.

As shown in schematic Fig. 2.1, a single heating element heats the water at the bottom, where also the cold water inlet is located. A mixing valve is used to mix the hot water – drawn from the top of the tank – with cold water. The heating element of conventional DEWHs heats the water with constant power and is controlled by a thermostat which keeps the water in a temperature band. The power is switched on at a lower temperature bound and switched off again when reaching an upper bound.

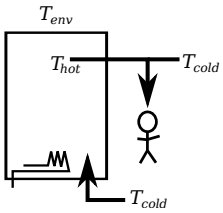

Figure 2.1: DEWH Schematic

A thermal model of a DEWH, which describes the temperature change over time, is required in order to optimize the heating schedule for DR while maintaining user comfort through temperature bounds. Furthermore, such a model allows simulation analysis of DR methods for DEWHs. Thermal models of different complexity are explained in this section.

2.5.1 Single-node model

The single-node model is a simplified thermal model assuming equal temperature distribution of the water in the tank. Energy loss occurs due to consumption of hot water and standby losses. Both processes decrease the overall temperature. When a user draws hot water from the top, cold water flows into the tank at the bottom and mixes with the remaining hot water. Standby losses occur due to the temperature difference to the environment and the heat conductivity of the insulation. The temperature increases when the heating element is turned on with constant power. Thus, the temperature change over time is described by the differential equation (2.18), which describes the power balance of stored, added and emitted energy as considered in [KHP15, NJPH07, PLC10, SMD+12].

$$C\frac{dT(t)}{dt} = P(t) - G\cdot(T(t) - T_{\text{env}}) - W_{HK}(t)\cdot(T(t) - T_{\text{cold}}) \tag{2.18}$$

Here C is the heat capacity [J/K] of the water in the tank, which is determined by the product of the volume V, density $\rho = 1$ kg/l and the specific heat capacity C_ρ [J/kgK] of the water. $P(t)$ is the current heater power [W], G the heat conductivity [W/K] of the insulation, W_{HK} the hot water consumption [W/K], T_{env} the temperature of the environment, and T_{cold} the temperature of the cold inlet water. The temperature change can be calculated by (2.19), which is the solution of (2.18) for given initial temperature T_0 and constant heating power as well as water consumption.

$$T(t) = \Bigg((G(T_0 - T_{\text{env}}) + W_{HK}(T_0 - T_{\text{cold}}) - P)\, e^{-\frac{t(G+W_{HK})}{C}} + P + GT_{\text{env}} + W_{HK}T_{\text{env}} \Bigg) \frac{1}{G + W_{HK}} \tag{2.19}$$

Resolving (2.19) according to t, allows to determine the duration until a specified target temperature T_x is reached. The resulting formula is given in (2.20).

$$t = \frac{C}{G + W_{HK}} \log\left(\frac{G(T_0 - T_{\text{env}}) - P_i + W_{HK}(T_0 - T_{\text{cold}})}{W_{HK}(T_x - T_{\text{cold}}) - P_i - G(T_{\text{env}} - T_x)} \right) \tag{2.20}$$

The simplification of this model has two advantages. First, it may also be considered to represent other types of TCLs such as waterbeds, but also space heating or air

conditioning systems. Secondly, the model allows the formulation of a solvable linear or integer optimization problem. For this purpose time needs to be discretised into time slots of length Δt and the heater power as well as the water consumption are to be considered constant and independent of the current temperature within each slot [KHP15]. Then the resulting solution of differential equation (2.21), given by (2.22)–(2.24), describes the temperature T_{i+1} at the end of a time slot i given the initial temperature T_i. The water temperature T_i converges exponentially to T_∞, with the temperature change rate τ defining the duration of changing about 63.2 % towards T_∞ (see (2.22)). Thus, the temperature changes faster for smaller τ-values and vice versa.

$$C\frac{dT(t)}{dt} = P(t) - G \cdot (T(t) - T_{\text{env}}) - W(t) \tag{2.21}$$

$$T_{i+1} = \left(1 - e^{-\Delta t/\tau}\right) T_\infty + T_i e^{-\Delta t/\tau} \tag{2.22}$$

$$T_\infty = T_{\text{env}} + \frac{P - W}{G} \tag{2.23}$$

$$\tau = \frac{C}{G} \tag{2.24}$$

2.5.2 Multi-Node models

While the single-node model already allows a good estimate of the state of charge, the estimation of the outlet temperature shows a high error [KHPP19]. As shown by several studies [KAY+05, FSUS07, KLH11], the assumption of an equal temperature distribution as used in the one-node model does not hold in reality. Especially, a water draw leads to a distribution with different temperatures inside the tank, as the water does not mix, but gets divided into different layers when the temperature difference is greater then 20 K. The height and time dependent distribution can be described by a partial differential equation (PDE) [XDL+14] or by multiple layers with ordinary differential equations (ODEs) [KLH11, KHP15].

Kondoh et al. [KLH11] define a simplified model considering two layers for a DEWH. The volume is divided into two nodes, which temperatures are described by power balance equations similar to the single-node model, but with an additional power flow between both nodes. The cold inlet water is fed in at the bottom node and the hot water is fed out from the upper node. When water is drawn, first only the temperature of the lower node is decreased until the volume of the node is consumed, then the upper layer is affected by further water consumption.

An alternative two-node model is used by Diao et al. [DLE+12]. Here, instead of two fixed nodes with changing temperature, the height of the hot water volume is changing while the temperatures of both nodes are fixed close to the cold and hot water temperatures. The change of the height is defined by an ODE. When the total volume is heated, the model switches to the single-node model. The two-node model can be extended by considering heat transfer between both nodes similar to [KLH11] in addition to the change of the height. Such a model then is described by three ODEs [KHPP19].

More complex models can be described by separating the volume into n layers and thus describing a system of n ODEs [KHP15, KHPP19] or using a PDE [XDL+14]. Both models allow calculating the temperature over time depending on height by considering thermal conductivity between adjacent heights. These models achieve the best accuracy for estimating the state of the water heater regarding stored energy and outlet temperature, but their higher complexity also leads to a high computational effort.

Besides the temperature estimation error of the outlet temperature, the one- and two-node models are also less accurate regarding the behavior of the heating element. Although the calculated start time of the heating is similar in case of a water draw, the one-node model stops heating earlier than the two-node model, which also stops before the PDE model [XDL+14].

2.6 DR Control Methods

With time-varying prices a DEWH may reduce its operational costs by primarily heating in times of lower prices. Given a thermal model allows predicting the temperature profile considering an expected water consumption and thus enables complex heating scheduling. DR control methods for DEWHs in literature follow different approaches in terms of the optimization objective and the solution method. A common objective is minimizing the costs of electricity, which is usually constrained with temperature limits to ensure user's comfort [DL11, SNSF16, ZSU11, KHP15]. An alternative is to define discomfort costs and consider a balance of both costs in the objective [KSH18]. Some works consider peak load reduction instead or in conjunction with electricity costs [NK05, SPM+10].

A simple solution is to map different temperature setpoints to given prices [GA04, NK05, VT16], i.e. low temperatures at high prices and vice versa. More sophisticated approaches use a heating schedule defining at what time the heater should

be turned on in order to achieve minimum costs and user discomfort. Solutions can be found with generic optimization methods, such as linear or binary integer programming [ZSU11, KHP15, WSF+17], but also (binary) PSO [SPM+10] or GA [LLX17]. Other approaches use stochastic dynamic programming [PMFH16], Dijkstra's algorithm [KH17] or Q-learning [AjXY+17]. Developing application specific heuristic algorithms is a promising alternative in order to achieve low computational performance requirements [DL11, SNSF16, GV17, KSH18].

This section describes selected control methods in more detail, starting with the conventional (non-DR) case up to scheduling optimization with a focus on computationally efficient heuristic algorithms.

2.6.1 Conventional bang-bang thermostat (BBT)

A conventional DEWH uses a bi-metal thermostat which automatically switches the heating element on or off as the metal bends at a certain temperature. Such a device maintains the water temperature with a hysteresis, as such a thermostat has a deadband and does not immediately switch the heater when the temperature changes slightly. The nominal temperature T_{nom} of the deadband is usually adjustable within a larger range by the user, e.g. 35 °C – 85 °C. The heating element is switched on when the temperature reaches a minimum T_{min} and it is switched off at a maximum temperature T_{max}.

More complex heating decisions can be achieved by adding a control device, which is capable of de-connecting the heating element, e.g. using an electromechanical relay. De-connecting the heating element allows a wider temperature range below the minimum switching point of the thermostat and thus power consumption can be deferred.

2.6.2 Proportional

A proportional adaptive nominal temperature (ANT) controller uses some reference signal to adjust the nominal temperature of the thermostat over time in some predefined temperature range ΔT_{nom}. When using time-varying prices as control signal, low prices are mapped to high temperatures and vice versa by considering the minimum and maximum price within a given time window [GA04, NK05, VT16]. The nominal temperature for time slot i is determined by (2.25), where $\overline{T}_{\text{nom}}$ is the maximum nominal temperature, $\underline{p}$ and $\overline{p}$ are the minimum and maximum value of the price

vector p, and ΔT_{nom} is the nominal temperature range. The price vector p contains all currently considered price values within the control horizon, where p_i is the price value of slot i.

$$T_{\text{nom},i} = \bar{T}_{\text{nom}} - \frac{p_i - \underline{p}}{\overline{p} - \underline{p}} \Delta T_{\text{nom}} \tag{2.25}$$

2.6.3 Optimization problem formulation

Kepplinger et al. [KHP15] use the single-node model to formulate a binary integer programming problem with on-/off decision variables u_i for each time slot i in the horizon. The objective function (2.26) is to minimize the operational costs resulting from the sum of price and heating decision products over all n time slots, given by the scalar product of price vector p and heating decision vector u. If all prices are equal ($p_i = c$), the objective function minimizes the energy consumption. The optimization is constrained by upper and lower temperature bounds for each slot, which are given by (2.27) in standard form. As heating decisions u_i are either 0 or 1 (power `off` or `on` respectively), the resulting problem describes a binary integer programming problem.

$$\min_u \; p^T u \tag{2.26}$$

$$\text{s.t.} \; Au \leq a \tag{2.27}$$

Defining temperature constraints for each slot requires calculating the temperature T_i in a discretized manner depending on u_i for each slot with slot-wise constant water consumption W_i as discussed in Section 2.5.1. Applying the recursive temperature calculation (2.22) for T_i depending on T_{i-1} allows defining the linear expression (2.28) determining T_i depending on an initial temperature T_0.

$$T_i = (1-\gamma) \cdot \sum_{j=1}^{i} \left(\gamma^{i-j} \cdot T_{\infty,j} \right) + \gamma^i \cdot T_0 \tag{2.28}$$

where

$$\gamma = e^{-\frac{\Delta t}{\tau}} \tag{2.29}$$

$$T_{\infty,j} = T_{\text{env}} + \frac{P_j - W_j}{G} \tag{2.30}$$

To ensure the user's comfort, the water temperature must remain above a minimum value $T_{\min}$ in any slot with an expected water demand. The upper bound $T_{\max}$ of the temperature must not be exceeded in all slots for safety reasons, e.g. respecting the specified maximum ratings of the DEWH. To acquire the standard form of (2.27) requires rewriting (2.28) as (2.31) and (2.32) with $P_j = P_{\text{heater}} \cdot u_j$. The first n rows then describe the constraint $T_i \leq T_{\max}$ and the next n rows $T_i \geq T_{\min}$.

$$T_i = \sum_{j=1}^{i} \left((1-\gamma) \cdot \gamma^{i-j} \cdot \frac{P_{\text{heater}}}{G} \cdot u_j \right) + T_i^* \tag{2.31}$$

$$T_i^* = \gamma^i \cdot T_0 + \sum_{j=1}^{i} \left((1-\gamma) \cdot \gamma^{i-j} \cdot (T_{\text{env}} - \frac{W_j}{G}) \right) \tag{2.32}$$

$$A_{i,j} = \begin{cases} (1-\gamma) \cdot \gamma^{i-j} \cdot \frac{P_{\text{heater}}}{G} & 1 \leq j \leq i \\ 0 & i < j \leq n \end{cases} \tag{2.33}$$

$$a_i = T_{\max} - T_i^* \tag{2.34}$$

$$A_{(i+n),j} = \begin{cases} -A_{i,j} & W_j > 0 \\ 0 & \text{else} \end{cases} \tag{2.35}$$

$$a_{i+n} = \begin{cases} -(T_{\min} - T_i^*) & W_j > 0 \\ 0 & \text{else} \end{cases} \tag{2.36}$$

For their simulative case study, Kepplinger et al. [KHP15] solve the problem every hour using a timescale of one minute per slot and thus use $n = 1440$ slots per day. Depending on the objective, the results show either a cost- or an energy-reduction of about 12 % on average when compared to a night-time switching, which heats to a maximum temperature between 11 p.m. and 6 a.m.

The behavior of the DEWH is simulated using the multi-node model. Using this model also for the optimization allows higher savings, as only the temperature of the uppermost layer is constrained. However, the resulting constraints become non-linear

and thus require a more complex solution method, e.g. dynamic programming by testing all decisions fulfilling the constraints. Furthermore, the optimization becomes more sensitive to demand prediction errors and may lead to a reduction of the user's comfort. [PGJ14]

2.6.4 Du-Lu heuristic

Instead of a time-consuming dynamic programming approach, Du and Lu [DL11] developed an algorithm to heuristically solve the energy cost minimization of a DEWH. Their two-step scheduling method handles the non-linearity of the thermal (single node) model as well as the uncertainty of price- and water demand forecasts. The objective function is defined by (2.37) and is identical to (2.26), because $P_{\text{heater}}\Delta t$ is a constant factor defining the energy consumed if the heater is turned on during one time slot.

$$\min_{u} \sum_{i=1}^{n} p_i \cdot u_i \cdot P_{\text{heater}} \cdot \Delta t \tag{2.37}$$

The algorithm is based on strategies previously developed for pumped-storage hydro-turbines [LCD04]. Given a hot water demand and real-time price forecast of the next day, the total required heating time t_{total} is determined with (2.38) and scheduled into the hours with lowest prices.

$$t_{\text{total}} = \frac{\sum_{i=1}^{n} W_i + E_{\text{loss}}}{P_{\text{heater}}} \tag{2.38}$$

The scheduling considers a price threshold p_{th} for the heating decision. The threshold is used to decide when the heater should be turned on or off depending on the current price at time slot i according to (2.39). The value of p_{th} is determined by sorting all prices p_i in ascending order and define a mapping of duration to sorted prices p_{sort} by selecting the element $p_{\text{th}} = p_{\text{sort},k}$ with index $k = \lfloor t_{\text{total}} / \Delta t \rfloor$.

$$u_i = \begin{cases} 1 & p_i < p_{\text{th}} \\ 0 & \text{else} \end{cases} \tag{2.39}$$

The resulting temperature curve is calculated considering the heating schedule u and consumption forecast W. Predefined minimum and maximum temperature constraints

are checked for each slot. When the curve violates one constraint, the heater is set to maintain the temperature at the upper or lower bound until the temperature reenters the allowed range, i.e. due to a water draw. When maintaining the temperature a deadband is considered to avoid frequent switching similar to a thermostat. The procedure starts over from that time until no violation occurs.

Whenever the consumer draws water or real-time price updates are received, the schedule is recalculated with adjusted forecasts considering the time window until midnight. However, it is not specified how the expected residual water demand is updated.

2.6.5 Shah heuristic

The algorithm proposed by Shah et al. [SNSF16] solves the minimization problem (2.37) also by a heuristic approach which iteratively computes the temperature over time. However, the procedure first computes the temperature profile and then schedules the heating decisions into the time before the minimum temperature limit is violated. This is done by selecting the single heating decision, which leads to the best objective value within that time interval. In order to take into account higher costs resulting from higher standby losses when heating earlier, the objective value is modified using an effective costs definition (2.40).

$$c_{\text{eff}} = \frac{p^T u}{(1 - \alpha t)\,\beta} \quad 0 \leq \alpha,\, 0 \leq \beta \leq 1 \tag{2.40}$$

Here, α is the penalty factor for too early heating, as t is the time difference between preheating and temperature violation. Furthermore, the heating efficiency is considered by the factor β. The first factor α is determined with a high computational effort, e.g. searched with some optimization procedure. Whereas, the other factor is considered to be given by the DEWH manufacturer.

After selecting a heating decision, the temperature profile is recalculated and checked for violations again. In case of an upper bound violation, a different slot is selected for heating and reevaluated. Otherwise the procedure starts over until no more violations occur.

Kapsalis et al. [KSH18] developed a similar heuristic algorithm, but used an extended objective function instead of fixed temperature constraints. The objective value then becomes a trade-off between minimal costs and experienced discomfort. The balance of both is defined using a factor. The best solution is found by solving

the problem several times with increasing discomfort factors until either an upper bound of resulting costs is reached or the optimal comfort was achieved. In contrast to [SNSF16], effective heating costs are not considered.

2.7 Water Consumption Models

To simulate a large set of individual water heaters which reproduce an empirical daily consumption profile as provided in [Dep08], either the original samples or an appropriate stochastic model can be used. Mufaris and Baba follow the simple approach assuming that every consumer follows the average [MB15]. More sophisticated approaches use some probability distribution to consider different profiles.

Kondoh et al. quantified the water consumption using a minimum energy and duration of a water draw [KLH11]. The individual profiles are then generated by a random decision whether or not to consume energy at a given time. To reproduce a predefined average curve, 10000 water heaters were simulated.

Instead of distributing time slots with equal energy consumption, some authors split the average profile into different use cases and consumption rates as in [LB96, JV01]. Jordan and Vajen [JV01] consider different empirical distributions for shower, baths, small and medium water draws. The sum of the weighted probabilities represents the daily consumption. The flow rates are normally distributed and combined with a fixed draw-off duration of 1, 5 or 10 minutes.

Comprehensive datasets of real water consumption measurements, which are publicly accessible are rare. The largest set known to the author was published by the Water Research Foundation in 1999 [MDF99]. The data includes about one million water draw events in total, which were recorded in 1188 households over a period of about 2–4 weeks in different seasons. In 2016 another study was performed and the corresponding detailed data for about 2 weeks of 94 households is accessible to research institutes [DMD+16]. The recent data includes individual measurements for hot water.

Chapter 3

Simulation Environment Implementation

In order to analyze the aggregated behavior of individual appliances responding to price signals a simulation environment was developed in the scope of this thesis. The simulation is implemented using the event-based simulation framework Omnet++, which is briefly explained in Sec. 3.1. The implemented modules of the simulation are discussed in Sec. 3.2.

3.1 Omnet++

Omnet++ [VH08] is fundamentally an event-based simulation environment commonly used for – but not limited to – simulation of communication networks. Written in C++, hierarchical architecture of simulation model allows high customizability Nodes interact with each other by sending messages which can contain arbitrary data structures. For this purpose, every simulation model implements the common method `handleMessage(*msg)`, which is called by the framework for any incoming message. All events are represented as messages, e.g. an internal timeout event is realized by scheduling a message to the module itself at a certain time in the future.

Interconnections of modules are described by the custom topology description language NED. It allows defining interfaces, modules, submodules, communication gates and their interconnections with submodules. Parameters of modules are defined in a separate configuration file, allowing to configure different setups for different runs.

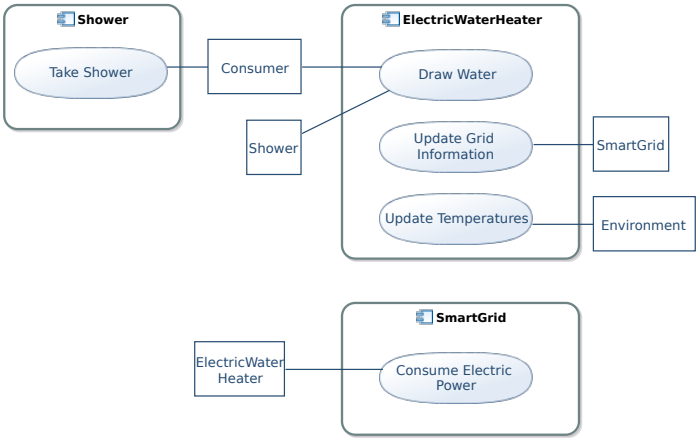

Figure 3.1: DR-TCL Simulation use case diagram

Further noticeable features of Omnet++ are an integrated development environment based on eclipse, a graphical user interface for simulation execution and an analysis tool allowing to plot and export results.

3.2 DR-TCL Simulation

The developed simulation environment essentially consists of four modules, which are the `Consumer`, `DEWH`, `SmartGrid` and `Environment`. The use case diagram shown in Fig. 3.1, summarizes the interactions of the modules. A `Consumer` may draw water either directly from the `DEWH` or by using the `Shower`. The `DEWH` may get notified by the `SmartGrid` about updated grid information, as well as by the `Environment` about changing temperatures. Whenever the `DEWH` switches its heating device, it will inform the `SmartGrid` about the change of its power consumption.

More implementation details are shown in the class diagram of Fig. 3.2. Note that most aggregations between objects are actually implemented using Omnet++'s interconnections of gates and sending messages. The obligatory generalization of `cSimpleModule` and its `handleMessage()` method is omitted in the diagram.

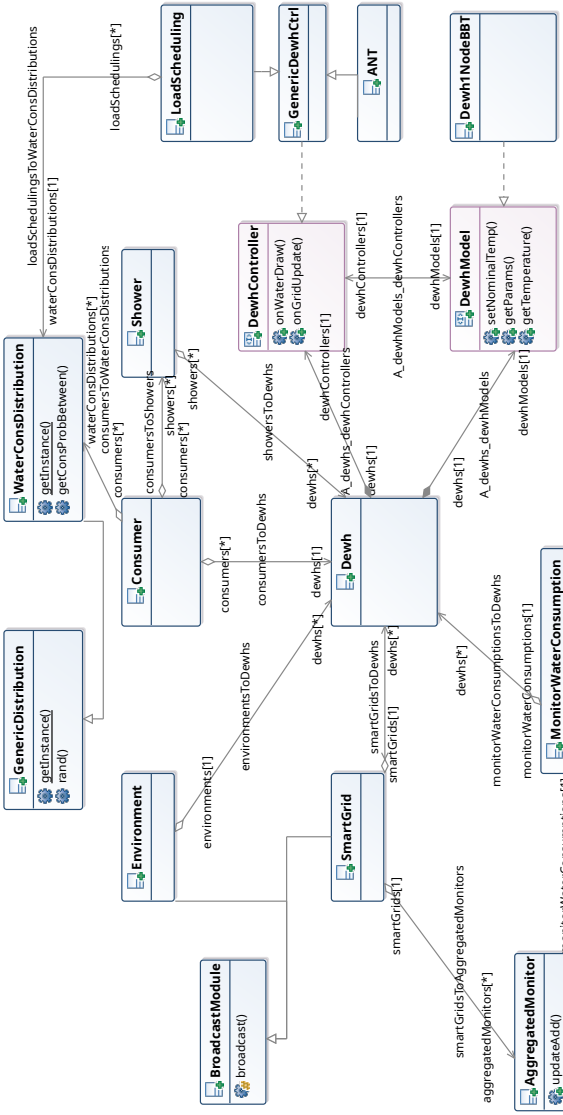

Figure 3.2: DR-TCL Simulation class diagram

3.2.1 Water consumption

Each `Consumer` schedules several water draw events at the beginning of a day. Depending on the configuration, water draws are chosen randomly following a specified distribution or read from an input file including. A water draw is specified by its starting time, duration, volume, desired and minimum-comfort temperature. When using randomly generated events, three different draw types can be configured. The number of events, their temperature and duration are specified with fixed values, whereas the volume is defined by some standard random distribution provided by Omnet++. Every water draw event triggers a message to be send to the `DEWH` or to the `Shower`. The `Shower` forwards the message to the DEWH directly or after a current shower is finished.

In order to generate random events following a certain distribution function, a pseudo-random number generator (RNG) was implemented in the base class `GenericDistribution`. Random numbers are drawn using the inverse transform method [Dev86]. For this purpose, a discrete probability distribution function (PDF) is read from an input file initially and the cumulative distribution function (CDF) as well as its inverse are calculated and stored. When calling `rand()`, a uniformly distributed random integer value is retrieved by Omnet++'s random number generator (RNG) and used as index for the inverse CDF, which selects the actual random value.

3.2.2 DEWH model and controller

The `DEWH` module consists of two sub-modules, the thermal model and the controller, which have to implement the interface `DewhModel` and `DewhController` respectively. The implementing classes to be used are specified in the configuration file. Available implementations are the single-node model of Sec. 2.5.1, a generic controller, and a load scheduling controller (see Sec. 4.2) as well as ANT (see Sec. 2.6.2).

The `DewhController` can modify the nominal temperature which is the setpoint for the thermostat of the `DewhModel`. The controller gets notified about updates from the `SmartGrid` and retrieves information about water draw events by the model. Furthermore, the controller may read all physical parameters as well as the current temperature of the model in order to make more complex heating decisions based on expected temperature profile. For this purpose, the controller has knowledge of the expected water consumption distribution.

The `DewhModel` calculates the temperature on any event regarding the thermal model and controls the power of the heating element regarding the specified minimum

and maximum temperature of the thermostat. The time to switch the heating on/off is also calculated using the model equation (2.20) using either the lower or upper thermostat bound as target temperature. Whenever the heating element is switched a message is send to the `SmartGrid` informing about the current power level. Received water draw events increase the current water flow and reschedule the received message with given duration to reduce it again. Water flow can either be modeled as mass flow or as a power consumption.

The impact on the energy drawn is significant, as the water temperature decreases during the mass flow. Thus, defining the water consumption as a power value instead of mass flow (temperature dependent power) has the advantage of matching to the desired energy drawn in total. As shown in the example temperature profile in Fig. 3.3, a short water draw leads to a fast temperature decrease compared to standby losses. In particular, the heating element cannot maintain the current temperature level but needs much more time to regain a higher temperature. Thus, the actual energy consumption caused by a water draw with fixed volume highly depends on the initial temperature. Furthermore, the energy is not equivalent to the initial expectation of drawing a volume with a certain temperature, as the temperature decreases during the draw and thus the effective power of the draw itself. For example, the shown water draw of 50 l with mix temperature 40 °C, duration of 300 s and an initial hot water temperature of 40.77 °C has an energy equivalent of about $50C\,(40 - T_{\text{cold}}) = 6.05 \times 10^6$ J, but the actual energy difference resulting from the temperature decrease equals to $C\,(T_0 - T_1) = 4.80 \times 10^6$ J, where T_1 is determined using (2.19).

In contrast, when using a water draw power equivalent, the temperature drops significantly lower and the heater has to stay on for a longer time and thus consumes more energy. This behavior is closer to the multi-layer model, assuming almost constant outlet temperature.

3.2.3 Aggregator and broadcast modules

In order to analyze the aggregated behavior of all loads, an `AggregatedMonitor` can be used to accumulate all received values over time. Additionally, a factor can be set which is multiplied for any value before accumulating. The factor may be changed at any time. This feature is used by the `SmartGrid`, which uses two aggregated monitors. One monitors the aggregated power consumption and the other uses the current price as factor, yielding the aggregated electricity costs.

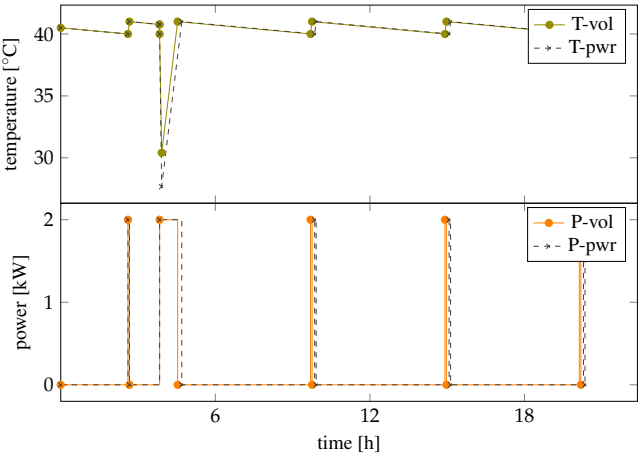

Figure 3.3: Single-node model example temperature profile for mass flow vs. power equivalent water draw

Another aggregator `MonitorWaterConsumption` is used for all water draw and temperature events. The module uses several aggregated monitors to track of the overall water consumption, its energy equivalent, the mean water temperature, the total energy lost through heat conductivity of insulation. Furthermore, low temperature events are aggregated, which occur when a water draw could not be satisfied regarding the desired temperature.

The `SmartGrid` additionally acts as a `BroadcastModule`, which sends the price information to all connected appliances. Another broadcast module is the `Environment`, which informs all appliances about changes of the environmental temperature as well as the inlet water temperature. Each appliances has a predefined offset to this centralized information in order to allow diversity.

3.3 Metrics

The goal of this dissertation is to shape the load given a target schedule by constructing retail prices. The goal of the considered control algorithms is to reduce electricity costs while maintaining consumer comfort by providing enough hot water at any time.

The following metrics are considered to rate performance of load shaping and control algorithms.

3.3.1 Energy consumption

The total energy consumption in kW h is determined by aggregating the energy consumed by the heating element. The energy proportions caused by insulation loss and the aggregated energy equivalents of every water draw events may be considered individually.

3.3.2 Energy costs

The costs of energy consumption is determined by the product of the consumed energy and the price at a certain price. Real day-ahead prices are considered in order to get an example profile of time varying prices, although these prices reflect the wholesale market in reality. Fig. 3.4 shows an example of hourly prices in EUR/MW h taken from the EPEX used for Germany and Austria, starting at midnight 2016-01-18. It is used as example for the simulations of this work.

The ability of shifting power consumption into times of low prices is expressed by the average price, which is determined considering the energy consumption given in (3.1), where E_i is the total energy consumed at time i and p_i the price at time i. The average price of the hourly prices in Fig 3.4 is 0.0357 EUR/kWh. Lower average prices represent a better ability of power shifting.

$$p_{\text{avg}} = \frac{\sum_{i=1}^{n} E_i p_i}{\sum_{i=1}^{n} E_i} \tag{3.1}$$

The energy efficiency of a DEWH and the utilized control method is given by the average price (3.2) payed for the useful energy. Here, the electricity costs are divided by the total energy of the water demand instead of the total energy.

$$p_{\text{use}} = \frac{\sum_{i=1}^{n} E_i p_i}{\sum_{i=1}^{n} W_i \Delta t} \tag{3.2}$$

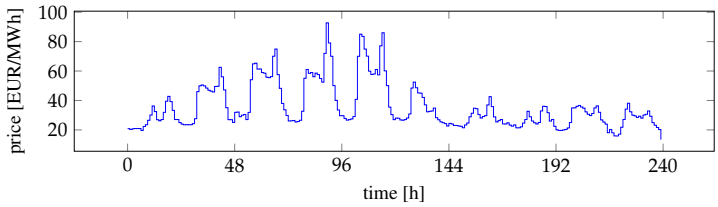

Figure 3.4: EPEX day-ahead price 10-day sample

3.3.3 Power availability

The day-ahead prices are considered as a measure for power availability. It is assumed that low prices reflect a high power availability, in particular from RES. Similarly, high prices are related to a low availability of RES. Thus, inverting the price profile leads to function of a power availability. This can be achieved using (3.3).

$$\hat{P}_i = \frac{\frac{n+1}{n}\overline{p_{\text{ex}}} - p_{\text{ex},i}}{(n+1)\,\overline{p_{\text{ex}}} - \sum_{j=1}^{n} p_{\text{ex},j}} \cdot 1\,\text{W} \tag{3.3}$$

3.3.4 Target deviation

The goal of load shaping is to minimize the difference between the aggregated load and the target profile. The error can be assessed by some vector norm, e.g. sum of squares is considered for the minimization objective in order to keep the error equally small in each time slot regardless of sign. Afterwards, the resulting performance is quantified by the mean absolute percentage error (MAPE) with (3.4). Here, $\hat{h}$ is the target schedule and h_k are the individual profiles of d loads.

$$M = 100 * \frac{\sum_{i=1}^{n} \left| \left(\sum_{k=1}^{d} h_{k,i} \right) - \hat{h}_i \right|}{\sum_{i=1}^{n} \hat{h}_i} \tag{3.4}$$

3.3.5 Consumer comfort

The consumer will be satisfied if the requested mix temperature of the hot and cold water is maintained within the total duration of the water draw. In this work it is assumed that the consumer always adjusts to the desired temperature at the water-tap, such that the temperature can not be too hot. Therefore discomfort is only experienced

when the temperature of the hot water drops below a defined minimum comfort value. This will be referenced as a low temperature event.

The average discomfort can be quantified with different complexity, e.g. by counting the total occurrences of low temperature events divided by the amount of draw-offs. To distinguish between a few households with many events and many households with few, the households which experienced one or more low temperature events in a given time interval is counted and divided by the number of intervals and households. More complex approaches, which consider the draw type, duration and difference of actual and minimum temperature are not further considered in this work, as the temperature of available hot water usually remains about constant or drops fast within a single draw-off due to the mixing layer, although this is not considered in the single-mass model.

In this work the number n_{lowT} of households experiencing one or more low temperature events per day is used to compare the satisfaction achieved by different configurations. It is assumed to be a more meaningful metric compared to the total count of events, because the majority of the water draw events are small draws which consume much less water than the few larger draws. Larger water draws have a stronger impact on the temperature decrease. Thus, the small taps only multiply the discomfort which is most likely caused by a previous large draw. For example when considering the same simulation results, where almost 100 % of the households experience at least one low temperature event, only about 20 % of all taps were affected. In contrast, with 80 % of the households, the count of affected events drops to only 5 %.

3.4 Preparation of data basis

Fundamental analysis of DEWH behavior and also theoretical performance of DR methods can be carried out with a few selected or randomly chosen values. However, in order to assess the practical performance of developed methods, a realistic setup of appliances and consumption profiles is required. This section describes the data basis of realistic DEWH setups and water consumption profiles.

3.4.1 Electric water heaters

In order to obtain a realistic set of different DEWHs, a sampling of devices available on the market from selected manufacturers [San14, SEG17, STI17, EHT17] was carried out. Figure 3.5 shows the observed diversity of 49 distinct devices regarding

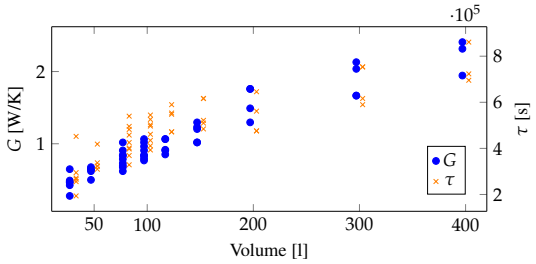

Figure 3.5: Volume / heat conductivity of DEWHs

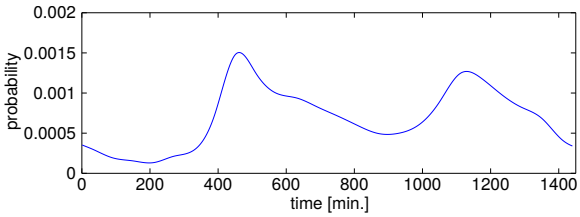

Figure 3.6: Water consumption pattern

heat conductivities and resulting τ-values (see Sec. 2.5.1) for the volume range of 30 to 400 l. Different types are available for each volume within a range of up to almost 50 % regarding the heat conductivity G. Calculating the τ-values with (2.24) shows that DEWHs of significantly different volume may have similar τ-values due to the diversity of the heat conductivity.

3.4.2 Water usage

Generating random water draw events allows to simulate arbitrary large set of households and also with unlimited simulation time. Households can either follow the same consumption patterns or may consider different profiles. In this work, randomly generated consumption follows the PDF shown in Fig. 3.6, which is derived from [Dep08] using interpolation. The drawback of this method is, that events do not follow routines of households, e.g. the time of a shower may differ significantly every day for a single household. Thus, it is not possible to learn and optimize for individual profiles rather than a total mean profile.

Real water usage data was published by the Water Research Foundation in 1999 [MDF99] and 2016 [DMD+16]. The databases include water draw events with an unique identifier for each household, the start time, volume, duration and type of the draw. Both databases do not state the mix-temperature of the water, thus assumptions have to be made. For this purpose, only events of type `Shower`, `Faucet` and `Bath/-tub` are considered. The mix-temperature is assumed with 40 °C and in the case of the 2016 database, which contains hot water measurements, a water temperature of 60 °C is used. To determine the hot water volume and energy equivalent, the inlet temperature is assumed with 11.1 °C. `Faucet` draws are considered with half the volume for the 1999 database, as they also may represent cold water draws.

Each household has about two weeks of measurement data, where the 1999 database mostly contains two periods of two weeks to cover different seasons of the same household. The measurement days are consecutive for single households, but spread over the year for different households. Fig 3.7(a) shows the distribution of the events per month. If many households need to be simulated in parallel, actual measurement dates have to be ignored and starting times need to be shifted to some common zero time. For a better balance of the water consumption profiles, events can be filtered by season. Furthermore, weekdays and weekends need to be distinguished, as the profiles may differ significantly.

In order to simulate households with the given data, each profile has to be mapped to a DEWH configuration. For this purpose, the maximum hourly water draw is considered to fit the tank size and the tank volume is as close to the draw volume as possible. Fig. 3.7(b) shows the resulting DEWH distribution of both databases. It can be seen that most households have larger ($> 150\,\mathrm{l}$) tank volumes, whereat the recent data shows a trend to smaller volumes. However, the earlier database dominates the total set.

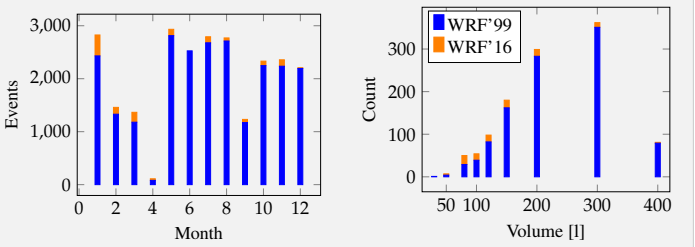

(a) Events per month

(b) Volumes

Figure 3.7: Real water usage data statistics

Chapter 4

Cost-Optimal Demand Response Algorithm for DEWHs

As a generic approach, customers may use solvers for linear programs or heuristic optimization methods to find appliance schedules minimizing their costs [PFM16, GSK16, RFFA12]. However, application specific algorithms promise a significantly lower computational effort and resource requirements that enable their execution on small controllers embedded in target devices. A well-known example was published by Du and Lu 2011 [DL11]. Their publication was cited more than 500 times as related work for optimizing costs and consumer comfort, in recent literature considering more general approaches including [PFM16, GSK16, RFFA12, KAK16, CAS13, WZWP13] and surveys [VZV15, WPSC13, Sia14]. Other work criticized beside the optimization itself, such as the limitation to a single load type [VDGJ12, SLLF13, MT13], the selfishness of the consumers which leads to high peaks at low prices [LNTL12, CAS13], and that uncertainties of consumption forecasts are not incorporated [PMFS16]. However, no work is known to the author that analyzed the algorithm in further detail, though it was used as comparison to a different optimization [AC14]. Although Shah et al. [SNSF16] published a similar algorithm in 2016, which improves the weaknesses of [DL11], they neither compared the behavior of both algorithms nor performed a comprehensive simulative study. As both papers claim to find the cost-optimal heating solution, a more detailed analysis and comparison of the algorithms is worthwhile.

In this chapter* the behavior of the Du and Lu algorithm [DL11], which is described in Sec. 2.6.4, is analyzed in more detail. In particular, several issues are identified and discussed. Furthermore, possible improvements are explained, which are partly also reflected in the algorithm of Shah et al. [SNSF16]. Simulations are used to analyse the effect of each improvement and all its combinations. Finally, an empirical study shows that the results of the algorithm are very close to optimal solutions.

4.1 Du-Lu algorithm issues & improvements

Although it is claimed to be optimal, there is no guarantee that the Du-Lu algorithm creates a cost-optimal heating pattern. The main issue is that a constant temperature bound is applied on the otherwise optimal schedule based on a price threshold heating decision, which may require the heater to be switched on at high prices, increasing the electricity costs and DR effect. Further suboptimal behavior results from binary heating decisions for whole time slots, a fixed optimization horizon, using a price threshold as heating decision and last but not least ignoring the efficiency of the heat storage, i.e. higher standby losses due to preheating.

4.1.1 Schedule minimum required energy

When the price optimal heating schedule leads to temperatures that fall below the lower limit, the heater will behave like a conventional thermostat to maintain the temperature. Thus the energy consumption will follow the water demand once the preheated water is used up until the next heating decision. As illustrated in Fig. 4.1, such a schedule may lead to a large energy consumption at high prices due to the strong correlation of the water demand and the exchange price. In the given example, the considered minimum prices of the first day are hour 23, 2 and 3, which correspond to a pre- and a post-heating phase (before or after a demand peak). At about hour 10 the preheated water is expected to be used up and the remaining water demand is scheduled to be heated in the last hours of the day and the heater is set to maintain the minimum temperature. If a water demand is expected at the end of the day, the last hour is used to heat although only a small amount of hot water may be required. Then the water remains preheated until the next day, increasing the standby loss and preventing to use lower prices on the next day for preheating.

*Minor extension of previous publication: Tobias Lübkert, Marcus Venzke, and Volker Turau. Appliance commitment for household load scheduling algorithm: A critical review. In *2017 IEEE International Conference on Smart Grid Communications (SmartGridComm)*, pages 539–544, Dresden, Germany, October 2017

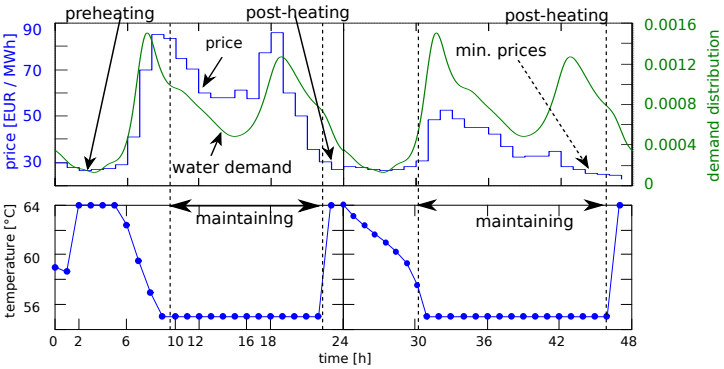

Figure 4.1: Maintaining minimum temperature

In the worst case, all considered minimum prices are at the end of the day. Then no preheating will be scheduled, as shown for the second day. This leads to a consumption pattern similar to a conventional thermostat.

To prevent such behavior, the energy demand after exceeding the lower temperature limit has to be scheduled within preceding lower prices, unless the heater is already scheduled to be on and it is impossible to maintain the temperature due to water draws. In the given example, a heating decision at hour 16 would improve the DR effect.

4.1.2 Variable heating duration

Using large time steps of one hour for the heating decision may lead to a higher energy consumption than required, as the heater may heat more than required by heating to the maximum temperature. This is especially the case for the last hour of a day. Because the water demand and the price are usually low at that time, the algorithm will decide to turn on the heater until the maximum temperature is reached, although it would be sufficient to heat the required demand. However, due to the low prices, this behavior can also have a positive effect if the following prices of the next day are higher.

To solve the issue, the heating duration needs to be adapted to the required demand. For this purpose smaller time steps can be used, e.g. in the order of minutes, but this significantly increases the computational effort. To prevent frequent switching Shah

et al. [SNSF16] propose to use a second controller, e.g. by applying partial power. Alternatively, the temperature setpoint corresponding to the desired heating duration can be calculated to adjust a thermostat. For this purpose, instead of a binary heating decision x_i, the total heating duration is scheduled within the minimum price hours. The decision variable then becomes a heating ratio $x_i \in [0,1]$. Thus the number of required time steps can be reduced to the number of available prices, while the heating resolution is increased with less computational effort.

4.1.3 Receding horizon

The scheduling algorithm always optimizes within a fixed horizon ending at midnight of the current day, including real-time updates, precluding the possibility to see lower prices on the next day. Alternatively a moving/receding horizon can be used that always considers a future time of same length, which is very common in model predictive control [MRRS00]. Depending on the horizon's length, this may require price prediction when the day-ahead prices are not yet available.

The heater will most probably consume a small amount of energy within the last hours, as the water demand is low and the forecast should have met the actual demand. However, the last hours of a day could already be considered to preheat for the next morning, which reduces the average cost if there are no comparable small prices that day. As shown in Fig. 4.2, this can be achieved by using a receding horizon for the real-time update, which always considers the water demand and exchange price forecasts of the upcoming 24 hours. Furthermore, a fixed horizon may lead to post-heating within the last hours if the actual water demand was below the forecast, which could reduce the preheating potential at lower prices of the next day.

However, a receding horizon may also be counterproductive due to suboptimal scheduling as discussed in Sec. 4.1.1, when the energy required to maintain the minimum temperature is not rescheduled. While a fixed horizon considers low prices during the day, a receding horizon may already consider lower prices of the next day instead, which leads to a higher energy consumption at higher prices when maintaining the minimum temperature.

4.1.4 Minimum price heating decision

Applying the temperature bounds on the optimal heating schedule may lead to a suboptimal actual heating profile when one of the prices considered for heating is

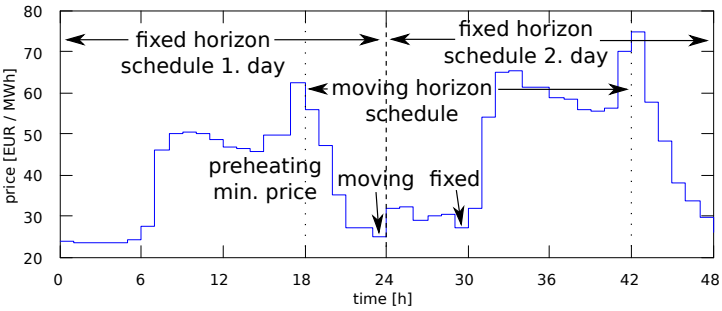

Figure 4.2: Preheating with fixed or receding horizon

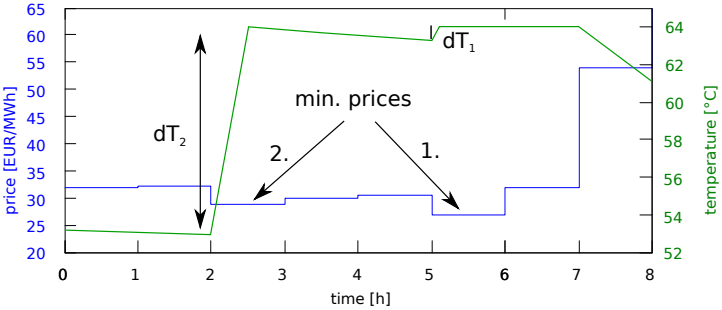

Figure 4.3: Violation of upper temperature bound

followed by lower prices, which are also considered for heating. As the temperature profile is calculated chronologically, the first violation of the upper temperature bound is selected to begin a new schedule. The heater may consume more energy at a slightly higher price unless the water demand in between significantly reduces the temperature. Fig. 4.3 shows an example schedule where hour 2 and 5 were selected to preheat the daily energy demand. As the heater needs less than an hour to heat from the minimum to the maximum temperature, the energy consumed with the minimum price in hour 5 may not exceed the demand between hour 2 and 5, which is comparably low. The issue also holds for different DEWH configurations which may not be capable to heat to the maximum within an hour unless the temperature decreases enough between two hours to completely utilize the minimum price.

This problem can be prevented, when instead of computing the temperature profile

for the complete heating schedule regarding a price threshold, only a single heating decision is considered per iteration, starting with the minimum price.

However, unless the rescheduling improvement of Sec. 4.1.1 is utilized, this method may be counterproductive. When the minimum price appears close to the end of the horizon, earlier prices will be ignored, which causes a long period where the minimum temperature has to be maintained.

4.1.5 Heat storage efficiency – effective price

High temperatures increase the standby losses, thus heating too early reduces the energy efficiency and may increase the costs. To prevent early preheating, effective costs may be considered for heating decisions instead of the minimum price. This also ensures to heat as late as possible at constant prices. Shah et al. [SNSF16] define the effective cost c_{eff} depending on the total daily costs by (2.40), considering a factor $\alpha \geq 0$. With the time difference t between the heating and the temperature violation, α specifies the balance of heating at low prices or close to the demand. The factor β represents the efficiency of the heating element as the relation of the heat energy demand to the required electrical energy. Furthermore, the choice of α depends on the characteristics of the DEWH and the consumption forecast.

In contrast, the proposed approach of this work is to calculate an effective price $p_{\text{eff},i}$ for each time slot i directly, without the need for parameter optimization with high computational effort. The effective price incorporates the costs for additional standby losses which occur when preheating to a higher temperature instead of directly heating to the desired temperature later. When sufficient knowledge about the DEWH parameters is available, $p_{\text{eff},i}$ can be calculated by Eq. (4.1).

$$p_{\text{eff},i} = \frac{\Delta T_i \cdot p_i}{\Delta T_{\text{min},i} + E_i / C} = p_i \cdot e^{\frac{\Delta t_i}{\tau}} \tag{4.1}$$

Here ΔT_i is the additional required temperature at time step i to reach a target temperature T_t at $t + \Delta t_i$, determined by (4.2). The target temperature (4.3) is the required temperature to reach the minimum bound after an expected water demand with energy E_i. $\Delta T_{\text{min},i}$ is the required temperature difference to reach $T_{\text{min},i}$ after Δt_i, given by (4.4). This allows to modify the temperature setpoint for non-binary

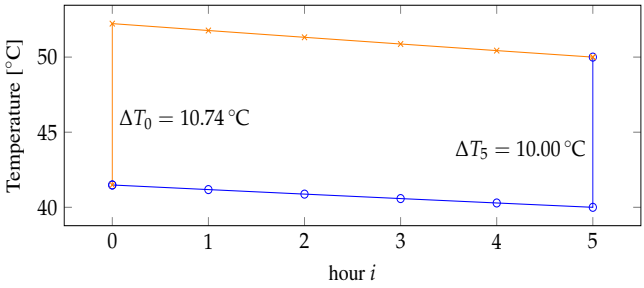

Figure 4.4: Example of a required preheating temperature

decisions variables.

$$\Delta T_i = (T_t - T_{\text{env}})\, e^{\frac{\Delta t_i}{\tau}} + T_{\text{env}} - T_t \tag{4.2}$$

$$T_t = T_{\text{min},i} + E_i / C \tag{4.3}$$

$$\Delta T_{\text{min},i} = T_{\text{min},i} - \left((T_i - T_{\text{env}})\, e^{-\frac{\Delta t_i}{\tau}} + T_{\text{env}} \right) \tag{4.4}$$

Fig. 4.4 shows an example of a required preheating temperature to reach 50 °C after five hours for a DEWH with $V = 60\,\text{l}$ and $G = 1\,\text{W/K}$. The target temperature is reached either by heating at the target time requiring a temperature difference of 10 °C or with increasing the temperature by 10.74 °C five hours earlier.

4.2 Enhanced Algorithm

When taking the improvements of Sec. 4.1.1–4.1.5 into account, the resulting algorithm becomes different from Du-Lu and similar to the Shah algorithm. Algorithm 1 describes the new recursive scheduling procedure. The complete steps including initialization are as follows:

1. Update price information for the current horizon. Initialize the heating schedule vector h with always off (0) and temperature schedule vector T with minimum bound T_{min}, but initial temperature T_0 with current temperature T_{cur}.

2. Determine the total heating duration t_h for the expected water demand within the specified horizon with n time steps, e.g. 24 hours.

3. Select the time slot i_m with minimum price and compute the heating duration t_h^+ to reach the maximum temperature $T_{\max}$ as well as the remaining time Δt_{i_m} to heat within that time step.

4. Add either the required or the available heating duration to h_{i_m}, subtract it from $\hat{t}_h$ and set the price at i_m to infinity if time step length Δt is reached.

5. Determine the new values for T by considering the temperature difference ΔT_i through heating, water draws and standby losses at time i. Check T for violations of the minimum and maximum temperature bound. Reduce the heating schedule such that the maximum temperature is not exceeded and set all prices up to the violation to infinity. If minimum is violated at i, create a schedule for required heating time t_h^- to maintain $T_{\min}$ within a horizon until i.

6. If the heating duration was not scheduled completely and at least one price is available, go back to step 3.

When the scheduling is completed, T_1 is used as new temperature setpoint for the thermostat. The scheduling gets recomputed when the next time step is reached, upon price changes, or water draw events.

4.3 Performance Analysis

To analyze the potential of the proposed enhanced algorithm and compare it to the Du-Lu algorithm, all combinations of the five improvements discussed in Sec. 4.1.1 – 4.1.5 were tested in a simulation. Furthermore, the difference of the algorithm results to optimal solutions was evaluated empirically by comparing results of 600 different scenarios to the solution of the equivalent LP.

In the evaluation of Du and Lu [DL11] only one day was considered, using a favorable price profile with low prices every few hours. Shah et al. [SNSF16] also evaluated a single day schedule for one DEWH regarding a time-of-use price profile with four prices. Deviations from the expected water demand and prices were considered by Du and Lu, but not Shah et al. Both utilized the savings of electricity payment to assess the algorithm. The claimed optimality of both was not proven.

Algorithm 1 Enhanced Scheduling Algorithm

$p \leftarrow$ updated prices for n time steps
$h_i \leftarrow 0 \, \forall i \in \{0, 1, \ldots, n\}$
$T_0 \leftarrow T_{\text{cur}}$
$T_{1..n} \leftarrow T_{\min}$
$t_h \leftarrow$ heating duration for water demand within horizon
SCHEDULE(t_h, n)
procedure SCHEDULE($\hat{t}_h$, $\hat{n}$)
  while $\hat{t}_h > 0$ & $\min\{p_{0..\hat{n}-1}\} \neq \infty$ **do**
    $i_m \leftarrow \arg\min\{p_{0..\hat{n}-1}\}$
    $t_+ \leftarrow \min\{\hat{t}_h, t_h^+, \Delta t_{i_m}\}$
    $h_{i_m} \leftarrow h_{i_m} + t_+$
    $\hat{t}_h \leftarrow \hat{t}_h - t_+$
    if $h_{i_m} == \Delta t$ **then**
      $p_{i_m} \leftarrow \infty$
    end if
    for $i = 0$ to $\hat{n} - 1$ **do**
      $T_{i+1} \leftarrow T_i + \Delta T_i$
      if $T_{i+1} \geq T_{\max}$ **then**
        $p_{0..i} \leftarrow \infty$
        $T_{i+1} \leftarrow T_{\max}$
        reduce h_{i_m} and update $\hat{t}_h$ accordingly
      else if $T_{i+1} < T_{\min}$ **then**
        SCHEDULE(t_h^-, i)
        $\hat{t}_h \leftarrow \hat{t}_h - t_h^-$
      end if
    end for
  end while
end procedure

4.3.1 Simulative comparison

The simulation setup utilized in this section considers 1,000 DEWHs with a single consumer each. Every consumer takes 1 shower, 6 medium (e.g. dish-wash) and 14 small (e.g. washing hands) water draw events per day, which is half of the profile of [JV01] to scale the demand for a single person. The flow rates are normal distributed as shown in [JV01]. The draw events are randomly distributed with the water demand profile of [Dep08] shown at the top of Fig. 4.5, as it is also used as consumption forecast as in [SNSF16]. Fixed day-ahead prices from EPEX shown in Fig. 3.4 are repeatedly used to analyze a period of 30 days. The water heater volume is selected to be equal to the mean daily demand of 65 l and has a rated power of 2 kW. The heat

conductivity is considered with 0.7 W/K, which was neglected by Du and Lu although it shows an impact on the DR effect [LVT17b]. The scheduling is performed utilizing 24 time steps per day, the temperature setpoint is updated by the current scheduling decision and is maintained within a deadband of 2 °C.

To assess the performance of the different improvements, the DR effect is measured by the resulting total costs and the average price paid for electricity [VT16]. The discomfort is evaluated considering the number of households which experience at least one shower with temperature below 35 °C per day.

Table 4.1 shows the simulation results for every possible combination of the improvements compared to the Du-Lu algorithm of Sec. 2.6.4, except the effective price, which is only applied once together with all other improvements. The first five columns indicate the selected improvements (`ep`: effective price 4.1.5, `hd`: variable heating duration 4.1.2, `rh`: receding horizon 4.1.3, `sT`: schedule T_{min} required energy 4.1.1, `sp`: select single minimum price 4.1.4). The combinations which improved the DR effect are highlighted.

The results show, that a variable heating duration (`hd`) per slot is required for all other methods to have a positive impact, but it does not improve the DR effect alone. The pre-scheduling of the energy required to maintain the minimum temperature (`sT`) has the most significant impact on DR. The other improvements (`rh`, `sp`) are more likely to be counterproductive for the given price characteristics unless combined with `sT`, then a further improvement is achieved. Furthermore, the discomfort is significantly reduced by `sT`, as it ensures the preheating before high demands. Using `hd` however increases the discomfort slightly due to a more accurate heating profile for an inaccurate demand forecast. In general, the discomfort can be reduced by using a higher minimum temperature or larger tank volume, which also impacts the DR effect [LVT17b]. Using the effective price (`ep`) instead of the original price information further reduces the costs by requiring less energy for standby losses. The improvements reduce the total costs by 0.28 EUR or about 5.6 % over all 30 simulated days. Thus the cost savings are doubled, as a conventional water heater with a constant temperature setpoint yields total costs of 5.24 EUR and an average price of 3.87 cent/kWh.

Detailed simulation results for a single day are shown in Fig. 4.5, including the total power consumption and mean temperature of the four highlighted beneficial combinations as well as the original Du-Lu algorithm. The starting temperature of all DEWHs is equally distributed within the allowed range, thus the mean temperature

Table 4.1: Effect of different improvements

ep	hd	rh	sT	sp	discomfort [%]	costs [EUR]	price [Cent/kWh]	Δ costs [%]	Δ price [%]
					2.91	4.96	3.57	0.00	0.00
				✓	3.09	5.04	3.64	1.60	1.87
			✓		0.23	5.13	3.62	3.42	1.35
			✓	✓	0.29	5.13	3.62	3.35	1.34
		✓			3.93	5.03	3.66	1.47	2.57
		✓		✓	4.22	5.06	3.70	2.06	3.66
		✓	✓		0.08	5.18	3.64	4.44	2.05
		✓	✓	✓	0.11	5.17	3.64	4.14	1.91
	✓				3.38	4.93	3.60	-0.53	0.85
	✓			✓	3.67	5.01	3.68	1.00	3.09
	✓		✓		2.05	4.77	3.46	-3.93	-3.24
	✓		✓	✓	2.16	4.75	3.45	-4.26	-3.42
	✓	✓			3.98	5.03	3.67	1.49	2.74
	✓	✓		✓	4.40	5.06	3.70	2.02	3.65
	✓	✓	✓		1.49	4.71	3.37	-5.13	-5.60
	✓	✓	✓	✓	1.63	4.69	3.36	-5.42	**-5.85**
✓	✓	✓	✓	✓	1.88	4.68	3.37	**-5.58**	-5.63

starts in the middle at 0 AM. The selected example illustrates all previously discussed improvements. Activated improvements are annotated to each curve in the figure.

The significant different heating decision of the Du-Lu algorithm and improved configurations are highlighted with 1–4 in the figure and discussed as follows.

1. At 1 AM all DEWHs heat to the maximum temperature unless `sp` is used, as the current price is the second lowest of the day. With `sp` only a few preheat slightly to avoid falling below the minimum temperature until 2.

2. The minimum price is found at 6 AM, where it is only possible with `sp` to consume a large amount of energy with a price difference of 0.06 cents/kWh.

3. As the current price at hour 14 is a local minimum, the Du-Lu algorithm will only decide to heat if the remaining demand does not fit the minimum price at hour 23. This is the case for only a few DEWHs, thus the mean temperature is slightly increased. The temperature is further increased when utilizing `sT`

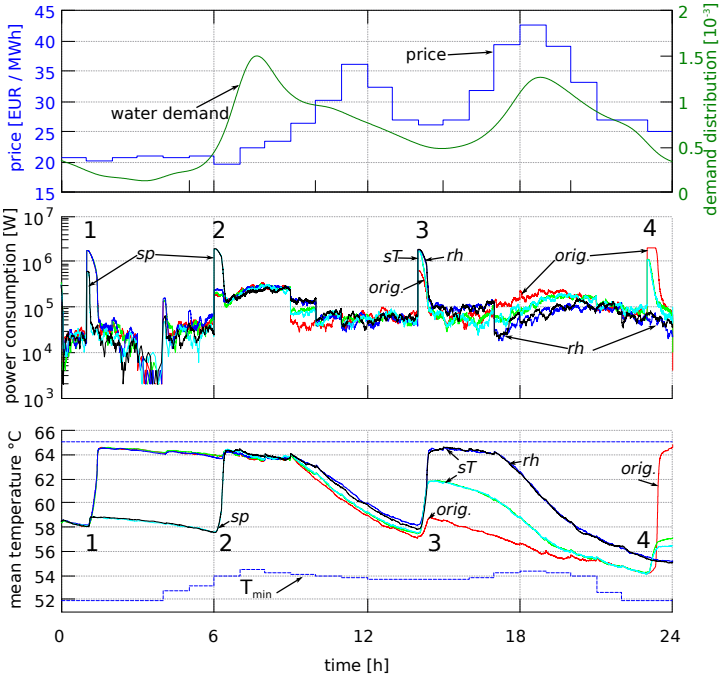

Figure 4.5: Simulation first day detail

to avoid falling below the minimum bound during the upcoming high demand and prices. A receding horizon (`rh`) causes heating to the maximum, as a large part of the next day's demand and further lower prices are already considered.

4. In the last hour, the Du-Lu algorithm decides to heat to the maximum because of the binary heating decision and a small expected demand. With variable heating duration (`hd`) and a fixed horizon the energy consumption is much smaller as the temperature setpoint is adapted to the expected demand. With a receding horizon (`rh`) the energy consumption is minimal, as smaller prices of the next day are considered.

4.3.2 Optimality

In order to evaluate the optimality of the developed algorithm, resulting heating schedules of several test cases are compared to the results of the equivalent LP-solution. The equivalent LP problem is derived from the integer linear program (ILP) problem defined in Sec. 2.6.3 and using a real value $h \in [0,1]$ instead of a binary heating decision. The solution is obtained using GNU Linear Programming Kit (GLPK) within Octave [EBHW17]. Algorithm 1 is solely used with the effective price method of Sec. 4.1.5.

In total 600 test cases are compared considering the mean absolute error of the heating decision. The scenarios cover all combinations of different values for volume, heat conductivity and temperature range specified in Table 4.2 as well as different price and water consmption profiles shown in Fig. 4.6(a) and Fig. 4.6(b) respectively. Fixed temperature values of cold water, environment, as well as the initial hot water temperature are given in Table 4.3.

The observed deviations are shown in the histogram of Fig. 4.7. The worst case error is about 6×10^{-5}. In the most cases, the error is 1×10^{-5} or even smaller.

Table 4.2: Optimality test cases varied parameter

V [l]	G [W/K]	ΔT_{nom} [°C]
30	0.4	2
50	0.8	5
100	1.0	10
150	1.4	20
300	2.0	30
	2.4	

Table 4.3: Optimality test cases fixed parameter

T_{cold} [°C]	T_{env} [°C]	T_0 [°C]
10	20	55

4.4 Conclusion

In this chapter a nearly cost-optimal DR algorithm for TCL appliances was developed on the basis of analyzing and enhancing multiple issues of the appliance commitment algorithm published by Du and Lu [DL11]. The resulting procedure shows similarities to the algorithm of Shah et al. [SNSF16]. The developed algorithm was analyzed by simulating 1,000 DEWHs. The DR effect was assessed as the total costs for electricity and average price paid regarding day-ahead prices. Furthermore, it is ensured that the

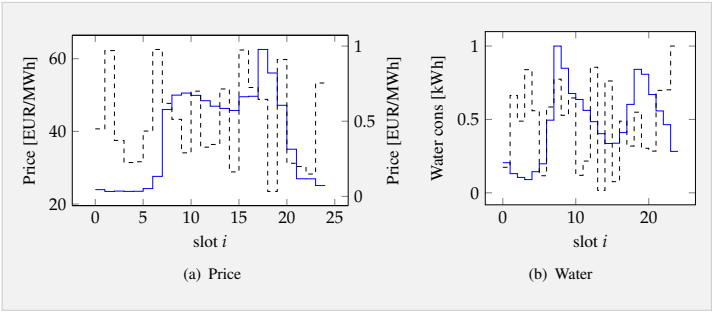

Figure 4.6: Optimality test cases

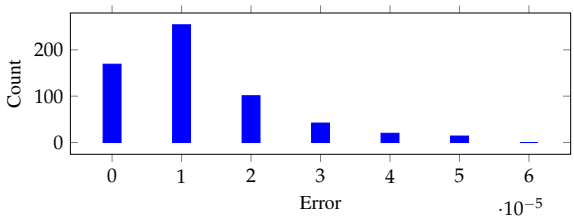

Figure 4.7: Histogram of mean absolute error to LP solution

requested hot water is provided by monitoring the consumer discomfort as percentage of households experiencing a low temperature water per day.

In total, five different issues were identified and resolved. The simulation results show that the most significant improvement is to schedule the required energy to maintain the minimum comfort temperature in the time before the limit is reached. The DR effect is further improved when using a receding horizon, which considers prices of the next day. Selecting a single minimum price per iteration instead of defining a price threshold may also increase the effect, as otherwise an earlier but higher price might be in favor of the minimum. All mentioned enhancements depend on utilizing a variable heating duration per price, e.g. by considering smaller time slots or by determining a temperature setpoint corresponding to the heating duration. Using an effective price function which considers the heat storage efficiency further reduces the total costs as less energy is required for standby operation.

Compared to the Du-Lu algorithm, the enhancements double the cost reduction

compared to conventional DEWHs with additional 5.6 % and also reduce the discomfort by 35 %. Furthermore, it was shown empirically that the developed algorithm yields near optimal solutions of the equivalent LP, with errors in the order of 1×10^{-5}. Thus, the algorithm may be considered as a substitute for a generic LP-solver.

Chapter 5

DEWH Parameter Impact Analysis for Demand Response

In order to construct prices, a supplier requires some knowledge about the customers' appliances and their demand to be able to estimate the resulting load profile. The parameters of interest are those which impact the effect of the DR program. Those parameters are also important for customers subscribed to a DR program, e.g. for the decision to invest in a new DEWH. Furthermore, devices may utilize different control methods, also affecting the parameter impact.

The effect of DR programs is difficult to quantify, thus market prices are often used to assess the capability to contribute to power balancing. It is often assumed that consumers directly benefit from reduced energy costs resulting from market prices.

When considering DEWHs, the energy consumption and the DR potential is influenced by many parameters. Besides the pattern of hot water consumption of the consumer it also depends on the tank volume, insulation and heater power as well as on control mechanism. The control mechanisms considered in this work set the nominal hot water temperature, which is manually defined by the consumer for commercially available DEWHs. The nominal hot water temperature may also be continuously varied by a DR mechanism considering future prices. This adds two more parameters, the allowed temperature range and the length of the price horizon.

In addition to the reduction of the energy consumption and contribution to power balancing, DR mechanisms must maintain the consumer satisfaction by providing enough hot water when required. However, the impact of the different dimensions of

the parameter space on DR effect and user satisfaction is not yet fully evaluated in literature. This also holds for the dependencies between parameters.

This chapter* analyzes the influence of the aforementioned parameters on DEWHs using different metrics and their interdependencies. The most significant parameters are identified in order to reduce the parameter space for assessing the performance of DR methods. For this purpose a common DEWH without DR mechanism and two energy scheduling methods from literature are evaluated by simulation. It is shown that all considered parameters but the heat conductivity have a significant impact on the consumer satisfaction. The average price particularly depends on the temperature range and the price horizon, but also on the volume and the heat conductivity.

5.1 Simulation Setup

To evaluate the metrics for different DR mechanisms and parameter values, 1000 DEWHs with one consumer each are simulated. The single-mass model is utilized for simplicity, as it is assumed that it allows to extract the same qualitative conclusions. Table 5.1 shows the settings of used default parameters. Furthermore, the volume, heat conductivity, rated power of the heater, nominal temperature, temperature range and forecast horizon are varied to evaluate their impact.

Table 5.1: Parameter settings to represent a realistic setup

Par.	Value	Description
V	65 l	tank volume
$\bar{W}$	62.5 l	avg. daily hot water consumption
$T_{\min}$	54 °C	thermostat lower threshold
$T_{\max}$	56 °C	thermostat upper threshold
T_{env}	$U\,(17.5, 22.5)$ °C	uniformly distr. ambient temp.
T_{cold}	10 °C	inlet / cold water temp.
C_ρ	4185.5 J/kg°C	heat capacity of water
P_{heater}	$U\,(1950, 2050)$ W	uniformly distributed rated power

*Major revision of previous publication: Tobias Lübkert, Marcus Venzke, and Volker Turau. Impacts of domestic electric water heater parameters on demand response. *Computer Science - Research and Development*, 32:49–64, 2017

5.1.1 Water Consumption

Following the model from [JV01], each consumer has a fixed amount of different water draws per day. The daily consumer pattern consists of 14 small draws (0.4 l), 6 medium draws (6 l) and 1 shower (40 l). All draw events are randomly distributed using the empirical daily consumption measured in [Dep08], which was interpolated in order to obtain a minute-scale probability mass function shown in Fig. 3.6. The draw volumes are normally distributed, as defined in [JV01], with $\mathcal{N}(0.4, 0.5)$, $\mathcal{N}(6, 1.25)$ in the same order as before, and $\mathcal{N}(40, 5)$. Water draws have a fixed duration of 1 min (small / medium) and 5 min (shower). The withdrawal temperatures, which result from mixing hot with cold inlet water, are set to 40 °C for small and shower draws, and 50 °C for medium draws as in [Sta06]. The minimum comfort thresholds are assumed to be 35 °C and 40 °C respectively.

5.1.2 Minimum Comfort Temperature

The required nominal temperature to achieve the maximum allowed discomfort with probability ω_{dcmf} can be estimated considering the largest temperature decrease in the single-mass model. The minimum setpoint temperature T_t at which the temperature drops below the minimum comfort threshold T_{cmf} with probability ω_{dcmf} at the end of a large draw can be determined by the equivalent probability threshold (5.1) that the amount V_{HW} of hot water drawn is less than the amount V_W necessary to reach temperature T_{cmf}. Where $P(V_{\text{HW}} < V_W)$ is expressed by the cumulative normal distribution of the large draw volume. The temperature setpoint can then be determined by (5.2).

$$\begin{aligned} P(T_t < T_{\text{cmf}}) &= P(V_{\text{HW}} > V_W) \leq \omega_{\text{dcmf}} \\ &\iff P(V_{\text{HW}} \leq V_W) \geq 1 - \omega_{\text{dcmf}} \end{aligned} \tag{5.1}$$

$$T_t = T_{\text{cmf}} - \frac{V_W}{V}(T_{\text{cold}} - T_{\text{use}}) \tag{5.2}$$

For example, considering a volume of 100 l, mean draw volume of 40 l and $T_{\text{cmf}} = 40\,°\text{C}$, yields a minimum setpoint of $T_{\text{min}} = 53.98\,°\text{C}$ for $\omega_{\text{dcmf}} = 0.01$.

Instead of a fixed temperature, the minimum temperature setpoint can be varied considering the probability P_S of a large draw at time t_i using the total probability (5.3) of experiencing a low temperature after a shower within a discrete time interval

of n slots. To determine the temperatures $T_{t,i}$, thresholds can be obtained for every t_i regarding the total probability of ω_{dcmf} using (5.4).

$$\sum_{i=1}^{n} P_S(t_i)\, P(T_{t,i} < T_{\text{cmf}}) \leq \omega_{\text{dcmf}} \tag{5.3}$$

$$P_S(t_i)\, P(T_{t,i} < T_{\text{cmf}}) \leq \omega_{\text{dcmf}} \cdot b_i,\ \sum_{i=1}^{n} b_i = 1,\ 0 \leq b_i \frac{\omega_{\text{dcmf}}}{P_S(t_i)} \leq 1 \tag{5.4}$$

In this work a minimum temperature setpoint schedule for energy scheduling comfort (ESC) was generated using $b_i = 1/n$, which gives a range of 51.97 – 54.55 °C when considering the consumption pattern of Fig. 3.6 as P_S. In general a greater variance of $T_{t,i}$ can be achieved when a sharper distribution P_S is given.

5.2 General Parameter Variation Effects

The energy consumption of a water heater per day depends on its total volume, heat conductivity of the insulation, temperature setpoint, the rated power of its heating element, and the control algorithm. The largest amount of energy is taken by the consumer drawing hot water from the tank, assuming a regular daily usage. The consumption shows a positive correlation with the market price, whereas the target of a DR mechanism is to achieve a negative correlation. To satisfy the consumer, the volume needs to be large or the temperature setpoint needs to be high enough regarding the average water consumption.

In this section the impact of changing the volume of a DEWH on the DR metrics is evaluated considering a fixed average water consumption and realistic heat conductivities for each volume. To reduce the parameter space, the volume is normalized by the average hot water consumption, as it is assumed to show similar effects for the same volume-consumption ratio. Furthermore, the impact of varying the heat conductivity and rated power DEWH is evaluated for different volume-consumption ratios considering the satisfaction, energy consumption, average price and mean temperature. The considered DEWHs are common devices utilizing a thermostat with fixed temperature setpoint, which is represented by a BBT controller.

5.2.1 DEWH Volume

Increasing the DEWH volume improves the consumer's satisfaction at the cost of a higher energy consumption, whereas the average price is slightly reduced. Increasing

the water heater volume also increases the heat conductivity if the same insulation is used, due to an enlarged surface. However, as the surface area does not scale linearly with the volume, the insulation per liter is improved while the total energy consumption is increased. Table 5.2 shows the simulation results for five volumes V from 50 l to 150 l. The heat conductivity is obtained by taking the median from available values shown in Fig. 3.5 for each volume. The average daily water consumption $\bar{W}$ remains unchanged, thus the volume-consumption ratio $V/\bar{W}$ increases with growing volume. The impact is evaluated by comparing the total energy consumption E_{total} per day, the proportion of insulation energy loss E_{loss}, the average price p_{avg} and the average proportion of consumers per day who experienced one or more discomforts n_{lowT}.

Table 5.2: Daily DEWH energy consumption comparison

V [l]	G [W/°C]	$V/\bar{W}$	E_{total} [kW h]	E_{loss} [%]	p_{avg} [Cent/kWh]	n_{lowT} [%]
50	0.65	0.8	4.06	12.7	3.91	58.5
80	0.79	1.28	4.18	15.5	3.90	2.2
100	0.87	1.6	4.25	17.1	3.89	0.1
120	0.92	1.92	4.29	18.2	3.89	0
150	1.2	2.4	4.53	23.6	3.87	0

The results show that the energy consumption caused by insulation heat loss already has a high proportion of about 13 % when the volume is smaller than the average water consumption and the discomfort is high. Increasing the volume significantly improves the satisfaction, but also increases the total energy consumption. By choosing a DEWH with a doubled volume, the energy consumption increases by about 5 %. The average price is above the mean price of 0.0357 EUR/kWh, because of the positive correlation of consumption and market prices. The average price slightly decreases with the volume, as the correlation is improved. Considering these results, the volume has to be selected appropriately small with respect to the water consumption. A sufficient satisfaction can be achieved with a ratio in the range $1.3 < V/\bar{W} < 1.6$. However, the high dissatisfaction with $V/\bar{W} < 1$ occurs because of the low mix temperature after large draws in the single-mass model. Furthermore, the satisfaction also depends on the nominal temperature and the heating power, as a higher temperature reduces

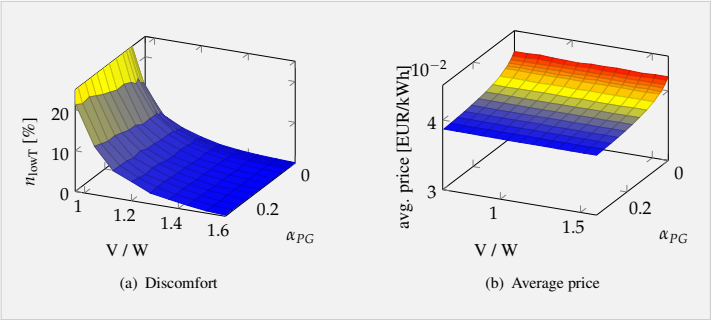

(a) Discomfort (b) Average price

Figure 5.1: BBT Variation of heat conductivity

the required hot water volume to achieve the same mix temperature and a higher rated power of the heating element reduces the heating duration.

Increasing the water consumption with a fixed volume shows similar effects as decreasing the volume with a fixed consumption, because the volume-consumption ratio also decreases. However, the same $V/\bar{W}$ ratio does not imply the same E_{total} or E_{loss}, because of different water consumptions and heat conductivities.

5.2.2 Heat Conductivity

A higher heat conductivity G (smaller heat resistance) reduces the effective power of the heater and the consumer satisfaction. The effective power is the difference of the rated power and losses to the environment P_G. A higher heat conductivity thus increases the heating duration and speeds up cooling. The effect is stronger at higher temperature, as the heat flow depends on the water temperature. Fig. 5.1(a) shows the impact of P_G on the average satisfaction n_{lowT} for different volumes at a fixed consumption. The values of G range from 1 mW/K to 20 W/K, normalized by the rated power P_{heater} using the mean temperature $\bar{T}$: $\alpha_{PG} = P_G / P_{\text{heater}} = G \cdot \bar{T} / P_{\text{heater}}$.

The observed discomfort increases about linearly with P_G, but the impact is generally low. As shown in Fig. 5.1(a), the slope is higher for smaller volumes which already have greater discomforts. For larger volumes ($V/\bar{W} > 1.2$), the heat conductivity has a low influence unless it is very high. The average daily energy consumption

for heating is the energy of the hot water drawn plus the losses to the environment. Thus, it increases linearly with P_G and is independent of the volume.

The average price shown in Fig. 5.1(b) generally decreases non-linearly with increasing G and converges for high values. As the share of standby energy increases, the power consumption particularly increases in low demand periods where prices are lower.

5.2.3 Rated Power

Increasing the rated power P_{heater} of the heating element improves the satisfaction, as the nominal temperature is regained faster, which allows to draw hot water with less delay after previous draws. This can be seen in Fig. 5.2(a) showing the average discomfort depending on the volume and the rated power. P_{heater} is normalized by the largest daily energy consumption of a single water draw with $\alpha_{PW} = P_{\text{heater}} / P_{\text{W}}$. The power P_{W} consumed by a water draw can be obtained by dividing the corresponding energy by the duration t_{W} of the water draw, as the duration of the water draw is fixed. Given the mix temperature T_{use} and volume V_{W} of the draw, P_{W} can be estimated by (5.5), derived by (2.18). The considered values of P_{heater} in Fig. 5.2 range from 0.2 kW to 5 kW, which yields a ratio range from about 0.01 to 0.3. The heat conductivity is set to a negligible value of 1 mW/K.

$$P_{\text{W}} = \rho C_\rho V_{\text{W}} \left(T_{\text{use}} - T_{\text{cold}}\right) / t_{\text{W}} \tag{5.5}$$

Combining a small volume with a low power heater leads to a high discomfort, as the temperature decreases faster due to water draws and regains slower to its nominal value. Both, increasing either the volume or the power improves the satisfaction. A large volume in combination with a very low heating power achieves a smaller average price as shown in Fig. 5.2(c), because the heating duration gets extended to the low price hours. However, the energy consumption cannot be improved by a smaller heating power, as the mean temperature stays about the same and a larger volume generally increases the heat conductivity significantly.

To maintain a maximum satisfaction a minimum power is required depending on the volume. The hatched area in Fig. 5.2(b) shows the non-linear dependency for a discomfort below 1 %. With a volume ratio of 1.6, the power ratio should not be less than roughly 0.03 (about 0.6 kW). However, as the heater needs to provide at least the

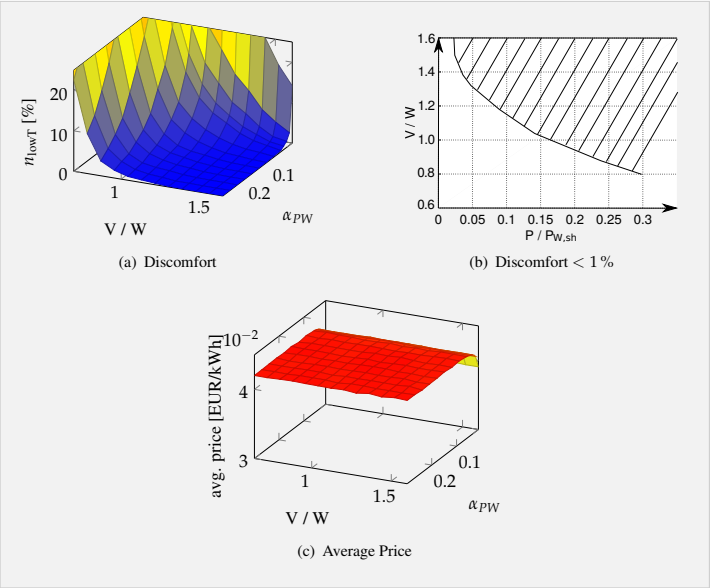

Figure 5.2: BBT Variation of heater power

daily energy consumption, the minimum required power converges at about 150 W (0.01) for larger volumes. Considering a maximum power of 2 kW (0.12), the volume ratio needs to be at least about 1.15 with the selected water consumption.

5.3 Parameter Variation Effects using BBT

Besides the physical parameters, the behavior of BBT can be influenced by the nominal temperature setpoint and the temperature range of the thermostat. The nominal temperature increases or decreases both, the minimum and maximum temperature, whereas the thermostat range maintains the nominal value and increases the allowed temperature difference. In this section their impact on the satisfaction, energy consumption, average price and mean temperature is evaluated for different volumes.

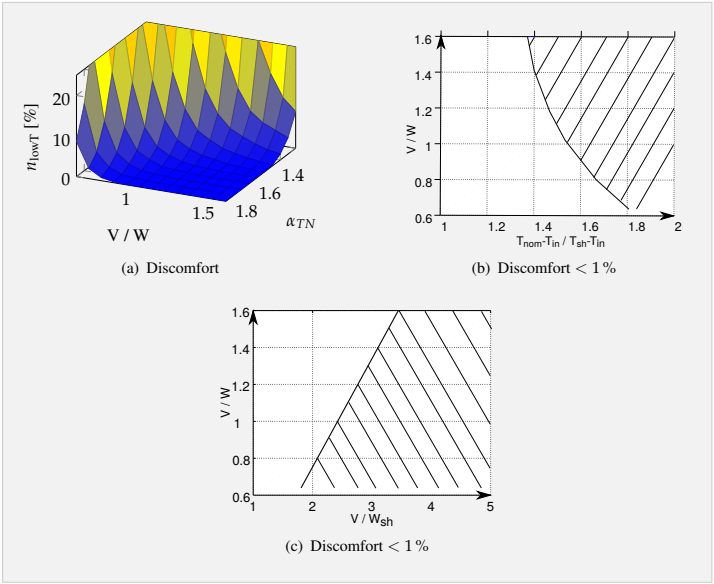

(a) Discomfort

(b) Discomfort $< 1\,\%$

(c) Discomfort $< 1\,\%$

Figure 5.3: BBT Variation of nominal temperature

5.3.1 Nominal Temperature

Increasing the nominal temperature – and thus the average hot water temperature – increases the amount of stored energy. The daily energy consumption is also increased due to the heat conductivity. The comfort is improved, as a higher temperature increases the volume of hot water that can be drawn with the same mix temperature. Fig. 5.3(a) shows the discomfort against volume ratio and normalized nominal temperature $\alpha_{TN} = \frac{T_{\text{nom}} - T_{\text{cold}}}{T_{\text{use}} - T_{\text{cold}}}$ within a range from 1.2 to 1.86 (respectively T_{nom} between 46 °C – 66 °C). The thermostat range is maintained at $\Delta T_{\text{nom}} = 2\,°\text{C}$.

The temperature ratio has a higher impact on the satisfaction than volume ratio, because the comfort does not only depend on the stored energy but also on the absolute temperature. For example, a DEWH with a large volume and temperature setpoint of T_{cmf} will always lead to a discomfort, whereas a DEWH of half size, and the same stored energy by having a higher setpoint may satisfy the consumer. As shown in Fig. 5.3(a), doubling the temperature ratio increases the satisfaction stronger than

doubling the volume.

However, the energy consumption also increases stronger with a higher nominal temperature than with a larger volume ($G \propto V^{\frac{2}{3}}$). Furthermore, both parameters have no significant impact on the average price.

The non-linear dependency of the required nominal temperature and volume to achieve a discomfort of at least 1 % is shown in Fig. 5.3(b). While a volume ratio of 1.4 requires a temperature ratio of about 1.4, with half of the volume the temperature only needs to increase to 1.7. Considering the amount V_{HW} of hot water drawn at a large draw, the satisfaction dependency can be approximately expressed linearly with (5.6) as shown in Fig. 5.3(c). Utilizing the linear factors allows to reproduce the non-linear dependency with (5.7) and the temperature ratio using (5.8).

$$\frac{V}{\bar{W}} = \frac{aV}{V_{\mathrm{HW}}} + b, \quad V_{\mathrm{HW}} = V_{\mathrm{W}} \left(\frac{\bar{T} - T_{\mathrm{use}}}{\bar{T} - T_{\mathrm{cold}}} \right) \tag{5.6}$$

$$\Longrightarrow \frac{V}{\bar{W}} = \frac{b \left(T_{\mathrm{use}} - T_{\mathrm{cold}} \right) V_{\mathrm{W}}}{V_{\mathrm{W}} \left(T_{\mathrm{use}} - T_{\mathrm{cold}} \right) + a\bar{W} \left(T_{\mathrm{cold}} - \bar{T} \right)} \tag{5.7}$$

$$\Longrightarrow \frac{T_{\mathrm{nom}} - T_{\mathrm{cold}}}{T_{\mathrm{use}} - T_{\mathrm{cold}}} = V_{\mathrm{W}} \left(\frac{1}{a\bar{W}} - \frac{b}{aV} \right), \quad T_{\mathrm{nom}} = \bar{T} \tag{5.8}$$

The linear factors $a \approx 0.6$ and $b \approx -0.45$ can be taken from Fig. 5.3(c) to reproduce the curve of 5.3(b), but they also depend on other parameters as the rated power, thermostat range and heat conductivity. Furthermore, the assumed linear dependency might not hold for much smaller or higher values.

5.3.2 Thermostat Range

Using a higher thermostat temperature range while maintaining the same nominal temperature decreases the satisfaction, because of the lower minimum temperature. Furthermore the heating and cooling durations increase, which impacts the cost correlation. The thermostat range ΔT_{nom} is varied from 0.02 °C to 24 °C and normalized by the nominal temperature $\alpha_{TR} = \Delta T_{\mathrm{nom}} / T_{\mathrm{nom}}$, which ranges from about 2×10^{-4} to 0.22.

Fig. 5.4(a) shows that the discomfort generally increases with larger thermostat range. The satisfaction remains almost constant for very small T_{nom}, but higher ranges require larger volumes in a non-linear relation.

The energy consumption increases with a larger range, as the mean temperature is slightly higher within periods of low water demand, which are much shorter than the

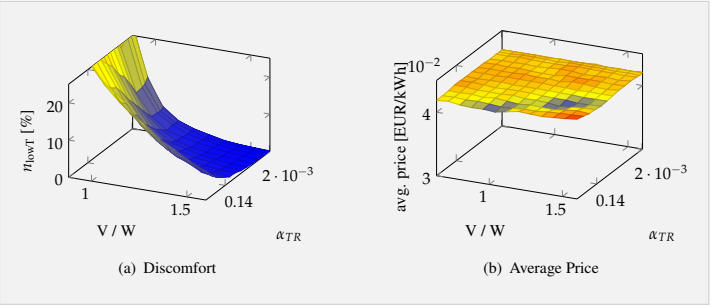

(a) Discomfort (b) Average Price

Figure 5.4: BBT Variation of thermostat range

cooling duration. The effect of the temperature range on the average price is small and as shown in Fig. 5.4(b) has a rather unpredictable behavior. Both, minimum and maximum prices are achieved above the maximum discomfort of 1 %.

5.3.3 Summary

The heat conductivity has a small influence on the satisfaction but linearly increases the energy consumption, whereas the average price decreases non-linear with larger G and converges for higher values. Increasing the rated power is more energy efficient than enlarging the volume to improve satisfaction. Although, with very low power the average price can be decreased, it would require a large volume to maintain the satisfaction which leads to higher standby losses in reality.

When considering a simplified constant heat conductivity model, it is slightly more efficient to increase the volume than the nominal temperature. The thermostat range should be small to reduce energy consumption and maintain a minimum satisfaction. Furthermore, the temperature settings and the volume have no impact on the average price.

5.4 Parameter Variation Effects using ANT

In addition to BBT, ANT changes the nominal temperature of the thermostat depending on the exchange price as described in Sec. 2.6.2. Thus the behavior of the water heater is affected by the allowed temperature range. As the current nominal

Table 5.3: ANT window configurations

window	-12	-6	0	6	12	18	24
Past	12	6	6	0	0	0	0
Future	12	12	6	6	12	18	24

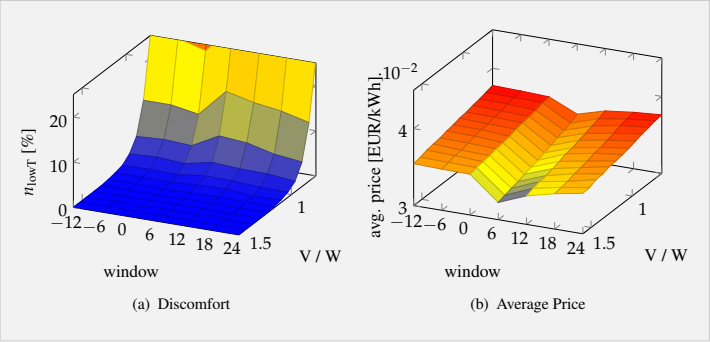

(a) Discomfort (b) Average Price

Figure 5.5: ANT Variation of volume

temperature is modeled as a function of the market price, the time window of considered prices impacts the heating decision. Table 5.3 shows the evaluated window configurations with regarded hours from the past and future. The default thermostat range is set to 2 °C and the nominal temperature ranges from 55 to 65 °C.

5.4.1 Volume

The discomfort shown in Fig. 5.5(a) depends more on the volume than the horizon, but is slightly improved when considering prices from past hours, as the nominal temperature is increased when the price decreases and the water demand still is high. But this leads to a higher average price as shown in Fig. 5.5(b). With increasing volume the average price decreases as more energy is being stored during low prices hours, as shown in Fig. 5.5(b). But this also increases the energy consumption because of the heat conductivity. The best average price is achieved with a small future window and without considering past values.

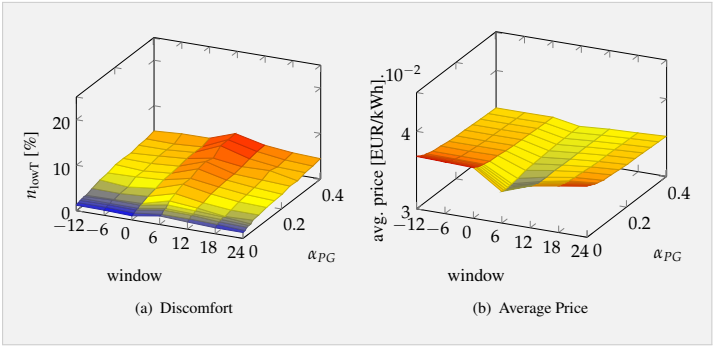

(a) Discomfort (b) Average Price

Figure 5.6: ANT Variation of heat conductivity

5.4.2 Heat Conductivity

Similar to BBT, the energy consumption increases linearly with the heat conductivity, which causes the average price to converge to a price close to the mean of about 0.035 EUR/kWh as shown in Fig. 5.6(b). The horizon has a small impact on the energy consumption. It is mostly increased when considering past hour prices and also slightly for smaller future windows. Considering past hour prices leads to heating at falling prices where the water demand also decreases. Small future windows lead to higher temperatures at the local minimum of price and water demand in the afternoon.

Whereas a window of 6 achieves the lowest price with improved insulation (small heat conductivity), it also shows a slightly increased discomfort (Fig. 5.6(a)). The discomfort generally increases slightly with P_G. The best satisfaction is achieved when considering past prices, because the exchange prices start decreasing while the water demand is high. But this also slightly increases the insulation energy loss as the temperature is kept high while the water demand decreases.

5.4.3 Rated Power

Similar to BBT the rated power has no influence on the average price unless it is very low and the satisfaction decreases, as shown in Fig. 5.7(a). Furthermore, the minimum price of BBT is already higher than the maximum of ANT when considering past hour prices as shown in Fig. 5.7(b). However, a window configuration of 6 future slots already achieves the minimum price independent of the rated power.

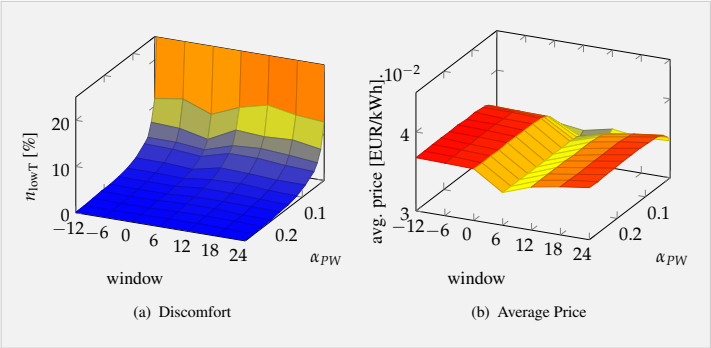

(a) Discomfort (b) Average Price

Figure 5.7: ANT Variation of rated power

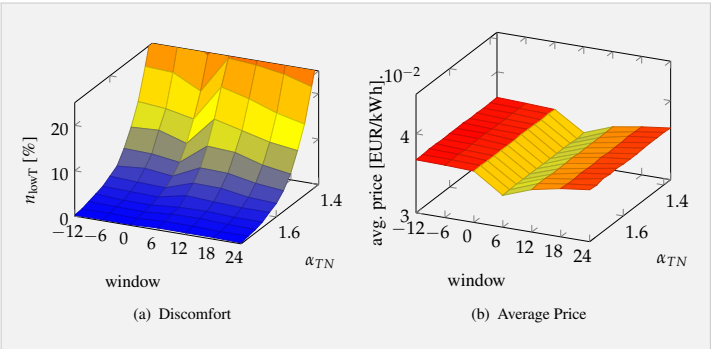

(a) Discomfort (b) Average Price

Figure 5.8: ANT Variation of nominal temperature

5.4.4 Nominal Temperature

As shown in Fig. 5.8(a) increasing the nominal temperature has a similar impact on the satisfaction as for BBT. The average price also does not depend on the nominal temperature as shown in Fig. 5.8(b). It does depend on the window configuration. However, increasing the nominal temperature will also increase the energy consumption due to the heat conductivity.

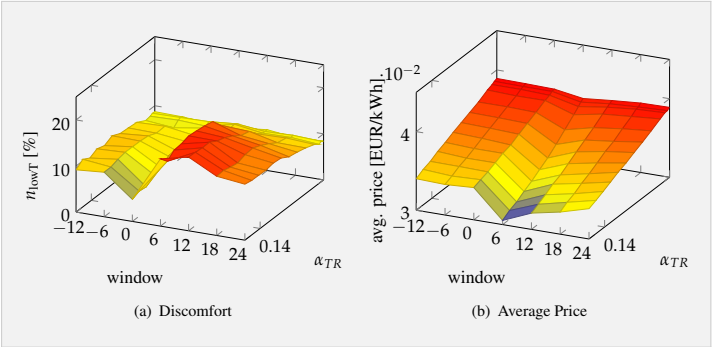

(a) Discomfort (b) Average Price

Figure 5.9: ANT Variation of nominal range

5.4.5 Nominal Temperature Range

Increasing the range of the nominal temperature generally decreases the average price (Fig. 5.9(b)), because more energy can be consumed in low price hours. But when the minimum temperature is also decreased, the satisfaction (Fig. 5.9(a)) decreases too. However, when past hour prices are considered, the satisfaction remains about constant with higher ranges, because the nominal temperature is increased at falling prices when the water demand is high. The best average price is still achieved by the smallest window configuration 6.

5.4.6 Summary

ANT generally achieves a lower average price than BBT. Furthermore, it allows an average price below the mean exchange price when using a small future window of a few hours. Window configuration and temperature range have the strongest impact on the average price, but also affect the satisfaction. In contrast to BBT, a larger volume also reduces the average price, whereas the minimum nominal temperature still has no impact. The minimum average price is achieved with a large volume, large temperature range and without considering past and about 3–5 future hour prices.

As for BBT, the satisfaction mostly depends on the volume and minimum nominal temperature, but also slightly on the window configuration of ANT. The best satisfaction can be achieved when past hour prices are considered, which allows large temperature ranges with a low minimum. However, the slightly decreased satisfaction

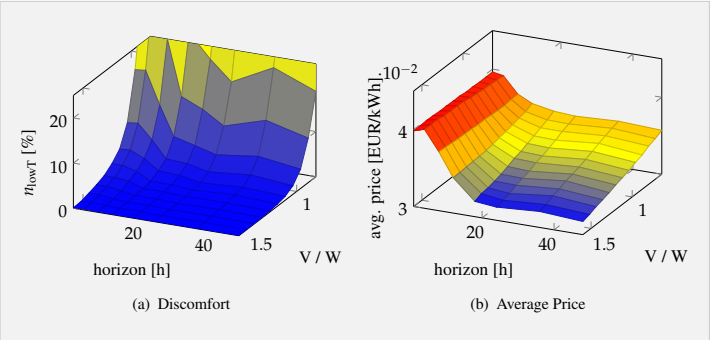

(a) Discomfort (b) Average Price

Figure 5.10: ESC Variation of volume

of a small future window may also be compensated by a larger volume or minimum nominal temperature.

The energy consumption can only be reduced by reducing the energy loss through heat conductivity, which depends on the volume and the nominal temperature. With ANT the energy loss is highest when past hour prices are considered and also slightly higher with smaller future windows, as both increases the mean temperature.

5.5 Parameter Variation Effects using ESC

As ANT, ESC changes the nominal temperature by considering future energy prices and the actual and prospective energy consumption. As the length of the horizon impacts the decision, different horizons from 1 to 48 hours are analyzed.

5.5.1 Volume and Horizon

The discomfort (shown in Fig. 5.10(a)) mostly depends on the volume and in general is lower when using a larger horizon, as more upcoming demand may be considered for preheating. In general the average price is lower for larger volumes and with larger horizons. The minimum average price is achieved with a horizon of about 18 hours or more. As shown in Fig. 5.10(b), further enlarging the horizon does not reduce the average price.

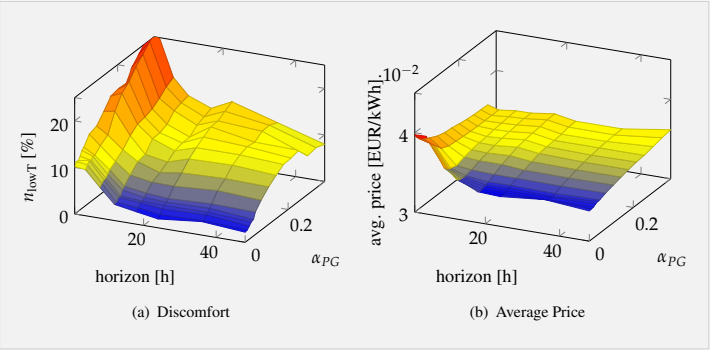

(a) Discomfort (b) Average Price

Figure 5.11: ESC Variation of heat conductivity

5.5.2 Heat Conductivity

As for BBT and ANT, the energy consumption increases about linearly with higher heat conductivity. The discomfort increases with higher G as shown in Fig. 5.11(a), because it impacts the effective price and leads to later heating decisions as well as a lower mean temperature.

Due to less preheating decisions, the average price also increases with higher G as shown in 5.11(b). Furthermore, the impact of the horizon becomes less significant, as preheating gets closer to the demand.

5.5.3 Rated Power

In principle a higher rated power improves comfort as the nominal temperature can be regained faster. Furthermore, with higher heating power more energy can be stored within the same time, which allows to achieve a lower average price, e.g. when prices vary with more often than each hour. As shown in Fig. 5.12(a), the rated power has a significant impact on the discomfort. However, the rated power has a no impact on the average price (Fig. 5.12(b)), unless it is very low, which leads to worse average price and high discomfort. A larger horizon improves the comfort, as long as the average price is also improved.

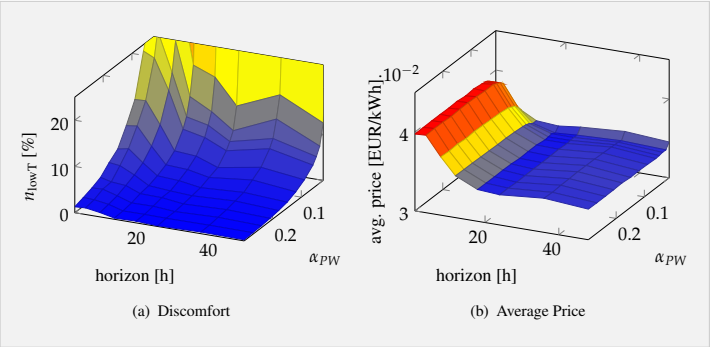

(a) Discomfort (b) Average Price

Figure 5.12: ESC Variation of rated power

5.5.4 Nominal Temperature

Similar to increasing the volume, a higher nominal temperature increases the comfort but also the energy consumption. Furthermore, larger horizons allow a slightly lower minimum and maximum temperature to achieve minimum discomfort, as a larger future demand is considered for preheating. However, the average price is independent of the nominal temperature as for ANT.

5.5.5 Nominal Temperature Range

Increasing the range of the nominal temperature reduces the minimum temperature and thus generally decreases the comfort, as shown in Fig. 5.13(a). The average price is significantly reduced with a larger range and smaller horizon as shown in Fig. 5.13(b), because more energy can be stored. The energy consumption decreases with larger range, because the mean temperature is reduced.

5.5.6 Summary

Similar to ANT, ESC achieves a lower average price than BBT. It is below the mean exchange price, and lower than ANT. The average price particularly depends on the horizon, temperature range, volume and also on the heat conductivity. The best average price is also achieved with a larger horizon of about 18 hours or more, as well as a lower heat conductivity, larger volume and temperature range. In contrast to

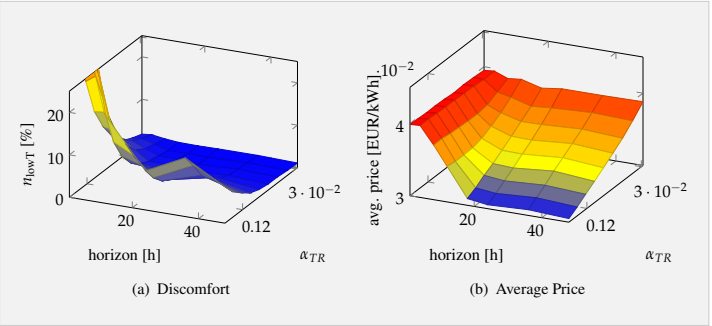

(a) Discomfort (b) Average Price

Figure 5.13: ESC Variation of nominal range

ANT, the impact of the horizon is more comprehensible, as more information may only improve, but not worsen the results.

5.6 Conclusion

In this chapter the impact of physical and configuration parameters of different DR mechanisms for DEWHs were analyzed in relation to energy consumption, DR effect and consumer satisfaction. The simulation results of the parameter variations show that the physical parameters not only influence the energy consumption and consumer satisfaction, but also the DR effect. The various DR algorithms must be assessed for DEWHs with the same configuration and the same consumer comfort. Energy savings must only result from lower losses to the environment, not by providing insufficient hot water.

The most important parameters for the DR effect are the price horizon, the range of the nominal temperature and the tank volume. To improve the consumer satisfaction the nominal temperature or the volume may be increased. Whereas the nominal temperature has no impact on the average price, a larger volume improves the effect on DR. However, increasing the temperature can simply be done by the controller or consumer, whereas a DEWH with larger volume requires a financial investment and more housing space. Furthermore, the deployment of a sophisticated DR controller already requires significant modifications, as a communication infrastructure and different sensors might be needed. The heat conductivity needs to be reasonable low, as this reduces the energy consumption and also may improve the DR effect for

appropriate DR mechanisms. Reducing the heat conductivity requires a different or thicker insulation. Theoretically, a perfect insulation allows to preheat at any time before a demand, but stronger insulation also implies higher expenses and may require more space. Rated power is the only parameter improving the DR effect for BBT, but it has insignificant impact for ANT and ESC and leads to higher discomfort.

The best DR effect can be achieved using a small future horizon with ANT and large horizon with ESC. ANT and ESC achieve a good DR effect, but also increase the energy consumption compared to the conventional BBT. Although ANT may achieve a good result with its simplicity, the more complex algorithm ESC allows a better DR effect and setting the horizon parameter is more transparent.

Chapter 6

DR Prices for DEWHs with Bilevel Optimization

The goal of this dissertation is to shape the aggregated power consumption profile of many DEWHs regarding a predefined target schedule (i.e. the power availability of RES) using a DA-RTP pricing scheme. A reasonable approach to find an optimal solution is to formulate and solve a corresponding bilevel problem. This chapter explains the system model as well as the resulting problem formulation and evaluates its solution using a state of the art solver.

6.1 System Model Preserving Privacy

In the considered system model* shown in Fig. 1.1, the supplier determines a target schedule for the aggregated power consumption of its customers in the planning phase a day-ahead. The target schedule reflects concluded trades at the energy exchange, which were made based on forecast of RES and the expected energy demand of customers. In the next step, the supplier has to define electricity retail prices for the next day, with fixed values for each time slot, which are broadcast to all customer households. Each household has a fixed price-insensitive load and a flexible DEWH load. The DEWH operates autonomously and optimizes its heating operation

*Problem description previously published in: Tobias Lübkert, Marcus Venzke, Nhat-Vinh Vo, and Volker Turau. Understanding price functions to control domestic electric water heaters for demand response. *Computer Science - Research and Development*, 33(1):81–92, February 2018
and: Tobias Lübkert, Marcus Venzke, and Volker Turau. Calculating retail prices from demand response target schedules to operate domestic electric water heaters. *Energy Informatics*, 1(1):31, October 2018

regarding received prices as defined in Sec. 2.6.3/4.2. The objective of the supplier thus is to find a price signal that leads to a minimal deviation of the resulting power consumption of flexible loads to the target schedule, e.g. with respect to the sum of squared errors. For this purpose the supplier has to estimate the behavior of the total flexible load of all DEWHs.

To protect the privacy of customers, only statistical knowledge of their DEWHs and their water consumption profile is considered. In particular, there is no back-channel, other than a smart meter, which is used for billing. Although, the power consumption of the DEWH is visible, customer's privacy is protected, as exact times of water usage are hidden by preheating decisions of the controller. This approach is especially different from DLC approaches, which remotely control the heating element of a DEWH and have knowledge of the current water temperature [YTP09]. Furthermore, the supplier's objective differs from the common objective of maximizing social welfare [MZ13, WLM15, ZMPM13], as the load has not only to be shifted into times of low prices, but needs to be distributed over the whole horizon regarding a given shape.

6.1.1 Follower's problem

The LP problem formulation describing the cost minimization of a DEWH is explained in Sec. 2.6.3, which uses the simplified thermal model of Sec. 2.5.1. Instead of binary heating decisions, real values are considered, as this improves the performance as shown in Sec. 4.3.1. The decision variables h_i determine the portion of each slot used for heating. It allows high precision of the solution while keeping the complexity low by using a LP with less time slots compared to an ILP considering binary heating decisions. However, the heating element can only be turned on or off. The resulting average power $h_i \cdot P_{\text{heater}}$ can thus only be achieved with many DEWHs equally distributing their heating times in the slot.

Additional constraints restrict the heating time in each slot from 0 to the length of the slot, that is, $0 \leq h_i \leq 1$. $h_i \leq 1$ leads to n more rows of A and a, one per slot, as

given in (6.1) and (6.2). Similarly, $0 \leq h_i$ leads to (6.3) and (6.4).

$$A_{(i+2n),j} = \begin{cases} 1 & i = j \\ 0 & i \neq j \end{cases} \tag{6.1}$$

$$a_{i+2n} = 1 \tag{6.2}$$

$$A_{(i+3n),j} = \begin{cases} -1 & i = j \\ 0 & i \neq j \end{cases} \tag{6.3}$$

$$a_{i+3n} = 0 \tag{6.4}$$

Together with (2.34)–(2.36), the block matrix A consists of four square submatrices. The upper two are lower triangular. The lower two are an identity matrix and a negative identity matrix. In total, $4n$ constraints have to be fulfilled. Formally, the follower's problem of the DEWH for given prices p is written as (6.5) with (6.6).

$$\min_h \; p^T \cdot h \tag{6.5}$$

$$s.t.\; A \cdot h^T \leq a \tag{6.6}$$

6.1.2 Leader's problem

The supplier induces the DEWHs to follow the target schedule by sending a price function to all customers. The price function consists of discrete time-dependent prices and is implemented as price vector p. To protect the customers' privacy, the supplier is assumed to have statistical knowledge about hot water usage and device parameters only. However, the subsequent discussion initially requires the supplier to have full knowledge of hot water usage and device parameters. This is relaxed to statistical knowledge later.

The objective of the supplier is to find the price vector p minimizing the difference of the target schedule $\hat{h}$ to the aggregated heating profile of all DEWHs (6.7). Prices are constant during each slot. The individual heating profile vector h_k of DEWH with

number k results from minimizing its operational cost for the given price vector (6.8)–(6.9).

$$\min_{p} \left\| \left(\sum_{k=1}^{d} h_k \right) - \hat{h} \right\| \tag{6.7}$$

$$\forall k \in [1,d] : \min_{h_k} p^T \cdot h_k \tag{6.8}$$

$$\text{s. t. } A_k \cdot h_k \leq a_k \tag{6.9}$$

Here, $\| \cdot \|$ is some vector norm. In this model, the common vector norm sum of squares is used to rate positive and negative deviations equally, leading to objective (6.10).

$$\min_{p} \sum_{i=1}^{n} \left(\left(\sum_{k=1}^{d} h_{k,i} \right) - \hat{h}_i \right)^2 \tag{6.10}$$

The supplier calculates the target schedule $\hat{h}$ from its total power availability $\hat{P}$ (for all customers), and from the expected energy requirements of each DEWH. Therefore, an estimation of each DEWH's energy requirement $E_{\text{total},k}$ is calculated with (6.11) by adding the energy required for hot water consumption $P_{\text{W},i}$ and the minimum of the energy lost to the environment in each slot. $\hat{h}$ is calculated from E_{total} with (6.12) by scaling it with the suppliers relative total power availability.

$$E_{\text{total}} = \sum_{i=1}^{n} \left(P_{\text{W},i} + G \cdot (T_{\min} - T_{\text{env}}) \right) \cdot \Delta t \tag{6.11}$$

$$\hat{h}_i = \sum_{k=1}^{d} E_{\text{total},k} \cdot \frac{\hat{P}_i}{\sum_{i=1}^{n} \hat{P}_i} \cdot \frac{1}{P_{\text{heater},k} \cdot \Delta t} \tag{6.12}$$

A supplier's constraint is assumed, that prices p_i must be greater than some minimum value p^ϵ due to fixed expenses. Otherwise, the solution of the follower's problem will include arbitrary heating rates for prices equal to zero and maximum rate for negative prices regardless of the water demand. The constraint is modeled with a vector p_n^ϵ with $p_{n,i}^\epsilon = p^\epsilon > 0$ and (6.13).

$$p_{n,i}^\epsilon \leq p_i \tag{6.13}$$

6.2 Solving the Bilevel Optimization Problem

Finding optimal solutions to a bilevel problem is NP-hard and thus the size of the considered problem is critical. To reduce the problem formulation of many DEWHs, clusters of similar DEWHs are used. After transforming the bilevel problem into a MILP, setups of different complexity are evaluated using the Gurobi optimization solver [Opt18]. As larger setups cannot be solved optimally, a heuristic optimization is performed using PSO.

6.2.1 Clustering of DEWHs

As the complexity of the bilevel problem significantly increases with the number of DEWHs, one approach of reducing the complexity is to consider a mean model clustering many devices. A reasonable parameter for clustering is the volume, because it shows a significant impact on the DR effect. Considering the concept of the effective price, a more promising clustering is done by the temperature change rate τ, as this is the only parameter of the thermal model in the equation, see (4.1). In particular, the effective price determines the times of preheating and thus times of higher power consumption for individual DEWHs.

A two step procedure is proposed, which reduces a set of many DEWHs down to a number of at most d. In the first step, DEWHs with similar τ-value are merged with Algorithm 2*. Afterwards the smallest adjacent clusters are merged with Algorithm 3 until the desired number of clusters is reached. Given a vector $\tilde{\tau}$ of τ-values containing all considered DEWHs in descending order and a minimum allowed difference $\Delta\tau$ of adjacent values, Algorithm 2 removes all values which have a smaller difference to the next lower value. The first and the last τ-value of the returned vector $\hat{\tau}$ are larger or lower than the maximum or minimum value respectively. Thus all DEWHs with $\hat{\tau}_i < \tilde{\tau}_m \leq \hat{\tau}_{i+1}$ belong to the cluster i.

If afterwards more clusters remain than desired, Algorithm 3 iteratively merges clusters, given the vector $\hat{\tau}$ together with the numbers of DEWHs per cluster in the vector d^τ and the desired number of clusters d. In each iteration it removes the τ-value, such that the new resulting cluster spanned by two adjacent τ-values has minimum size.

*Algorithm 2 previously published in: Tobias Lübkert, Marcus Venzke, and Volker Turau. Calculating retail prices from demand response target schedules to operate domestic electric water heaters. *Energy Informatics*, 1(1):31, October 2018

Algorithm 2 τ-Cluster

```
function TAU_CLUSTER(τ̃, Δτ)
    τ̂_0 ← τ̃_1 + Δτ
    τ̂_1 ← τ̃_1
    k ← 1
    for m = 2 to d do
        if |τ̂_k − τ̃_m| < Δτ then
            τ̂_k ← τ̃_m
        else
            k ← k + 1
            τ̂_k ← τ̃_m
        end if
    end for
    τ̂_{k+1} ← τ̃_d − Δτ
    return τ̂
end function
```

Algorithm 3 τ-Cluster merge

```
function TAU_CLUSTER_MERGE(τ̂, d^τ, d)
    while d < length of d^τ do
        k ← arg min_k d^τ_k + d^τ_{k+1}
        τ̂_k ← τ̂_{k+1}
        remove τ̂_{k+1} and update d^τ accordingly
    end while
    return τ̂
end function
```

6.2.2 Temperature violation penalty

The fixed minimum and maximum temperature constraints may lead to an infeasible LP, e.g. when considering a small temperature range, a large water draw within a short duration makes preheating and not falling below the minimum temperature unavoidable. In order to solve these type of scenarios, the hard constraint can be converted to an additional term of the objective using the penalty method. Instead of not allowing solutions with less than minimum temperature, these solutions will lead to high virtual costs due to penalty factors p_{pty} and thus will be avoided by the solver if possible. This is achieved, by moving constraint (2.35)–(2.36) to the objective, which leads to the new objective (6.14).

$$\min\ p^T \cdot h + \max\left\{0, {p_{\text{pty}}}^T \cdot (T_{\min} - T)\right\} \tag{6.14}$$

The equivalent LP formulation (6.15) then allows a solver to find a feasible solution. The number of decision variables is doubled.

$$\min\ p^T \cdot h + {p_{\text{pty}}}^T \cdot x \tag{6.15}$$

$$\text{s. t. } x \geq 0 \tag{6.16}$$

$$x \geq T_{\min} - T \tag{6.17}$$

6.2.3 KKT Transformation

In order to solve the formulated bilevel problem (6.7) – (6.9), it has to be converted into an equivalent one-level problem. A common approach is the KKT transformation (see Sec. 2.3.2), which converts the objective function of the follower's problem into a constraint of the leader's problem. By applying the KKT conditions and the reduction of the complementary constraints (2.7) – (2.15) for each follower problem of DEWH k, the resulting problem becomes a mixed-integer nonlinear problem described by (6.7), (6.13) and (6.18) – (6.21) $\forall k \in \{1,\ldots,d\}\,,\ j \in \{1,\ldots,4n\}$.

$$p + {A_k}^T \lambda_k = 0 \tag{6.18}$$

$$0 \leq \lambda_{k,j} \leq Q_\lambda z_{k,j} \tag{6.19}$$

$$-Q_A \left(1 - z_{k,j}\right) \leq A_k h^T - a_k \leq 0 \tag{6.20}$$

$$z_{k,j} \in \{0,1\} \tag{6.21}$$

6.2.4 Setup and simple pricing schemes

A realistic setup of DEWHs and water consumption profiles is used based on the real usage data described in Sec. 3.4.2 and DEWHs available on the market described in Sec. 3.4.1. Only weekdays in the winter half year (Oct.–Mar.) with at least five days of data are considered, which results in a total of 893 households and a mean daily energy consumption of about 6.25 MW h. An inaccuracy of the volume is assumed between –2 % and 2 % with a step size of 1 %. The resulting τ-values are shown in descending order in Fig. 6.1. After applying the clustering with a total size of $d = 50$ and a minimum τ-difference of $\Delta\tau = 0.4\,\%$, the size distribution of τ-cluster size shown in Fig. 6.2 is obtained. The average cluster includes 18 DEWHs.

The complexity of the optimization problem is varied by creating setups with different amounts of decision variables and constraints. Thus, several setups are

created for all combinations of $d \in \{1, 10, 20, 30, 40, 50\}$ and $n \in \{6, 12, 24\}$. Here, d determines how many clusters are included in the problem formulation instead of recomputing the clusters. With smaller n, the time duration of slots increases respectively. The minimum price is defined with $p^{\epsilon} = 1$ [EUR/MWh], as prices must be greater than zero and can be scaled by any constant factor without effecting the follower's objective. Its absolute value does not influence interpretation of results. Only the relation of prices to each other influences heating decisions of DEWHs, not absolute values. Absolute retail prices are out of scope of this work. The large numbers of the complementary reduction are selected with $Q_A = 1000$ and $Q_\lambda = 100$.

An example target schedule is created using the power availability of wind and solar power from the German TSO Tennet [Gmbb, Gmba] for 1. Jan. 2018. The power profile is scaled to the expected mean demand of all DEWHs using (6.11) – (6.12) assuming a mean temperature of 55 °C, as the allowed temperature range is defined with $T_{\text{min}} = 40\,°\text{C}$, $T_{\text{max}} = 70\,°\text{C}$, and $P_{\text{heater}} = 2\,\text{kW}$. The target schedule is shown at the bottom of Fig. 6.3 in comparison to load profiles resulting from simple pricing schemes, which are constant prices and prices that are inverse proportional to the target schedule. Both schemes lead to huge deviations from the target schedule. This motivates the need for a more suitable pricing algorithm as proposed in this dissertation.

The closest power profile results from a flat price of $p = 1$, although it makes the heating decision independent of the target schedule. The cost-optimal heating profile maintains the minimum temperature and heats as late as possible. With inverse proportional prices, loads are shifted to times of high availability. Thus, DA-RTP prices, shown in the top figure, lead to larger deviation from the target schedule. The energy exchange price of the same date is mostly negative and thus leads to a higher power consumption in total with peak consumption around the minimum and no load during the last third of the day. Adding an offset of 200 to that price profile removes all negative prices, but the resulting power consumption shows a similar profile with lower total demand. The heating profile is far lower than desired at most times and exceeds the desired demand by a factor of about four in three hours.

A price profile with the inverse shape of the target schedule was calculated with (3.3), which leads to a similar price profile as the exchange price, however the minimum price occurs a few hours later. Thus, this price also leads to a high deviation of the target, as it only shifts the peak consumption.

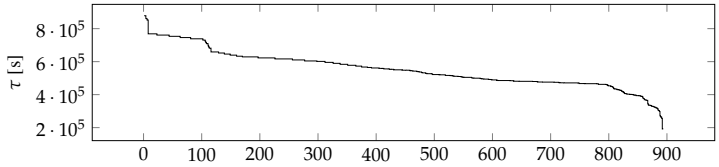

Figure 6.1: τ-values

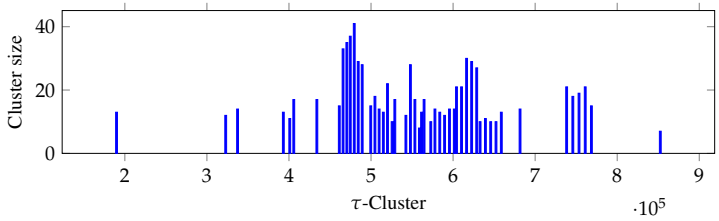

Figure 6.2: Clusters

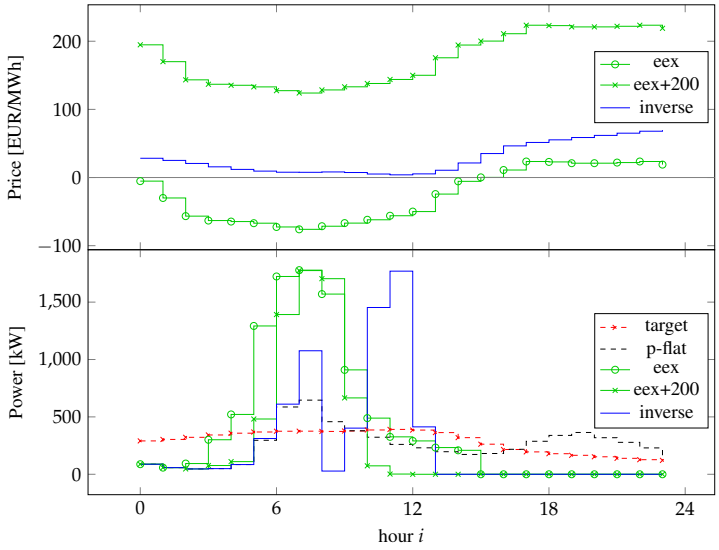

Figure 6.3: Simple prices

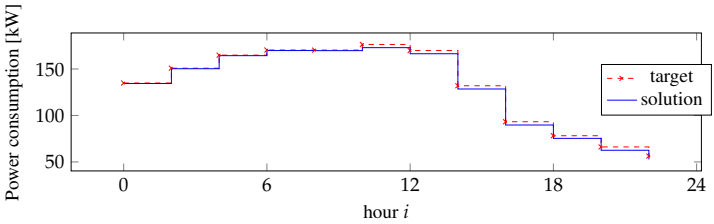

Figure 6.4: Heating schedule of best found solution for largest solvable setup

6.2.5 Optimal price evaluation

The Gurobi optimization solver [Opt18] is used to solve all considered setups. The optimization was performed on 32 cores of an AMD Opteron 6282 SE processor with 2.6 GHz for each setup with a time limit of four hours. Solutions were found for setups with $d \leq 10$ or $n \leq 12$ within less than 10 s. All other setups stopped without any solution, with two exceptions. For $d = 5, n = 24$ and $d = 10, n = 12$, no optimal solution is found within the time limit. However, good solutions are found after 2 minutes and about 1 hour respectively.

The best found solution for $d = 10, n = 12$ is shown in Fig. 6.4. The resulting power consumption approximates the target schedule as desired. It does not perfectly fit, as the total energy demand is slightly below the expected.

The resulting prices of the best solutions found for each setup are shown in Fig. 6.5. The top shows setups with $n = 6$, the bottom shows the other (with $n = 12$ on the left and $n = 24$ on the right). With two exceptions (shown on the top right) for $n = 6$, all found prices follow monotonic increasing functions with different slope, which is the same for different time resolution but equal DEWHs. Surprisingly, the price solution for a single DEWH cluster is very similar to solutions of more than one DEWHs, only the slope is slightly different. This allows to assume that these prices follow a certain principle depending on a physical parameter. Further investigation is done in Ch. 7.

6.3 Particle Swarm Optimization

A common alternative approach to solve bilevel problems is to use heuristic optimization such as PSO. The PSO solver solves the leaders problem by initially chosing random prices. The fitness is evaluated by solving the follower's problem using a

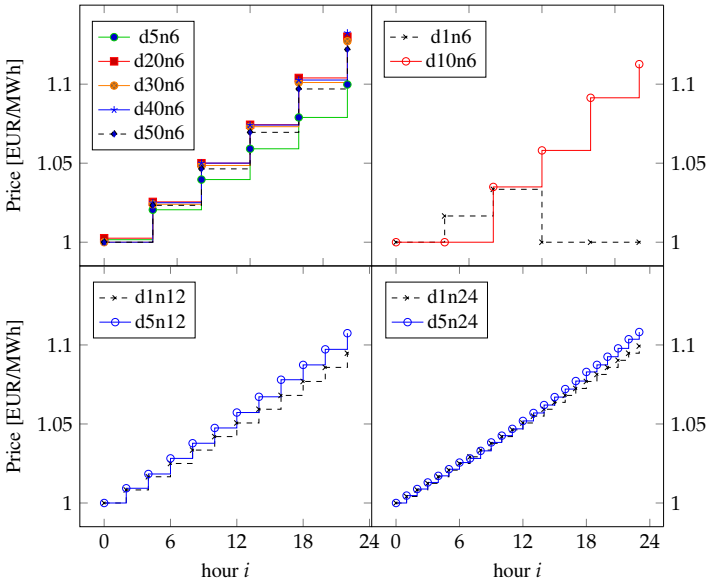

Figure 6.5: Found prices of all setups

LP solver and determining the error regarding the target schedule. The behavior of PSO depends on several parameters, the swarm size s, inertia weight ω, and the attraction weights ϕ_p and ϕ_g. Pedersen [Mag10a] suggests different parameters for different particle dimensions and number of iterations, which have shown good performance. Four parameter configurations shown in Table 6.1 are selected for evaluation. The SwarmOps implementation of Pedersen [Mag10b] for Matlab is used with Octave [EBHW17] as PSO solver. The resulting squared error is also shown in Table 6.1. Detailed results in Fig. 6.6 and Fig. 6.7 show the resulting power consumption profiles and prices respectively.

Configurations A, B and D lead to comparable results. Prices show small variations with a maximum difference of up to 2 % and the resulting power consumption profiles are similar as for a flat price. In contrast, the price of configuration C switches five times between two price levels, the maximum and minimum. The resulting power profile differs the most from the others. However, the resulting error is the highest. Thus, it seems unlikely for PSO to find better results other than near the local optimum

Table 6.1: PSO parameters and results

	Dim	iter [1×10^3]	s	ω	ϕ_p	ϕ_g	Err [1×10^5]
A	20	40	69	-0.4438	-0.2699	3.395	1.8
B	20	400	149	-0.3236	-0.1136	3.9789	1.5
C	30	60	134	-0.1618	1.8903	2.1225	2.3
D	30	600	95	-0.6031	-0.6485	2.6475	1.4

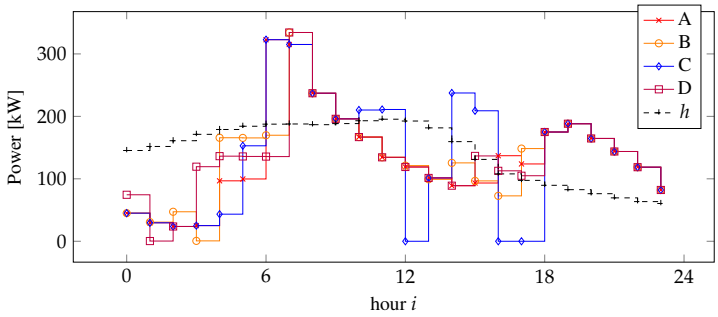

Figure 6.6: Heating schedule of PSO solutions

of almost flat prices.

6.4 Conclusion

The bilevel optimization problem of a supplier was formulated, which is to induce a power consumption profile of many DEWHs following a target schedule as a result of individual cost optimization to a broadcasted price vector. Clustering of many DEWHs reduces the complexity of the optimization problem. However, a state of the art solver practically finds solutions only for rather small problem sizes, i.e. less than five clusters or less than 12 time slots. Resulting price profiles for different setups follow the same principle of a monotonic increasing price. An alternative heuristic optimization approach using PSO did not lead to satisfying results. Thus, further investigation of the price principle resulting from bilevel optimization is done in the next chapter.

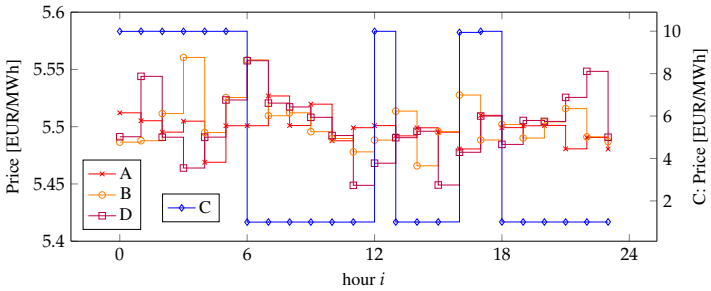

Figure 6.7: Found prices with PSO

Chapter 7

τ-Price Principle

This chapter further investigates the feasibility of suppliers to use price functions to shape their customers' load profile giving a desired profile, while customers optimize their consumption regarding their electricity costs. The results of Ch. 6 have shown that optimal prices from different bilevel problem setups follow the same principle, a monotonic increasing price.

As the resulting prices for a single or many DEWHs only differs in the slope, the resulting price for a single DEWH scenario is evaluated in more detail. The gained understanding allows a deep insight into the procedure of selecting price functions and their ability to induce a desired load profile. It is shown that price functions obtained by bilevel optimization cannot uniquely induce a desired load profile for a single DEWH. However, the acquired understanding allows identifying a procedure to generate price functions that induce a desired aggregated load profile of many DEWHs.

The optimal price to shape the load profile of a single DEWH is numerically evaluated in Sec. 7.1[*]. Sec. 7.2 outlines an approach for fixing prices to control many DEWHs. Sec. 7.3[#] explains how the resulting price function impacts the optimal heating decision.

[*] Sec. 7.1–7.2 partly previously published in: Tobias Lübkert, Marcus Venzke, Nhat-Vinh Vo, and Volker Turau. Understanding price functions to control domestic electric water heaters for demand response. *Computer Science - Research and Development*, 33(1):81–92, February 2018

[#] Sec. 7.3 previously published as part of: Tobias Lübkert, Marcus Venzke, and Volker Turau. Calculating retail prices from demand response target schedules to operate domestic electric water heaters. *Energy Informatics*, 1(1):31, October 2018

Table 7.1: Parameters of reference configuration.

Parameter	Value	Parameter	Value
n	24	T_0	40 °C
Δt	3600 s	$T_{\min}$	40 °C
V	65 l	$T_{\max}$	70 °C
G	1 W/K	T_{env}	19 °C
τ_{ref}	272 100 s	T_{cold}	15 °C
P_{heater}	2 kW	p^{ϵ}	1 EUR/MWh
$\bar{W}$	$130\,\text{l} = 2 \cdot V$		

7.1 Computational results

This section analyzes the results of the bilevel program and shows the limits of its application for a single DEWH. In particular, the properties of resulting price functions are discussed.

7.1.1 Configuration

The reference configuration used for numerical validation of a single DEWH is given in Table 7.1 and Fig. 3.6. The DEWH has a volume V of 65 liters and a heat conductivity $G = 1\,\text{W/K}$ leading to temperature change rate τ_{ref}. G and heating power P_{heater} are selected from available devices (see Sec. 3.4.1). The total hot water consumption volume $\bar{W}$ is selected with twice the tank volume V at minimum temperature $T_{\min}$, which roughly represents an average demand of two persons [Dep08]. The demand is distributed over the day with the distribution c_i shown in Fig. 3.6. Given a daily total hot water consumption volume $\bar{W}$, W_i is obtained by (7.1).

$$W_i = c_i \cdot \bar{W} \cdot C \left(T_{\min} - T_{\text{cold}}\right) / \Delta t \tag{7.1}$$

The required heating duration for the total water demand is about two hours ($\bar{W}C \left(T_{\min} - T_{\text{cold}}\right) / P_{\text{heater}}$), which allows a highly flexible optimization, as the total demand can be scheduled into roughly 10% of the available time.

An exemplary power availability was derived from exchange prices p_{ex} taken from EPEX ELIX [SE18] of a single day (2016-01-17) by transforming it into power availability with (3.3). The minimum retail price p^{ϵ} was selected as 1 EUR/MWh.

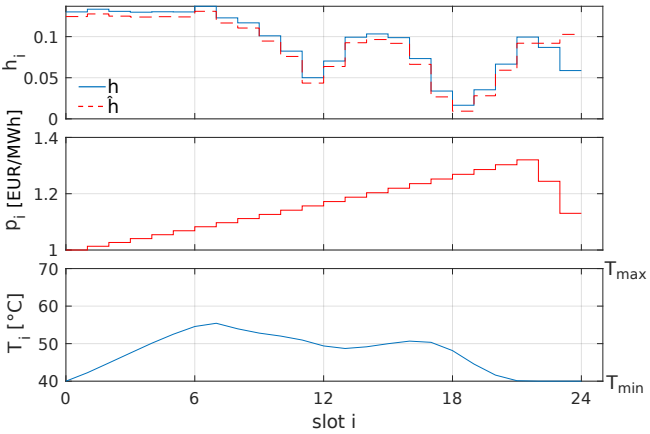

Figure 7.1: Bilevel solution.

7.1.2 Numerical results

The example optimization problems in this section are solved with an implementation in Matlab [Mat16] using the toolbox YALMIP. The toolbox YALMIP simplified the implementation. It works as a generic interface to many solvers and helps users to deal with various optimization problems, e.g. by selecting suitable solvers, converting bilevel problems into ordinary problems and converting constraints into the matrix notation. YALMIP selects the solver *quadprog*, as the objective function (6.10) of the leader's problem is quadratic.

The optimization problem is solvable. The resulting heating decision of the bilevel solution is very close to the desired profile as shown in Fig. 7.1 (top). The greatest deviation occurs at the end of the day, where the heating rate falls below the desired profile. A higher heating rate is not reasonable, as an end temperature above the minimum would lead to higher costs within the planning horizon for announced and fixed prices (DA-RTP). However, this could be changed using a larger horizon for the follower's problem, e.g. with forecasts of future prices. The maximum temperature is never reached, as shown in Fig. 7.1 (bottom). Only half of the allowed temperature range is required for this scenario. Hence, the main limiting factor is the price.

The resulting price function shown in Fig. 7.1 (middle) is basically monotonic increasing and non-linear, and does not force the desired heating profile. It exactly

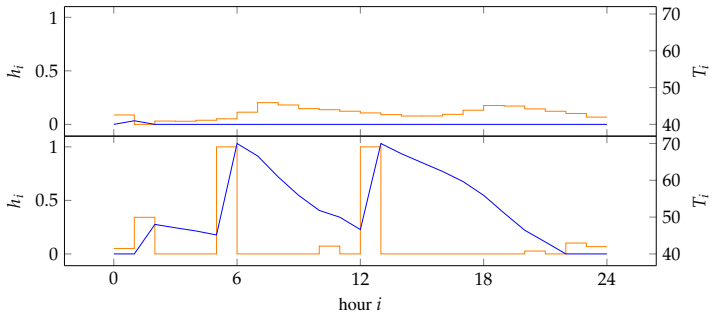

Figure 7.2: Follower's solutions of same costs.

compensates the costs for earlier heating due to higher standby losses. This property is achieved due to a constant effective price (see Sec. 4.1.5), which exactly compensates the slope of the given price. Thus, a DEWH has many options for heating decisions leading to the same minimal cost. Some options are close to the desired heating profile while others differ a lot. In this case, the bilevel solver chooses the option that leads to the best solution of the leader's problem, that is, the option with smallest deviation to the desired heating profile. However, in reality this model is unrealistic as a DEWH would probably choose a different option. This finding can be understood from the following observations.

The solution of the bilevel solver was tested for uniqueness by solving the follower's problem (6.5) with LP for the price function determined by bilevel optimization. The resulting consumption profile shown at the top of Fig. 7.2 is almost equal to the solution of a flat price and thus substantially different from the desired profile. In fact, the followers solution is almost arbitrary. Because of the flat effective price, the consumption profile shown at the bottom leads to the same total costs. The only constraint here is, that the minimum temperature is reached at hour 22, where the price is decreasing. Thus, the solution of the follower's problem is not unique and the approach to derive a price function to control a single DEWH for DR is questionable.

The slope of the price function only depends on temperature change rate τ. Fig. 7.3 shows the price functions for different values of τ. For comparability the constraint $p_1 = p^\epsilon$ was added to ensure that the first price is always the same.

The price slope observed from bilevel optimization can be described with (7.2). It only depends on γ and thus on the quotient τ of heat capacity C and heat conductivity

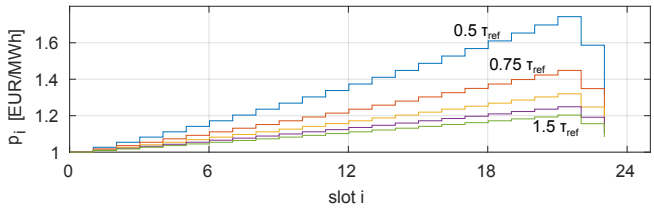

Figure 7.3: Bilevel prices for different time constants τ.

G (see (2.24) and (2.29)). It can be derived for the assumption, that alternatively heating in different slots $i-1$ or i lead to the same temperature T_i for the same costs. The required target temperatures of heating in either slot $i-1$ or i are given by (7.3) and (7.4) respectively, based on (2.22). Subtracting (7.4) and (7.3) leads to (7.5), the ratio of the required additional temperature in either slot. The requirement that the costs paid in both cases are the same is stated by (7.6), which leads to (7.2).

$$p_i = \frac{p_{i-1}}{\gamma} \tag{7.2}$$

$$\text{Heat in slot i-1: } T_i = (1-\gamma)T_{\infty,i} + \gamma T_{i-1} + \gamma \Delta T_{i-1} \tag{7.3}$$

$$\text{Heat in slot i: } T_i = \Delta T_i + (1-\gamma)T_{\infty,i} + \gamma T_{i-1} \tag{7.4}$$

$$\gamma = \frac{\Delta T_i}{\Delta T_{i-1}} \tag{7.5}$$

$$\Delta T_i \cdot C \cdot p_i = \Delta T_{i-1} \cdot C \cdot p_{i-1} \tag{7.6}$$

In fact, the above calculation is the opposite of calculating the effective price discussed in Sec. 4.1.5, which is crucial for the optimal heating decision of the DEWH. Thus, determining the effective price (4.1) with $\Delta t_i = (n-i)\,\Delta t$ for a price defined by (7.2) leads to a constant price (7.7).

$$p_{\text{eff},i} = p_i \cdot e^{(n-i)\Delta t/\tau} = p_1 \cdot e^{n\Delta t/\tau} \tag{7.7}$$

The bilevel solver may include steps in the price function where these cannot influence heating decisions as shown in the example in Fig. 7.4 with higher water consumption and higher target schedule $\hat{h}$ than in Fig. 7.1. An upward step has no effect when the maximum temperature is reached, as it cannot force further heating before, because the temperature reaches the maximum anyway. Similarly, a downward

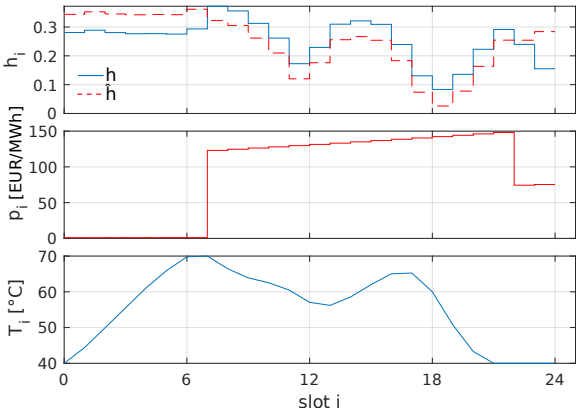

Figure 7.4: Bilevel solution for large water consumption.

step shows no impact when the minimum temperature is reached. Therefore, these steps can always be increased, reduced or removed.

If the temperature change rate τ of a DEWH slightly differs from the value assumed to find the price function, its consumption is far from the desired profile to minimize costs. Fig. 7.5 shows LP-solutions of the follower's problem for the price function with $\tau = \tau_{\text{ref}}$ and DEWHs having a larger and smaller time constant ($\tau_1 = 1.01\tau_{\text{ref}}$ and $\tau_2 = 0.99\tau_{\text{ref}}$). With larger τ, the DEWH immediately heats to the maximum temperature as fast as possible and maintains it until no further heating is required. Heating earlier reduces costs, as the standby losses are more than compensated by the price gain. But this leads to a large peak in power consumption. The smaller τ makes the DEWH maintain its minimum temperature, directly compensating water consumptions ($h_i \propto W_i$). Heating as late as possible reduces its costs, as standby losses are not compensated by the price gain. But then there is no effect for DR.

Considering different DEWHs for the bilevel problem, prevents the solver from selecting a price allowing arbitrary heating profiles of the same cost for a particular target device. A setup with three DEWHs of different size, demand and τ-value is used to further analyze the bilevel solution. The parameters of the considered DEWHs are shown in Table 7.2. The number of slots per day was changed to $n = 8$ to reduce the complexity and computational effort.

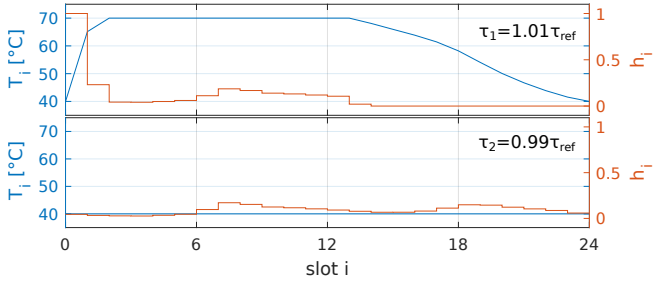

Figure 7.5: Deviation of follower's τ.

Table 7.2: Parameters of three DEWHs for bilevel optimization

k	V_k	$\bar{W}_k / V_k$	$\tau_k / \tau_{\text{ref}}$
1 (S)	55	3	0.99
2 (M)	65	4	1.00
3 (L)	75	5	1.01

As a single price function applies for three different DEWHs, the bilevel optimization may at most select one device per slot with arbitrary heating decision, while the others either decide to heat with maximum or minimum rate. The results in Fig. 7.6 show that a price function with slopes piece-wise following (7.2) achieves the optimal aggregated heating profile, by most of the time selecting the τ-value of the medium sized DEWH ($p \sim \text{M}$) to compensate the heating rate of the other devices. In the first and second slot the price slope correspond to the τ-value of the medium DEWH (M), which forces the large DEWH (L) to heat to the maximum temperature and the small DEWH (S) to heat only the required energy to maintain minimum temperature. Within the second slot all devices heat with maximum duration as the price increase is related to the small DEWH ($p \sim \text{S}$) in the third slot. All reach maximum temperature, as the price of the fourth slot shows a higher slope than any τ-value yields ($p > *$). From the fourth slot, the slope of the price continues to compensate the standby costs of the medium DEWH ($p \sim \text{M}$), allowing to select desired heating rates, while the large DEWH continues to maintain the maximum temperature and the small device heats as late as possible, such that it reaches minimum temperature at the end of slot four. In the last slot all devices heat with the maximum possible rate that leads to minimum

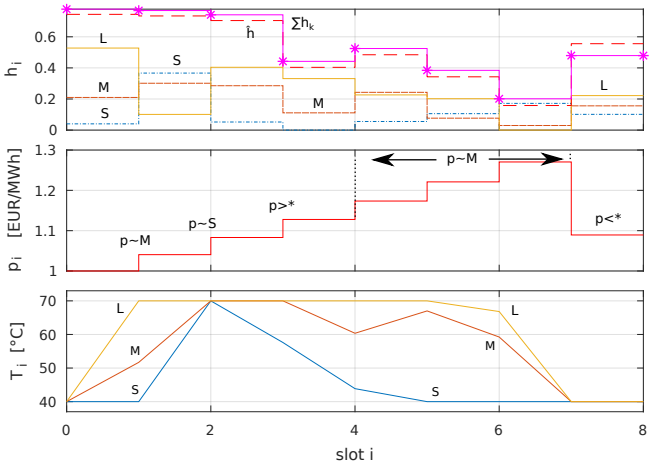

Figure 7.6: Bilevel solution of system with three DEWHs.

temperature, as the price is a local minimum $(p < *)$.

7.2 Control of many DEWHs

Observations from Section 7.1 lead to an approach for controlling many DEWHs with the same price function to approximately consume a desired load profile. Section 7.1 showed that this is impossible for individual DEWHs, as an "optimal" price function has a slope depending on its temperature change rate τ that only compensates energy losses allowing many possible heating decisions for the same lowest cost. However, it also showed that a price function that is optimal for a DEWH with τ_{ref} leads to one of two heating states for DEWHs with a different τ. Every DEWH k having $\tau_k > \tau_{\text{ref}}$ heats as much and as early as possible. Those with $\tau_k < \tau_{\text{ref}}$ heat as few as possible to maintain minimal temperature. These two states can also be selected for time intervals, if the slope of the price function is selected suitably for each interval as described in the following.

For many DEWHs with different τ_k, this allows selecting a desired number m of DEWHs doing maximal and the rest doing minimal heating. Therefore, assume that all DEWHs have a different, known τ_k and are sorted descending by that value, that is

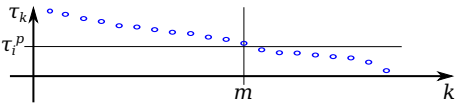

Figure 7.7: Selection of τ^p for many DEWHs sorted by τ_k.

$a < b \Rightarrow \tau_a > \tau_b$. The price function is then constructed with (7.8) given a vector $\tau^p = \left(\tau_1^p, \ldots, \tau_n^p\right)$ of τ-values, where each value τ_i^p is selected with any m such that $\tau_m < \tau_i^p < \tau_{m+1}$ as illustrated in Fig. 7.7. Thus m DEWHs with bigger τ_k are doing maximal heating and the rest having a smaller τ_k are doing minimal heating. The total power consumption results from the number of DEWHs in each state and their heating capabilities. If the heating capabilities are known, a price function can be constructed that brings the correct number of DEWHs into each state for every slot i to produce a power consumption that approximates the desired load profile.

$$p_i = p_{i-1} \cdot e^{\Delta t / \tau_{i-1}^p},\ 2 \leq i \leq n,\ p_1 = p^\epsilon \tag{7.8}$$

A price function has been constructed for an example with 24 slots and five DEWHs that shows that one or two DEWHs can be selected for heating with maximum rate for a slot, with all devices optimally solving the follower's problem (6.5) independently. Fig. 7.8 shows the price function and the corresponding τ^p at the top left, followed by the temperature profile and heating rate of each device, starting with highest $\tau_1 = 1.02\tau_{\text{ref}}$ and ending with lowest temperature change rate $\tau_5 = 0.98\tau_{\text{ref}}$. The constructed price function causes three simple peaks in slot 3–5 and a double peak in slot 13. After using a smaller slope for the first two slots, the price slope of the third slot is slightly higher than the slope corresponding to τ_1 but below the slope for τ_2 or less, thus only the first DEWH heats with maximum rate, while the others maintain the minimum temperature. In the subsequent slot, the slope is increased to match $\tau_2 > \tau_i^p > \tau_3$ respectively. This leads the second device to start heating with maximum rate, causing a strong increase, whereas the first device is already limited by the maximum temperature and may only heat the remaining difference or compensate the water demand, similar to all other DEWHs which maintain the minimum temperature. The slope is increased for the following slot in the same way, with similar effect on the heating rates. The slope continues according to $\tau_3 > \tau_i^p > \tau_4$ until slot 13, where the slope is changed with $\tau_i^p < \tau_5$, which causes the fourth and fifth DEWH to heat with peak rate at the same time. In this scenario, the

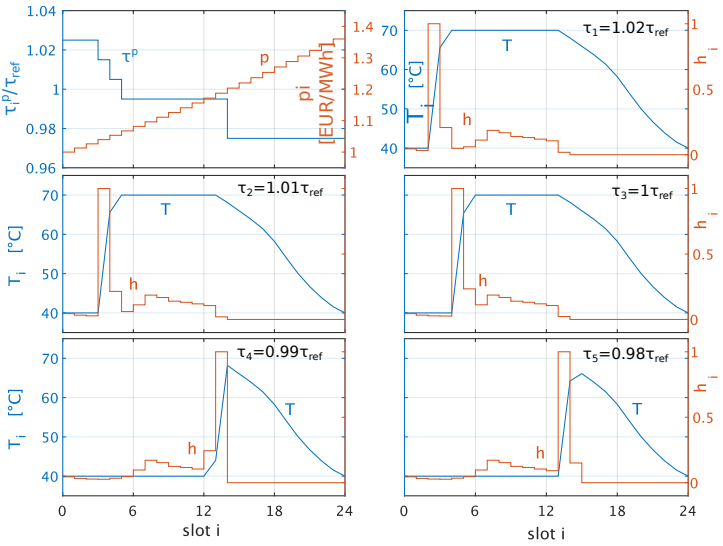

Figure 7.8: Peak distributing price for 5 DEWHs

total costs are highest for the DEWH with smallest τ, although this device spends the least time at high temperatures. However, the cost difference is small with about 1 %.

A generalized method can be developed for a large set of diverse DEWHs, which allows a higher resolution for selecting powered on devices per slot and thus different levels of the aggregated heating rate peaks to achieve more arbitrary profiles. With full knowledge of DEWH parameters and water demand, the peak values for each slot may be determined by considering the non-peak heating rates of all devices to reach the desired aggregated profile. Alternatively, it is also possible to induce multiple peaks of a single device by decreasing the slope at later slots, which enables more complex solutions with a less diverse set of DEWHs. However, the flexibility at the end of the planning horizon remains limited, because all devices intend to end at minimum temperature. This flexibility can be improved by extending the horizon at the end of the day, e.g. as receding horizon [MRRS00]. Later prices may be forecasted. Alternatively, prices of the next day may already be announced in the middle of the previous day. The permanently increasing price may be reset to a low price when all devices shall reach minimum temperature.

As all devices show different heating rates before and after a desired peak, constructing a direct method is challenging even with full knowledge. The procedure is further complicated when only statistical knowledge is given about device class distribution and hot water demands, as would be the case for more realistic applications.

7.3 Impact of τ-Prices on Cost-Optimal Heating Profiles

Creating price functions to induce an energy consumption following a target schedule requires understanding the impact of prices on the cost-optimal solution beyond inducing a single peak load per τ-cluster. This section describes the impact of the τ-price on the load profile of a DEWH which changes its target temperature and thus the heating state at certain times. Furthermore, it is explained how the heating rate is chosen in each individual hour, allowing to predict the total heating profile.

7.3.1 Changes of heating state

The effective price (4.1) is crucial for the heating decision of a DEWH. With a price defined by 7.8, the values of τ^p determine the heating states of all DEWHs in each slot.

If parameter τ_i^p is smaller or larger than the τ-value of the DEWH, the heating profile will deterministically either heat to the maximum or it will always maintain minimum temperature respectively. Preheating is always beneficial when prices are generated with $\tau_i^p < \tau$, as this leads to a monotonic increasing effective price, whereas $\tau_i^p > \tau$ leads to a monotonic decreasing effective price and thus prevents any preheating. Thus, the heating state H_i in slot i can be determined directly as shown in (7.9).

$$H_i = \begin{cases} \text{MAX} & \text{if } \tau_i^p < \tau \\ \text{MIN} & \text{if } \tau_i^p > \tau \\ \text{UNDEFINED} & \text{otherwise} \end{cases} \tag{7.9}$$

A change of the heating state from maintaining minimum $(H_i = \text{MIN})$ to heating to maximum temperature $(H_{i+1} = \text{MAX})$ leads to a local minimum in the effective price (4.1) and thus to a peak in the resulting heating profile as a rise from minimum to maximum temperature is required to fulfill the upcoming demand. Changing the

heating state from MAX to MIN generates a local maximum in the effective price, which stops the heating until the temperature reaches the minimum again.

7.3.2 Prediction of cost-optimal heating profiles

Price functions generated with (7.8) cause changes in the heating state H_i of a cost-optimizing DEWH depending on the temperature change rate τ, as discussed in the previous section. In order to induce an aggregated heating profile of many DEWHs, the impact of such state changes on the heating profile needs to be known in detail. This section extends the findings of Sec. 7.2, which only considered monotonic decreasing τ_i^p values to induce peak loads at certain times.

In principle, whenever the heating state changes, the DEWH will either start or stop preheating. Before the start of a preheating phase $(H_i = \text{MIN})$, the DEWH will heat as late as possible and thus heats the demand of the slot to maintain minimum temperature and only preheats when heating the full slot is insufficient. At the start of a preheating phase $(H_i = \text{MAX})$ the heating rate will be at a maximum level, e.g. heating the full slot $(h_i = 1)$. However, the actual heating rate depends on the maximum required temperature, which depends on the demand of later slots and also on later heating states as well as on the effective price (4.1).

The required temperature is selected such that the minimum temperature will be reached at the next local minimum effective price which is the start of next heating phase. When the maximum temperature is reached during the preheating phase, the temperature will be maintained until the effective price is below the next local minimum. Thus, any drawn energy will be restored by heating, similar to maintaining minimum temperature, but with higher standby losses. If the required temperature cannot be reached within a single slot, the heating rate will continue to be higher than the demand to reach the temperature. A different behavior occurs, if the effective price of the slot before the heating phase starts is below the price of the slot after the start $(p_{\text{eff},i-1} < p_{\text{eff},i+1})$. Then, the heating rate is selected such that the resulting temperature allows to reach the required temperature within the next slot.

Figure 7.9 shows an example LP solution for a price, which was generated to induce two changes from heating state MIN to MAX. The resulting heating and temperature profile is shown at the top and the selected τ^p as well as the resulting effective price at the bottom of the figure. The local minima of the effective prices are at slot 5, 16, and 24. At both state changes (first two minima), the heating rate is set to maximum value $(h = 1)$. A preheating before the state change occurs in both cases, as the preceding

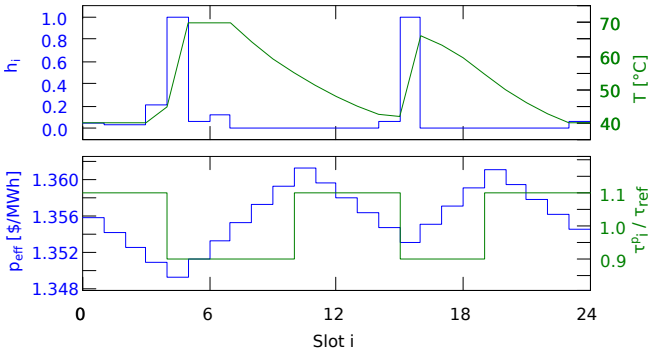

Figure 7.9: Example LP solution and effective price for price determined with (7.8) and τ^p to induce two peaks

effective price is slightly lower than the following price. The maximum temperature is maintained in slot 6 and 7 until it is sufficient to fulfill the energy demand until the next state change. The second preheating phase heats below the maximum allowed level and thus may turn off heating until the very last slot, where the effective price is slightly smaller than in slot 15 and thus the demanded energy will be restored by heating as it occurs to maintain minimum temperature.

7.4 Conclusion

The feasibility to use day-ahead pricing for controlling DEWHs to adapt their power consumption to a given profile was analyzed. The principle of optimal solutions of the bilevel problem formualtion considering a single DEWH was understood. The gained knowledge was then applied to many DEWHs.

The analysis of the bilevel optimization showed that the resulting price function is not reasonable to control the load of a single DEWH. With bilevel optimization, the solver selects a price function directly depending on the temperature change rate τ of the DEWH. This price function makes heating times irrelevant by compensating the costs for standby losses. Power consumptions were close to the desired profile, because the solver is then able to choose the desired heating profile from the many different solutions. Applying the same price function for a DEWH with different τ

leads to either heating as early or as late as possible and thus generates high peaks or does not shift consumption at all.

Exploiting this observation allows developing an approach for generating price functions that adapt the aggregated load of many DEWHs approximately to a desired profile, provided that the hot water demands and all parameters of all DEWHs are known. Therefore, the price function selects the number of DEWHs heating as much as possible at different times with appropriate price slopes to achieve a desired aggregated load profile. An iterative algorithm based on this approach is developed in the next chapter.

Chapter 8

τ-Price Heuristic Algorithm

This chapter* discusses the design of an algorithm that calculates a price function for a given target schedule based on the τ-price principle, such that a set of DEWHs consumes power approximately to the schedule. The algorithm is validated numerically by simulations. In a first step, perfect knowledge about every DEWH is assumed. In a second step this assumption is relaxed by only using statistics about clusters of many similar DEWHs, bringing the approach closer to practical application.

8.1 τ-Price Algorithm

Results from the previous chapter allow constructing an algorithm, which generates a price function that induces an aggregated heating profile of a known set of DEWHs following a target schedule $\hat{h}$. It exploits the effect that price functions resulting from (7.8) determine the heating state of a DEWH depending on the relation of the τ-value of the DEWH and of the prices. Thus, the solution space is reduced to prices corresponding to (7.8) and the decision variable p of the leader's problem is replaced with τ^p.

In principle the proposed Algorithm 4 utilizes a hill climbing approach by increasing or decreasing the number of DEWHs which are in the heating state MAX or MIN at each time slot i. The direction of change depends on whether the heating profile resulting from the current price is below or above the desired profile.

*Extension and revision of previous publication: Tobias Lübkert, Marcus Venzke, and Volker Turau. Calculating retail prices from demand response target schedules to operate domestic electric water heaters. *Energy Informatics*, 1(1):31, October 2018

Algorithm 4 τ-Price Algorithm

function FIND_PRICE($\hat{h}$)
  $\delta \leftarrow 0_{1,n}$ ▷ initialize vector for target error with zeros
  $\delta_{\text{last}} \leftarrow \infty_{1,n}$
  $\Gamma \leftarrow 0_{1,n}$
  while $\delta \neq \delta_{\text{last}}$ **do**
    $\delta_{\text{last}} \leftarrow \delta$
    for $i = 1$ to n **do**
      $\delta \leftarrow \text{ERROR}(\Gamma, \hat{h})$
      $\tilde{\Gamma} \leftarrow \Gamma$
      $\tilde{\Gamma}_i \leftarrow \tilde{\Gamma}_i + \text{SGN}(\delta_i)$ ▷ SGN(x): $\frac{x}{|x|}$ (sign of x)
      if $0 \leq \sum_{k=1}^{i} \tilde{\Gamma}_k \leq d$ **then**
        $\tilde{\Gamma} \leftarrow \text{APPLY\_PEAK\_BOUNDS}(\tilde{\Gamma})$
        $\delta_{\text{next}} \leftarrow \text{ERROR}(\tilde{\Gamma}, \hat{h})$
        if $\|\delta_{\text{next}}\| < \|\delta\| - \epsilon$ **then**
          $\delta \leftarrow \delta_{\text{next}}$
          $\Gamma \leftarrow \tilde{\Gamma}$
        end if
      end if
    end for
  end while
  return $\{\text{PRICE\_BY\_PEAK\_PLAN}(\Gamma),\ \Gamma\}$
end function
function PRICE_BY_PEAK_PLAN($\tilde{\Gamma}$)
  for $i = 1$ to n **do**
    $\tau_i^p \leftarrow \hat{\tau}_m - \frac{1}{2}\Delta\tau$ with $m = \sum_{j=1}^{i} \tilde{\Gamma}_j$
    $p_i \leftarrow$ compute with (7.8)
  end for
  return p
end function
function ERROR($\tilde{\Gamma}$, $\hat{h}$)
  $p \leftarrow \text{PRICE\_BY\_PEAK\_PLAN}(\tilde{\Gamma})$
  $h \leftarrow$ approximate heating profile(p)
  return $h - \hat{h}$
end function
function APPLY_PEAK_BOUNDS(Γ)
  $\theta_0 \leftarrow 0$
  $\theta_{1..n} \leftarrow \text{cumsum}(\Gamma)$
  for $i = 1$ to n **do**
    $\theta_i \leftarrow \max(0, \theta_i)$
    $\theta_i \leftarrow \min(d, \theta_i)$ ▷ limit to d, number of DEWHs
    $\tilde{\Gamma}_i \leftarrow \theta_i - \theta_{i-1}$
  end for
  return $\tilde{\Gamma}$
end function

As a change of the heating state at one time slot may impact the heating profile in a later or earlier slot, the algorithm iteratively tries to improve the aggregated profile and only considers changes that reduce the total error within the regarded horizon. The algorithm terminates when the error converges with respect to some precision ϵ (see lines 5 and 14). In Algorithm 4, planned state changes are represented by the peak plan vector Γ, which is initially zero for each slot and thus all DEWHs remain in heating state MIN. A positive value Γ_i will induce additional Γ_i DEWHs to change from MIN to MAX heating state in slot i, whereas a negative value will do the opposite. The sum of all Γ-values until time slot k thus determines the number of DEWHs which are in heating state MAX at that moment and must be positive at all time slots.

For each time slot in the horizon, the algorithm determines the total error resulting from the current peak plan Γ and adjusts the value at time slot i in the direction of the error at slot i (line 8–10). Because of the iterative approach, not only current bounds (line 11) but also the subsequent bounds have to be ensured (line 12). For this purpose, the cumulative sum of the peak plan is determined. The minimum and maximum number of devices is applied in each time slot and then converted back into the adjusted peak plan by taking the difference (see line 35–44). If the new resulting total error is below the previous achieved error, the adjusted peak plan $\tilde{\Gamma}$ is accepted or otherwise rejected (line 14–18). Incrementing the peak plan only by one step per time slot avoids an early depletion of flexibility, as once all DEWHs are in MAX heating state, the aggregated heating profile cannot be further increased in the following slots.

In order to determine the aggregated heating profile and the corresponding error (line 30–34) regarding the desired profile, the peak plan Γ is converted into a price vector p (line 23–29) which is applied to a method for approximating the resulting heating profile (line 32), e.g. by solving the LP for each DEWH or using some heuristic. The vector p results from applying vector τ^p to (7.8). The values τ_i^p are determined from the vector $\hat{\tau}$ containing the available values in descending order. To set m DEWHs into heating state MAX at slot i, τ_i^p is selected slightly smaller than $\hat{\tau}_m$ (line 25) such that all DEWHs of the cluster are affected but none of the next. The border values $\hat{\tau}_0$ and $\hat{\tau}_{d+1}$ are defined by some value significantly outside of the considered range of τ-values.

The available values within the vector $\hat{\tau}$ need to be unique, because otherwise an increment of Γ_i would have no effect. In practice, adjacent values must have an adequate minimum difference, due to a limited precision of LP solvers. Otherwise a τ^p value between two very close τ-values may induce an undefined behavior of two

DEWHs instead of changing the heating state to MIN or MAX. Thus, considering DEWHs with non-unique or similar τ-values leads to the effect, that incrementing Γ_i actually changes the heating states of multiple DEWHs.

Algorithm 2 creates a vector $\hat{\tau}$ regarding this limitation, given any vector $\tilde{\tau}$ of sorted τ-values of considered DEWHs and minimum difference of $\Delta\tau$. This is done by ignoring every $\tilde{\tau}_k$ which has a smaller difference to its preceding value. The drawback of this method is that the reduction may be unevenly distributed. This leads to a few larger gaps, were a change in the peak plan Γ changes the heating state of many DEWHs at once. However, an alternative approach, where instead of the difference to the previous value in $\tilde{\tau}$, the difference to the last value in $\hat{\tau}$ is considered, may again lead to the case that the selected τ^p is too close to the τ-value of a DEWH.

8.2 Evaluation for a Single Day

The performance of the proposed algorithm is assessed with a realistic setup of DEWHs for a fixed horizon of one day in this section as well as with a receding horizon over 6 days in the next section. The results are compared to alternative price scenarios of simple schemes, using constant or inverse proportional prices shown in Figure 6.3. For this purpose, the algorithm was implemented in Octave [EBHW17]. The follower's LP is solved using GLPK.

8.2.1 Scenario Configuration

The proposed algorithm requires a set of DEWHs with a sufficient diversity of τ-values in order to produce reasonable results. The hypothesis is that the existing DEWHs in German households fulfill this requirement. However, although only a limited range of volumes is available, the considered device base discussed in Sec. 3.4.1 shows that it is likely to have an adequate distribution of clustered τ-values for DEWHs on the market. This allows concluding that the existing DEWHs in Germany fulfill the requirement of a sufficient diversity in their τ-values.

Two scenarios are evaluated in this section, both consider the DEWH and demand configuration as described in Sec. 6.2.4, including all 50 clusters. The first scenario uses the same target schedule and the second uses the target schedule of Sec. 7.1.1. The algorithm terminates when no further reduction of the error is possible ($\epsilon = 0$).

8.2.2 Numerical Results

With the prices generated by the proposed algorithm, the aggregated energy consumption follows the desired shape of the availability profile in both scenarios. The energy consumption is shown in Fig. 8.1(a), with the aggregated heating profiles (target schedule and LP solution) at the top and the resulting p with corresponding τ^p at the bottom. The individual heating profiles h_k of all considered DEWHs are shown in a heat map in Fig. 8.1(b) and the error reduction per iteration is shown in Fig. 8.1(c).

The algorithm terminates after 5 iterations. The root-mean-square deviation (RMSD) is reduced from about 84 to 21. The resulting MAPE (M) reaches 11 % related to $\hat{h}$ with (3.4), which is a significantly improvement compared to an MAPE of 53 % for constant and 109 % for inverse proportional prices p_{inv}. The resulting total load is 5 % below the target schedule.

During the first five hours of the day, the algorithm increases the energy consumption following the increasing availability by changing τ^p such that in each hour a few DEWHs change to heating state MAX. As the DEWHs have different volumes and water demand, the resulting consumption peaks differ in length and height. As the load of the remaining DEWHs increases from slot six, the algorithm increases τ^p again. As a result, some DEWHs rely on preheated water without need for further heating. Others continue heating to maintain either minimum or maximum temperature.

More devices are added to the peak plan after the high water demand in the morning at slot 10, because the target schedule remains high and still increases slightly. The resulting load peaks are shorter and preheat the total remaining demand of those DEWHs. Thus, the total load decreases with the target schedule while more devices change to the heating state MAX.

The largest remaining error occurs at slot eight, where the load is higher than desired. Although the load could be increased in the time before to improve the error locally, any single change of the peak plan leads to a worse total error.

The algorithm achieves a similar total error reduction for the other example, but requires three times the number of iterations. The target schedule increases with a greater slope, which leads to a smaller error in the first ten slots. The schedule decreases earlier allowing more devices to stay in heating state MAX, as they do not require additional heating. The example availability increases again in the afternoon, where more devices are added to the peak plan. They stop heating shortly after, as the maximum temperature now is sufficient to serve the remaining demand of the

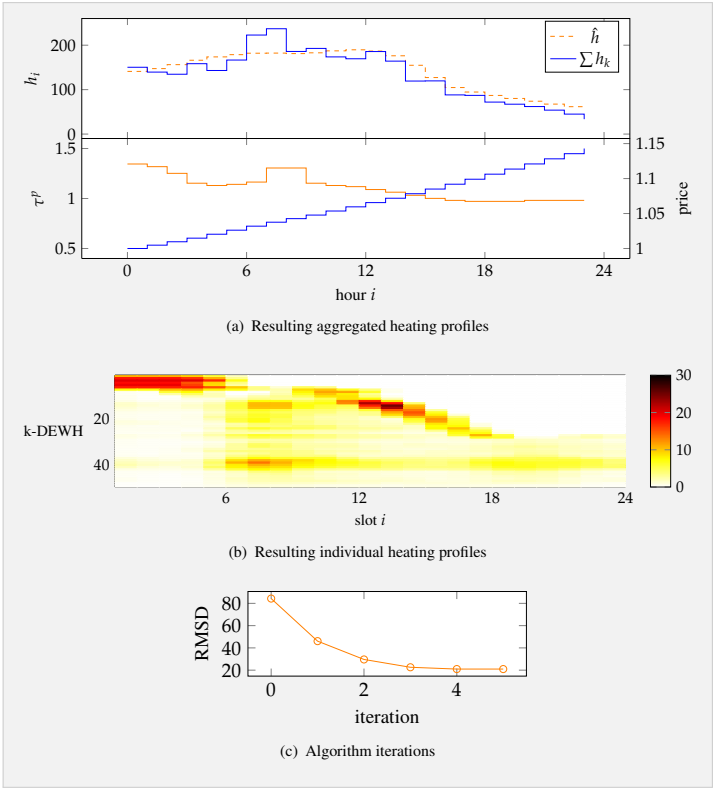

(a) Resulting aggregated heating profiles

(b) Resulting individual heating profiles

(c) Algorithm iterations

Figure 8.1: Results for τ-price with fixed 1-day horizon and virtual power availability

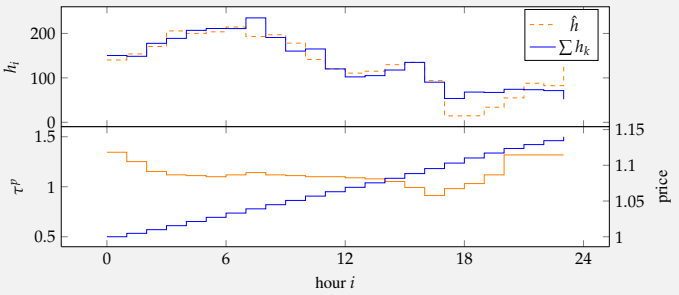

(a) Resulting aggregated heating profiles

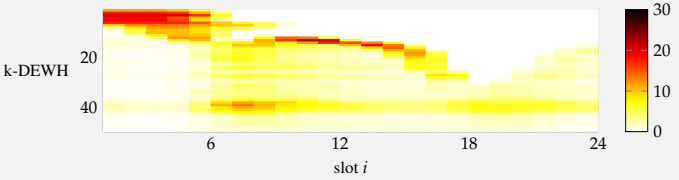

(b) Resulting individual heating profiles

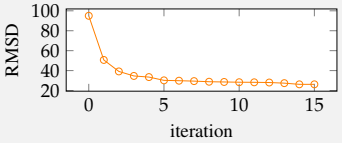

(c) Algorithm iterations

Figure 8.2: Results for τ-price with fixed 1-day horizon and virtual power availability

day. Afterwards, the availability quickly drops to a minimum value in slot 18 and the algorithm increases τ^p accordingly. However, the aggregated consumption cannot be reduced sufficiently, because many devices did not preheat and still require to heat to satisfy the demand.

The largest errors occur at the end of the horizon, as the target schedule increases. The algorithms fails to increase the energy consumption, as there is no remaining demand to preheat and it is always optimal to finish at minimum temperature. In order to increase the flexibility and include the demand of the next day, a receding horizon can be used. This is done in the next section by sending new prices for the next day during the current day.

In both scenarios about half of the DEWHs remain in heating state MIN all the time. These have the smallest considered τ-values, due to smaller volumes or a less efficient insulation. With an average heating duration of 3.5 h, the total energy demand is lower than in the scenario using exchange prices or constant prices when maintaining medium temperature. Although DEWHs with better insulation or larger volume preheat to higher temperatures, they still have lower operational costs for the same energy demand. The average price paid for consumed hot water energy (3.2) increases monotonically with τ. The DEWH having the largest τ-value has to pay about 1.14 EUR/MWh, whereas the smallest τ-value leads to costs of 1.39 EUR/MWh in relation to the arbitrary reference price p_{ref}.

At most times of the day, the resulting heating profile follows the availability favorable in both cases, except at slot eight or the end of the horizon. Although an increase or decrease of the peak plan Γ could reduce the local error, it would not reduce but increase the total error. However, it is possible to find a combination of increase and later decrease which would improve the total error. Thus, results could be further improved by a more complex post-optimization method, e.g. selecting multiple slots to be changed at once or using a recursive approach which first reduces the local error and then tries to find an additional change of the peak plan to reduce the total error again. Alternatively, only the local error could be considered to modify the peak plan, which may lead to better results for the first part, but much higher errors at the end of the day. In combination with a receding horizon, this still can lead to better results, but requires some mechanism to ensure convergence. Further alternatives are using a more sophisticated logic, e.g. modifying Γ around minimum and maximum error in one step, or a general heuristic optimization method like genetic algorithm or particle swarm optimization.

8.3 Improvements

The results from the previous section suggest that further improvement can be achieved by a second-stage, which changes multiple entries of the peak plan at once. Additionally, a receding horizon can improve the ability of the proposed algorithm to reduce the error at the end of a day, as the water demand of the next day can be considered for further preheating. Otherwise, all DEWHs will always end at minimum temperature at the same time, independent of the desired heating profile. However, by introducing a receding horizon, the prices would continue increasing exponentially, which is impractical as customers would not accept such prices. Thus, the price needs to be reset to a lower value after some time.

8.3.1 Second Stage Max-to-Min

The evaluation of the first example scenario shown in Fig. 8.1(a) allows the assumption that the resulting error can be further reduced by increasing the peak plan before the maximum error at slot eight. However, any single slot change of the peak plan would lead to a worse total error. Thus, a combination of at least two peak plan changes has to be considered.

Algorithm 5 iteratively changes two values of the peak plan. In principle, it tries to shift the load of the maximum error to the preceding minimum error. In a first step the slot indices of maximum and minimum error are determined (line 6–7), then the peak plan is increased at the maximum and decreased at the minimum. The peak plan bounds are applied as defined in Algorithm 4 line 35. This step is repeated until the error cannot be reduced further. As the peak plan may differ significantly afterwards, single slot changes are evaluated in a second step. Here, increase and decrease of the peak plan are evaluated separately. The procedure also ends when no further improvement is achieved.

The resulting load profile after applying Algorithm 5 is shown in Fig. 8.3. The maximum error of slot seven and eight is reduced successfully, by increasing the load before, which also reduces the local error at that time. The total RMSD is reduced by 3.4 % from 21 to 18.

Further constructed scenarios are shown in Fig. 8.4 considering basic shapes as target schedule. The only shape which cannot be improved by the second stage algorithm is a linear decreasing function (bottom left), which can be approximated with a RMSD of 16.4 in 13 iterations. The worst scenario is the opposite, a linear

Algorithm 5 τ-Price Heuristic Second Stage

```
1:  function PEAK_PLAN_MAX2MIN(Γ, ĥ, joint_inc_dec)
2:      δ_last ← ∞
3:      δ ← ERROR(Γ, ĥ)
4:      while δ ≤ δ_last − ε do
5:          δ_last ← δ
6:          i_− ← arg max δ_{1..n}
7:          i_+ ← arg min δ_{1..i_−}
8:          if joint_inc_dec then
9:              increase Γ_{i_+}, decrease Γ_{i_−}, apply bounds
10:             reset Γ if ERROR(Γ, ĥ) > δ
11:         else
12:             increase Γ_{i_+}, apply bounds and reset unless error reduced
13:             decrease Γ_{i_−}, apply bounds and reset unless error reduced
14:         end if
15:         δ ← ERROR(Γ, ĥ)
16:     end while
17:     return Γ
18: end function

19: function PEAK_PLAN_IMPROVE(Γ, ĥ)
20:     Γ ← PEAK_PLAN_MAX2MIN(Γ, ĥ, True)
21:     return PEAK_PLAN_MAX2MIN(Γ, ĥ, False)
22: end function
```

increasing target schedule (top left), where the second stage helps improving the error, but still leads to a high RMSD of 88. Similarly hard scenarios are a inverse triangle (bottom right) or a random schedule (middle right), both leading to a RMSD of about 62. It is impossible to increase the load at the end of the horizon and the algorithm cannot find a peak plan which induces two near peaks at noon, although the second stage helps to better fit the random peaks and valleys before. The other two scenarios, constant flat (middle left) and triangle (top right), achieve a similar RMSD of about 36. In both cases the second stage is beneficial. The flat schedule requires the most execution time in the first stage which stops after 35 iterations.

8.3.2 Receding Horizon and Price Reset

A receding horizon is implemented by calculating a new price vector for the next horizon and replacing the remaining prices of the current horizon. For example, 36 prices are broadcasted every 24 hours, which continue from the previous value. To

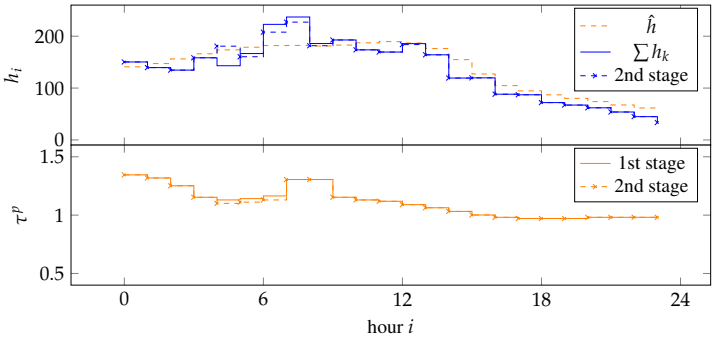

Figure 8.3: Second stage improvement

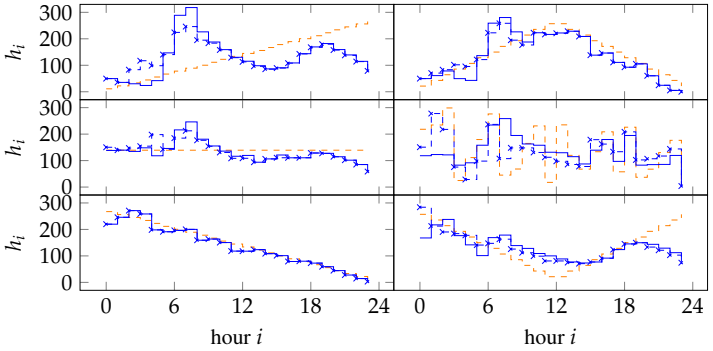

Figure 8.4: Limitations of target schedules

prevent an infinite increase of the price, a reset has to be included within the horizon. A fixed price reset hinders the benefit of a receding horizon, as again all DEWHs will end at minimum temperature at that time. However, the moment of the reset can be selected such that its impact on the resulting heating profile is small or even beneficial. Because the price reset causes the same behavior as the end of the scheduling horizon, the price finding problem can be split into two independent horizons before and after the reset. Algorithm 6 utilizes this effect to calculate a price including a reset to a lower value.

After determining the price for the whole horizon, the time slot r is selected to reset

the price afterwards. A reasonable time to reset the price is where most DEWHs are either in heating state MIN or finished preheating and thus the cumulative peak plan is at a local minimum level. However, the reset must occur before the start of the next horizon, as otherwise it could be removed again. Alternatively, the reset needs to be enforced in the next schedule. Algorithm 6 selects several candidate reset points $\hat{r}$ and in the next step determines the price again as a combination of two computed price functions for consecutive sub-horizons. The first sub-horizon ends at slot $r+1$ and the second starts at $r+2$.

An exhaustive search ($\hat{r} = \{1 \dots n\}$) for an example receding horizon for a RES availability of 30 days (01–30 Jan. 2018) has shown that the best reset option is most likely either at a local minimum or in an adjacent slot. When testing only those candidate solutions, the search space is reduced from 24 to 9.5 on average. Fig. 8.5 shows three sample peak plans (cumulative sum), the reset candidates and the actual best reset index. The optimum reset point of these scenarios are at the global minimum (top left), in the slot after (top right), or within the second lowest local minimum (bottom left). However, further studies have to be performed to ensure that the best reset position is always included in $\hat{r}$. The distribution of all 30 best reset indices is shown in the bottom right figure. Most optimal resets are found around slot 21–23 or at slot 12. Prices are updated every day at noon (12 p.m.) covering a horizon of 36 hours until midnight, thus a price reset at slot 24 is the last slot before the next update.

Algorithm 6 τ-Price Heuristic with price reset

$\Gamma \leftarrow$ FIND_PRICE($\hat{h}$)
$\hat{r} \leftarrow$ indices around local minima of cumulative sum of Γ
for $r \in \hat{r}$ **do**
  $\hat{p}_{1..r+1} \leftarrow$ FIND_PRICE($\hat{h}_{1..r+1}$)
  $\hat{p}_{r+2..n} \leftarrow$ FIND_PRICE($\hat{h}_{r+2..n}$)
  $p \leftarrow \hat{p}$ if minimum error
end for

The results for a receding horizon with and without price reset are shown in Fig. 8.6(a) and Fig. 8.6(b), both considering power availability from January 1 to 6 respectively. The aggregated heating profile follows the shape of the availability in both cases. The target schedule includes significant jumps (e.g. at slot 48, 72, or 120), because the total availability of RES is different for each day, but gets scaled to the expected demand of all DEWHs, which remains about the same. Only the upcoming

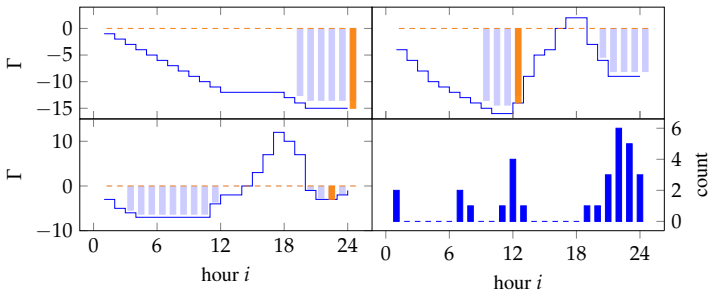

Figure 8.5: Price reset positions of exhaustive search

availability is re-scaled, the remaining 12 slots of the previous target schedule remain unchanged.

However, there are some noticeable errors in both cases. Without a price reset, the algorithm fails to induce increasing or flat shapes. The most significant errors occur around slot 24. Here the receding horizon is actually not beneficial, as the target schedule of that horizon is increasing for most of the time until the end. Although it is possible to reduce this error, the proposed second stage is not sufficient, as more complex modifications are required, e.g. more than two changes at once. The large errors around slot 24, but also later errors (e.g. around slot 60 and 84) are significantly reduced by introducing a price reset. However, it also introduces new errors mostly close to the reset, e.g. at slot 120. The overall M is reduced from 17.8 % to 12.1 %. Selecting the best reset time is crucial, as e.g. using a fixed price reset at slot 12 or 24 leads to M of 18.8 % or 21.8 % respectively. In any case, the calculated prices achieve significantly better results than a flat price $(M = 54.6\,\%)$ or inverse proportional prices $(M = 130\,\%)$.

The price resets often occur close to an increase of the target schedule. A period starting with high availability followed by a decreasing target leads the algorithm to select more devices to create peaks and remain in MAX heating state. This increases the overall energy demand and also the maximum price, as the price gradient needs to be steeper for DEWHs with smaller τ-values. Due to the price reset, the maximum price difference is about 20 % for the considered DEWH setup.

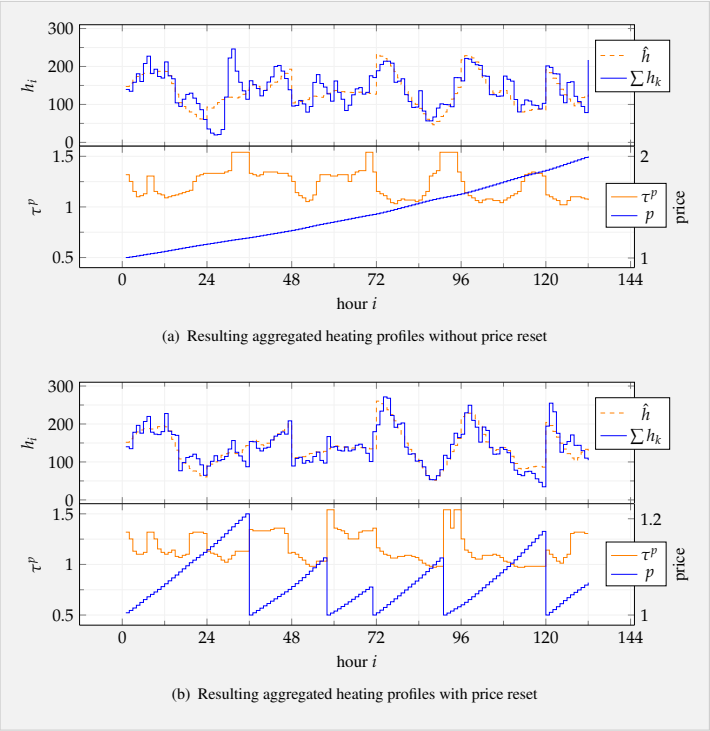

(a) Resulting aggregated heating profiles without price reset

(b) Resulting aggregated heating profiles with price reset

Figure 8.6: Results for τ-price with receding horizon for Jan. 1–6

8.4 Average Optimization Model vs. Statistical Behavior

In the previous sections the behavior of a set of known DEWHs was analyzed. However, in practice, each DEWH considered for price construction would represent the average behavior of a group of similar DEWHs for which only a stochastic water demand profile is known. In order to assess the applicability of this approach, a Monte-Carlo simulation as well as an event-based simulation with real measurement data is conducted to analyze the additional error due to a variance of the water consumption patterns.

8.4.1 Monte-Carlo analysis

To understand the effect of an averaged cluster model, 1000 optimal heating profiles are calculated for a single DEWH cluster with a volume of $V = 65\,\mathrm{l}$ considering different water demand profiles. The total water demand is randomly chosen with $2V \cdot f_N$ [l at $T_{\min}$], where f_N is normally distributed with mean $\mu = 1$ and standard deviation $\sigma = 0.25$. The total demand is distributed into 10 randomly chosen slots regarding the average profile. Figure 8.7(a) shows three example profiles on the left and a histogram of the total demand on the right.

The results of the previous section have shown that the most common individual heating profiles include a single pre-heating at beginning, two pre-heating phases, or maintaining minimum temperature during all slots of the horizon. The resulting heating profiles of the Monte Carlo simulation for these three scenarios are shown in Figure 8.7. In the case of maintaining minimum temperature (Fig. 8.7(b)), the average of all heating profiles is equal to the result of the average optimization model. Only small deviations occur, due to the randomization. Thus, in the considered scenario of the previous section, about 10 %–50 % of the profiles can be considered as correct.

In the other two cases slightly larger deviations occur. In the case of continuous heating to maximum temperature (Fig. 8.7(c)) both results begin with a similar profile, but differ at the end. This is because, some of the consumption patterns have a focus in the morning, which allows to turn off heating earlier. Others have a major consumption in the evening, which still requires some heating at later times. In total the resulting profiles differ from the average model by stretching the demand in the second part of the day, which causes a shortfall first and then a surplus. In the case of a second pre-heating peak in the afternoon (Fig. 8.7(d)), this leads to significant reduction of the peak height and a low additional load before and after the peak. The first pre-heating peak remains equal to the average model, but also distributes the demand afterwards into the time between both peaks.

Overall, the resulting heating profiles from the average optimization model are a good estimate of many different optimized profiles. Especially the first part of the horizon fits well, but at later slots additional errors are introduced as the energy consumption is higher than expected at times where it is intended to be reduced.

Deviations in volume or heat conductivity would lead to a different τ-value and thus are crucial, as this would change the number of devices considered for a cluster in the averaged model. Different temperature ranges have an impact on the peak height as DEWHs may either heat more or less in a time slot, which reduces the main peak,

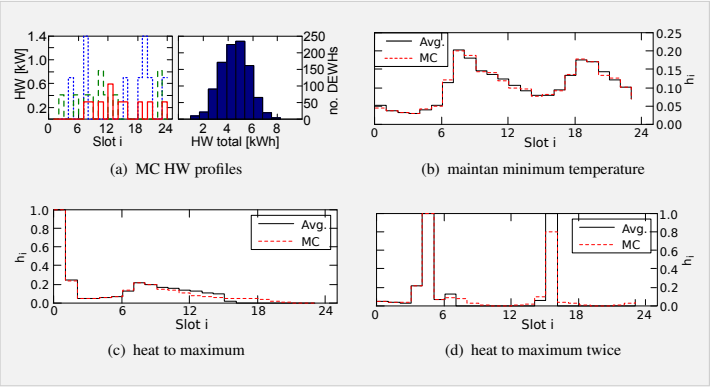

(a) MC HW profiles (b) maintan minimum temperature

(c) heat to maximum (d) heat to maximum twice

Figure 8.7: Comparison of averaged optimization and Monte Carlo simulation

but increases the consumption before the peak. The rated power has a similar impact, as some devices require more time to heat the same amount of energy. However, in practice rated power is restricted to a few common discrete values.

8.4.2 Real water consumption profiles

In practice, additional deviations from the average optimization model are to be expected, as the actual water demand may differ significantly from the expected profile used for determining the optimal heating schedule. The impact of real water demand profiles is analyzed in this section by an event-based simulation using the real water usage data described in Sec. 3.4.2. The dataset contains 893 DEWHs which optimize their heating decisions as described in Sec. 4.2 with continuous updates. The optimization considers the individual mean water demand profile of each household and the given fixed price information resulting from Sec. 8.3.1. Although the average cluster size of 18 DEWHs is too small to reproduce the expected average profile of each cluster, it allows to identify systematical errors.

The total load of all DEWHs still approximates the target schedule as shown in Fig. 8.8 (sim-24n). However, it deviates significantly from the expected load profile (cl-50d) obtained by the average optimization model with a MAPE of 14 %. The total load is about 7.5 % higher than expected, although the mean temperature of 43.4 °C is about 20 % lower than expected.

The largest errors occur at the end, where the load was expected to decrease steeper, but also at slot seven, where it increases less than expected. These deviations cannot be explained sufficiently by different average profiles used by each device of a cluster, as the aggregation of all individual LP solutions is much closer to the clustered profile (see Fig. 8.8, cl-893d and cl-50d).

The main reason for the additional errors are significant deviations of the actual water demand and the expected average profile. The demand may occur at other times or the total daily demand may be higher or lower. As shown in Fig. 8.9, this may lead to significant errors in both MAX heating and MIN heating states. Fig. 8.9(a) shows a problematic cluster with 13 DEWHs, which creates two separate peak loads. The expected load profile of the averaged cluster model deviates from the event-based simulation with a MAPE of about 75 %. The aggregation of all individual profiles reduces the error to 40 %, as the peak loads are decreased and some demand is shifted next to the peaks.

Some profiles are close to the expected behavior, others differ significantly as shown by the four individual profiles of Fig. 8.9(b). The profile on the top left shows a good match for the first peak, but a small deviation occurs before, because of the thermostat heating 1 °C to maintain the minimum temperature. The second peak shows higher deviation, as the demand was higher than expected before the planned peak and delayed afterwards. The bottom left profile shows even smaller deviation, as the demand is only slightly higher or lower than expected for the first and second peak respectively. Both profiles on the right show a significant deviation of the expected water demand, it occurs either too early (top) or too late (bottom), which reduces the desired peak and adds load where it was not intended.

The total demand is higher than expected, as some DEWHs have to restore the minimum temperature after higher water demands and DEWHs with lower demand preheated for the expected profile. Thus, the mean temperature of all devices is higher than expected with about 42.5 °C. A deviation of the end temperature also impacts the behavior of the next horizon as it lowers the initial preheating capability.

A DEWH heats with a fixed rated power and does not always fully utilize a time slot for heating, but stops before the end of the slot if the required temperature is reached. This can lead to higher load deviations within a time slot as shown in Fig. 8.8 (sim-192n) using eight samples per hour. In the example scenario, this leads to unintended load peaks caused by DEWHs which synchronously start heating at the beginning of a slot and stop after different duration. To reduce this effect, DEWHs

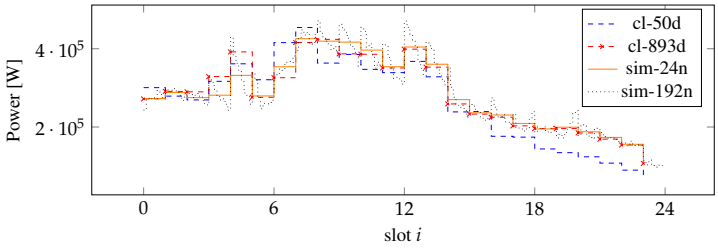

Figure 8.8: Event-based simulation compared to averaged cluster model

either need to randomly distribute their power consumption voluntarily or the number of prices per day can be increased, e.g. every 15 minutes.

8.5 Discussion

With the proposed algorithm, prices increase exponentially with a single reset to a minimum value per day. This successfully shapes the energy consumption of many DEWHs. However, it is unclear if the prices generated by the algorithm are applicable in practice.

Customers might accept such prices. They lower the operating costs of the DEWHs. The ratio between maximum and minimum price is only about 20 %, which is far less compared to other approaches, e.g. using IBR can lead up to a price ratio of roughly 400 % as in [HSW17]. Furthermore, prices are similar every day and change very little between the hours.

However, the same price function needs to be applied for many different appliances, unless each DEWH has its own electricity meter. In most households with a single meter measuring the entire household consumption, sending different prices to individual appliances is unrealistic. The integration of price insensitive loads (e.g. cooking, lights, multimedia) is still not a problem, as these behave the same for any price function. Its consumption can be forecasted as common today and subtracted from the target schedule. A bigger issue is the integration of cost optimizing shiftable loads (e.g. washing machines, dryer, charging electric vehicles). These devices will run as early as possible after the price reset to exploit the lowest prices.

The effort for integrating other TCL may be low due to their similar thermal model. In fact, the proposed algorithm only requires that TCLs know their τ-value and

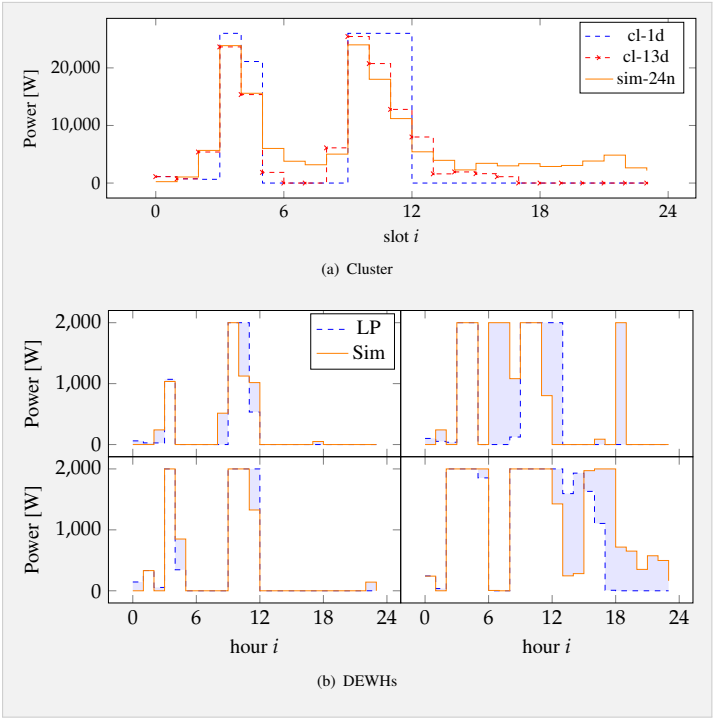

Figure 8.9: Comparison of averaged optimization and real water draw event simulation

optimally minimize their operational costs according to it. Devices with smaller τ-values than DEWHs (e.g. waterbeds [VT15]) are less likely selected for preheating, as first all DEWHs and devices with larger τ-values have to be in MAX heating state. However, if the loads use a different control mechanism, not fully optimizing for lowest costs, the resulting total consumption is different and deviates from the target schedule. Thus, loads may react with undesirable behavior, e.g. causing synchronized load peaks at lowest prices.

The major challenge with non-DEWH-loads is likely to occur around the price reset. Even though this point in time is selected to have low effect on the consumption of DEWHs, other loads will react on this large price change. Their consumption will

be low before and large after the reset. In many cases this prevents following a given target schedule, even though DEWHs account for a large part of the domestic energy demand.

8.6 Conclusion

In this chapter an algorithm was developed that constructs a price function from a target schedule to shape the load of many DEWHs such that they approximately consume power according to the schedule. With the setup used for validation, prices vary by about 20 %. Prices increase exponentially but can be reset to some smaller value in the late evening or at noon. Selecting the time of the price reset carefully is beneficial for the overall performance and leads to better results compared to not using a price reset.

The prices can be used for a realistic case of clusters consisting of many similar DEWHs only described by statistics. However, this leads to deviation from the expected behavior, as DEWHs of one cluster optimize according to different water demand profiles. Further deviation occurs due to the difference of expected and actual water demand. Additionally, the load within a time slot is not constant but decreases.

Chapter 9

Conclusion and Outlook

An increasing share of renewable energy sources (RES) complicates the process of balancing power supply and demand, as the energy generation becomes more uncertain. Beside expensive energy storage systems, the development of a Smart Grid helps to maintain a stable power grid. In particular demand response (DR) programs allow to change the power consumption of consumers such that the utilization of RES availability is improved. A possible approach is to send time-varying electricity prices to smart appliances some time ahead, e.g. a day before, which allows scheduling the power consumption such that the electricity costs are reduced. Thermostatically controllable loads (TCLs) and in particular domestic electric water heaters (DEWHs) can make a significant contribution to DR programs, as their thermal energy storage allows to shift a large part of today's domestic electricity demand. Price functions, such as day-ahead real-time pricing (RTP) (DA-RTP), are known to lead to load synchronization if appliances autonomously optimize their electricity payments.

This dissertation developed a novel approach allowing to shape the aggregated load of many TCL using DA-RTP. The energy supplier constructs a price function based on statistical knowledge about all customers' TCLs and broadcasts the price. Each TCL autonomously determines a cost-optimal heating schedule regarding the received price and controls the heating element accordingly. As the supplier's and the customers' optimization problems are interdependent, the cost-optimal behavior of the TCLs was studied in detail first.

An application specific scheduling algorithm was developed as alternative to a generic linear program (LP) solver, as it is promising to have much smaller resource requirements, which is favorable for the implementation embedded in the target device.

The algorithm results from applying several improvements to a previously published algorithm. A simulative analysis showed a doubling of cost-savings. Furthermore, it was shown empirically, that the resulting schedules are close to optimal solutions.

When assessing the performance of DR methods, it is important to ensure that the consumer comfort is respected, as otherwise achieved DR effects are unreasonable. A parameter study has shown, that the most important factors impacting the DR effect are the control horizon and the allowed temperature range as well as the volume. The comfort can be increased by a higher minimum temperature or a larger volume. Whereat changing the temperature is simple, it is also less efficient as only a larger volume improves the DR effect and also less increases the standby loss. Furthermore, a better insulated DEWHs benefits more from a DR program, as a higher energy efficiency allows longer duration between preheating and demand.

The goal of the supplier to shape the load of many TCLs finding a suitable DA-RTP signal was formulated as bilevel optimization problem. It was shown that optimal solutions can practically only be found for very small scenarios, e.g. for about six time slots or 5 appliances. Furthermore, a satisfying heuristic solution is also hardly found. Particle swarm optimization (PSO) did not find any solution which is significantly better than a constant price, because many prices either lead to the same load profile as a constant price or cause load peaks resulting in higher errors.

However, analyzing the optimal result for a single or a few TCLs allowed to construct a principle for prices which exploits the diversity of storage efficiency for many TCLs. It was understood that an exponentially increasing price can either compensate the storage efficiency of a TCL (which makes the time of heating irrelevant) or it forces heating as early or as late as possible. The slope of the price determines the heating state of the appliances and is directly related to its temperature change rate τ, the ratio of volume and heat conductivity. Changing the slope from one time slot to another also changes the heating state of effected TCLs. This effect allows to distribute load peaks of different devices to different times.

Based on the found principle an algorithm was developed, which constructs a price function for shaping the load of many TCLs to approximately match a target schedule. Several similar appliances are statistically modeled in clusters represented by an average optimization problem. The algorithm iteratively changes the slope regarding τ-values of the known clusters. Prices are updated once per day before the end of the current horizon, allowing to incorporate of the next day. As prices increase exponentially, the price function needs to be reset, e.g. once per day. Within the considered example scenario the price reset was actually beneficial as it reduced the

total error to about 12 % compared to not resetting the price (18 %) or a constant price (55 %). The maximum price variation was about 20 %. Simulating many real water demand profiles showed that the load approximates the target schedule. However, it also showed a deviation of the expected average cluster profile in particular to the end of the horizon with a decreasing load.

Future work should investigate efficient methods to improve the precision of the average cluster model, e.g. using Monte-Carlo simulation. Also, additional improvements of the algorithm are imaginable, e.g. different post-optimization steps. Furthermore, the practical applicability should be studied in further detail. An inventory analysis mapping actual TCL to their location in the power grid would help to find out whether the diversity of TCLs is also sufficiently distributed to also ensure stability of low voltage grids and transformers. A higher quantity of real measurement data is also required to have a sufficient data basis to evaluate the precision of an averaged cluster model. Another open question is, whether it is reasonable to integrate other smart appliances – especially non-TCL – to be used with the same price signal or if separate metering for TCLs is a cost-effective alternative.

Bibliography

[AC14] M. Arora and S. Chanana. Residential demand response from PV panel and energy storage device. In *2014 IEEE 6th India International Conference on Power Electronics (IICPE)*, pages 1–6, December 2014.

[AjXY+17] Khalid Al-jabery, Zhezhao Xu, Wenjian Yu, Donald C. Wunsch, Jinjun Xiong, and Yiyu Shi. Demand-Side Management of Domestic Electric Water Heaters Using Approximate Dynamic Programming. *IEEE Transactions on Computer-Aided Design of Integrated Circuits and Systems*, 36(5):775–788, May 2017.

[BOA13] T. Borsche, F. Oldewurtel, and G. Andersson. Minimizing communication cost for demand response using state estimation. In *PowerTech (POWERTECH), 2013 IEEE Grenoble*, pages 1–6, June 2013.

[Bor05] Severin Borenstein. The long-run efficiency of real-time electricity pricing. *The Energy Journal*, 26(3):93–116, 2005.

[CAS13] Tsung-Hui Chang, Mahnoosh Alizadeh, and Anna Scaglione. Real-Time Power Balancing Via Decentralized Coordinated Home Energy Scheduling. *IEEE Transactions on Smart Grid*, 4(3):1490–1504, September 2013.

[CL12] Adela Conchado and Pedro Linares. *Handbook of Networks in Power Systems I*, chapter The Economic Impact of Demand-Response Programs on Power Systems. A Survey of the State of the Art, pages 281–301. Springer Berlin Heidelberg, Berlin, Heidelberg, 2012.

[Dem02] S Dempe. *Nonconvex Optimization and Its Applications - Foundations of Bilevel Programming*. Kluwer Academic Publisher, Dordrecht, 2002.

[Dep08] Department for Environment, Food and Rural Affairs (Defra). Measurement of Domestic Hot Water Consumption in Dwellings. Technical report, Department for Environment, Food and Rural Affairs (Defra), 2008.

[Dev86] Luc Devroye. *Non-uniform random variate generation*. Springer, New York, 1986. OCLC: 13269466.

[dJufV] Bundesministerium der Justiz und für Verbraucherschutz. Erneuerbare-energien-gesetz vom 21. juli 2014 (bgbl. i s. 1066), das zuletzt durch artikel 1 des gesetzes vom 17. juli 2017 (bgbl. i s. 2532) geändert worden ist.

[DKPVK15] Stephan Dempe, Vyacheslav Kalashnikov, Gerardo A. Pérez-Valdés, and Nataliya Kalashnykova. *Bilevel Programming Problems*. Energy Systems. Springer Berlin Heidelberg, Berlin, Heidelberg, 2015.

[DL11] Pengwei Du and Ning Lu. Appliance Commitment for Household Load Scheduling. *IEEE Transactions on Smart Grid*, 2(2):411–419, June 2011.

[DLE+12] R. Diao, S. Lu, M. Elizondo, E. Mayhorn, Y. Zhang, and N. Samaan. Electric water heater modeling and control strategies for demand response. In *2012 IEEE Power and Energy Society General Meeting*, pages 1–8, July 2012.

[DMD+16] William B DeOreo, Peter W Mayer, Benedykt Dziegielewski, Jack Kiefer, and Water Research Foundation. *Residential end uses of water, version 2: executive report*. Water Research Foundation, 2016. OCLC: 953583940.

[DOE06] DOE. Benefits of demand response in electricity markets and recommendations for achieving them. Technical report, U. S. Department of Energy, 2006.

[EBHW17] John W. Eaton, David Bateman, Søren Hauberg, and Rik Wehbring. *GNU Octave version 4.2.1 manual: a high-level interactive language for numerical computations*, 2017.

[EHT17] EHT Haustechnik GmbH / Markenvertrieb AEG. Warmwassergeräte wandspeicher. `https://www.aeg-haustechnik.de/de/home/produkte-loesungen/warmwassergeraete/wandspeicher.html`, 2017. [Online; accessed 14-Dec-2017].

[EK16] B. Priya Esther and K. Sathish Kumar. A survey on residential Demand Side Management architecture, approaches, optimization models and methods. *Renewable and Sustainable Energy Reviews*, 59:342–351, June 2016.

[ES18] Agora Energiewende and Sandbag. The european power sector in 2017. state of affairs and review of current developments. `https://www.agora-energiewende.de/fileadmin2/Projekte/2018/EU_Jahresrueckblick_2017/Agora_EU-report`, 2018.

[FMXY12] Xi Fang, Satyajayant Misra, Guoliang Xue, and Dejun Yang. Smart Grid — The New and Improved Power Grid: A Survey. *IEEE Communications Surveys & Tutorials*, 14(4):944–980, 2012.

[FSUS07] José Fernández-Seara, Francisco J. Uhía, and Jaime Sieres. Experimental analysis of a domestic electric hot water storage tank. Part II: dynamic mode of operation. *Applied Thermal Engineering*, 27(1):137–144, January 2007.

[fSuWFBWH] Zentrum für Sonnenenergie-und Wasserstoff-Forschung Baden-Württemberg and Umweltbundesamt (Hrsg.). Erneuerbare energien in deutschland – daten zur entwicklung im jahr 2017. `https://www.umweltbundesamt.de/sites/default/files/medien/376/publikationen/180315_uba_hg_eeinzahlen_2018_bf.pdf`.

[GA04] Chong Hock K Goh and Jay Apt. Consumer Strategies for Controlling Electric Water Heaters under Dynamic Pricing. In *Carnegie Mellon Electricity Industry Center Working Paper*, 2004.

[GGSW17] Sebastian Gottwalt, Johannes Garttner, Hartmut Schmeck, and Christof Weinhardt. Modeling and Valuation of Residential Demand Flexibility for Renewable Energy Integration. *IEEE Transactions on Smart Grid*, 8(6):2565–2574, November 2017.

[Gil16] Hans Christian Gils. *Balancing of intermittent renewable power generation by demand response and thermal energy storage*. PhD thesis, Universität Stuttgart, January 2016.

[Gmba] TenneT TSO GmbH. Tatsächliche und prognostizierte solarenergieeinspeisung - tennet. `https://www.tennet.eu/de/strommarkt/transparenz/transparenz-deutschland/netzkennzahlen/tatsaechliche-und-prognostizierte-solarenergieeinspeisung/tennet-regelzone-gesamt/`. [Online; accessed 01-May-2018].

[Gmbb] TenneT TSO GmbH. Tatsächliche und prognostizierte windenergieeinspeisung - tennet. https://www.tennet.eu/de/strommarkt/transparenz/transparenz-deutschland/netzkennzahlen/tatsaechliche-und-prognostizierte-windenergieeinspeisung/. [Online; accessed 01-May-2018].

[Gra14] Dietmar Richard Graeber. *Handel mit Strom aus erneuerbaren Energien: Kombination von Prognosen*. Research. Springer Gabler, Wiesbaden, 2014. OCLC: 869290424.

[GSK16] A. Gupta, B. P. Singh, and R. Kumar. Optimal provision for enhanced consumer satisfaction and energy savings by an intelligent household energy management system. In *2016 IEEE 6th International Conference on Power Systems (ICPS)*, pages 1–6, March 2016.

[GV17] G Safouri and Vassilis Kapsalis. A Heuristic Algorithm for Operation Scheduling of Electric Water Heaters under Dynamic Pricing. In *18th European Roundtable for Sustainable Consumption and Production*, pages 288–297, Skiathos Island, Greece, October 2017.

[Gä16] Johannes Gärttner. *Group Formation in Smart Grids : Designing Demand Response Portfolios*. PhD thesis, Karlsruher Institut für Technologie, 2016.

[Has80] B.F. Hastings. Ten years of operating experience with a remote controlled water heater load management system at detroit edison. *Power Apparatus and Systems, IEEE Transactions on*, PAS-99(4):1437–1441, July 1980.

[HDS10] Klaus Heuck, Klaus-Dieter Dettmann, and Detlef Schulz. *Elektrische Energieversorgung: Erzeugung, Übertragung und Verteilung elektrischer Energie für Studium und Praxis*. Studium. Vieweg + Teubner, Wiesbaden, 8., überarb. und aktualisierte aufl edition, 2010. OCLC: 669170746.

[HSW17] Christoph Hunziker, Nicola Schulz, and Holger Wache. Shaping aggregated load profiles based on optimized local scheduling of home appliances. *Computer Science - Research and Development*, August 2017.

[JDDA17] José Horta, Daniel Kofman, David Menga, and Alonso Silva. Novel market approach for locally balancing renewable energy production and flexible demand. In *IEEE International Conference on Smart Grid Communications*, pages 545–551, Dresden, 2017.

[Jor19] A. Rezaee Jordehi. Optimisation of demand response in electric power systems, a review. *Renewable and Sustainable Energy Reviews*, 103:308–319, April 2019.

[JV01] Ulrike Jordan and Klaus Vajen. Realistic Domestic Hot-Water Profiles in Different Time Scales (v. 2.0). *Project Report for IEA-SHC Task 26*, May 2001.

[KAK16] Azim Keshtkar, Siamak Arzanpour, and Fazel Keshtkar. Adaptive residential demand-side management using rule-based techniques in smart grid environments. *Energy and Buildings*, 133:281 – 294, 2016.

[KAY+04] J. Kondoh, H. Aki, H. Yamaguchi, A. Murata, and I. Ishii. Consumed power control of time deferrable loads for frequency regulation. In *IEEE PES Power Systems Conference and Exposition, 2004.*, pages 1013–1018 vol.2, October 2004.

[KAY+05] Junji Kondoh, Hirohisa Aki, Hiroshi Yamaguchi, Akinobu Murata, and Itaru Ishii. Future consumed power estimation of time deferrable loads for frequency regulation. In *CIRED 2005-18th International Conference and Exhibition on Electricity Distribution*, pages 1–4. IET, 2005.

[KE95] J. Kennedy and R. Eberhart. Particle swarm optimization. In *Proceedings of ICNN'95 - International Conference on Neural Networks*, volume 4, pages 1942–1948, Perth, WA, Australia, 1995. IEEE.

[KH17] Vassilis Kapsalis and Loukas Hadellis. Optimal operation scheduling of electric water heaters under dynamic pricing. *Sustainable Cities and Society*, 31:109–121, May 2017.

[KHP15] Peter Kepplinger, Gerhard Huber, and Jörg Petrasch. Autonomous optimal control for demand side management with resistive domestic hot water heaters using linear optimization. *Energy and Buildings*, 100:50–55, August 2015.

[KHPP19] Peter Kepplinger, Gerhard Huber, Markus Preißinger, and Jörg Petrasch. State estimation of resistive domestic hot water heaters in arbitrary operation modes for demand side management. *Thermal Science and Engineering Progress*, 9:94–109, March 2019.

[KLH11] Junji Kondoh, Ning Lu, and Donald J. Hammerstrom. An Evaluation of the Water Heater Load Potential for Providing Regulation Service. *IEEE Transactions on Power Systems*, 26(3):1309–1316, August 2011.

[Kon13] Panos Konstantin. *Praxisbuch Energiewirtschaft - Energieumwandlung, -transport und -beschaffung im liberalisierten Markt*. Springer Vieweg, Berlin Heidelberg, 3 edition, 2013.

[KSH18] Vassilis Kapsalis, Georgia Safouri, and Loukas Hadellis. Cost/comfort-oriented optimization algorithm for operation scheduling of electric water heaters under dynamic pricing. *Journal of Cleaner Production*, 198:1053–1065, October 2018.

[KVH17] Raimund M. Kovacevic, Nhat-Vinh Vo, and Josef Haunschmied. Bilevel approaches for distributed DSM using internal individualized prices. In *IEEE International Conference on Smart Grid Communications 2017*, pages 533–538, Dresden, October 2017.

[KW98] Horst Kuhrwahl and Werner Wölfle. *ABC der Elektro-Warmwasserversorgung*. Energie-Verl., Heidelberg, 1998. OCLC: 174474483.

[LB96] I.E. Lane and N. Beute. A model of the domestic hot water load. *IEEE Transactions on Power Systems*, 11(4):1850–1855, November 1996.

[LCD04] N. Lu, J.H. Chow, and A.A. Desrochers. Pumped-Storage Hydro-Turbine Bidding Strategies in a Competitive Electricity Market. *IEEE Transactions on Power Systems*, 19(2):834–841, May 2004.

[Lin10] David Lindley. Smart grids: The energy storage problem. *Nature*, 463(7277):18–20, January 2010.

[LLX17] Bo Lin, Shuhui Li, and Yang Xiao. Optimal and Learning-Based Demand Response Mechanism for Electric Water Heater System. *Energies*, 10(11):1722, October 2017.

[LNTL12] Y. Li, B. L. Ng, M. Trayer, and L. Liu. Automated residential demand response: Algorithmic implications of pricing models. *IEEE Transactions on Smart Grid*, 3(4):1712–1721, December 2012.

[LVT17a] Tobias Lübkert, Marcus Venzke, and Volker Turau. Appliance commitment for household load scheduling algorithm: A critical review. In *2017 IEEE International Conference on Smart Grid Communications (SmartGridComm)*, pages 539–544, Dresden, Germany, October 2017.

[LVT17b] Tobias Lübkert, Marcus Venzke, and Volker Turau. Impacts of domestic electric water heater parameters on demand response. *Computer Science - Research and Development*, 32:49–64, 2017.

[LVT18] Tobias Lübkert, Marcus Venzke, and Volker Turau. Calculating retail prices from demand response target schedules to operate domestic electric water heaters. *Energy Informatics*, 1(1):31, October 2018.

[LVVT18] Tobias Lübkert, Marcus Venzke, Nhat-Vinh Vo, and Volker Turau. Understanding price functions to control domestic electric water heaters for demand response. *Computer Science - Research and Development*, 33(1):81–92, February 2018.

[LZLK16] Sen Li, Wei Zhang, Jianming Lian, and Karanjit Kalsi. Market-Based Coordination of Thermostatically Controlled Loads—Part I: A Mechanism Design Formulation. *IEEE Transactions on Power Systems*, 31(2):1170–1178, March 2016.

[Mag10a] Magnus Erik Hvass Pedersen. Good Parameters for Particle Swarm Optimization. Technical Report HL1001, Hvass Laboratories Technical Report, 2010.

[Mag10b] MagnusErik Hvass Pedersen. SwarmOps for Matlab. `http://www.hvass-labs.org/projects/swarmops/matlab/files/SwarmOpsMatlab1_0.pdf`, November 2010.

[Mat16] MathWorks. Matlab. `https://de.mathworks.com/products/matlab.html`, 2016.

[MB15] A. L. M. Mufaris and J. Baba. Coordinated consumer load control by use of heat pump water heaters for voltage rise mitigation in future distribution system. In *2015 Seventh Annual IEEE Green Technologies Conference*, pages 176–182, April 2015.

[MDF99] Peter W. Mayer, William B. DeOreo, and AWWA Research Foundation, editors. *Residential end uses of water*. AWWA Research Foundation and American Water Works Association, Denver, CO, 1999.

[MRLG10] Amir-Hamed Mohsenian-Rad and Alberto Leon-Garcia. Optimal Residential Load Control With Price Prediction in Real-Time Electricity Pricing Environments. *IEEE Transactions on Smart Grid*, 1(2):120–133, September 2010.

[MRRS00] D.Q. Mayne, J.B. Rawlings, C.V. Rao, and P.O.M. Scokaert. Constrained model predictive control: Stability and optimality. *Automatica*, 36(6):789 – 814, 2000.

[MT13] B. Moradzadeh and K. Tomsovic. Two-stage residential energy management considering network operational constraints. *IEEE Transactions on Smart Grid*, 4(4):2339–2346, December 2013.

[MZ13] Fan-Lin Meng and Xiao-Jun Zeng. A Stackelberg game-theoretic approach to optimal real-time pricing for the smart grid. *Soft Computing*, 17(12):2365–2380, December 2013.

[MZZ+17] Fanlin Meng, Xiao-Jun Zeng, Yan Zhang, Chris J. Dent, and Dun-Wei Gong. An integrated optimization+ learning approach to optimal dynamic pricing for the retailer with multi-type customers in smart grids. *CoRR*, abs/1612.05971v2, 2017.

[NJPH07] M.H. Nehrir, Runmin Jia, D.A. Pierre, and D.J. Hammerstrom. Power Management of Aggregate Electric Water Heater Loads by Voltage Control. In *IEEE Power Engineering Society General Meeting, 2007*, pages 1–6, June 2007.

[NK05] Ning Lu and S. Katipamula. Control strategies of thermostatically controlled appliances in a competitive electricity market. In *IEEE Power Engineering Society General Meeting, 2005*, pages 202–207 Vol. 1, June 2005.

[Oli69] JB Oliver. Radio control of water heaters and distribution station voltage regulators. In *IEEE Summer Power Meeting, Dallas, Texas*, 1969.

[Opt18] Gurobi Optimization. Gurobi optimization - the state-of-the-art mathematical programming solver. `http://www.gurobi.com/index`, 2018. [Online; accessed 17-Apr-2019].

[PD11] Peter Palensky and Dietmar Dietrich. Demand Side Management: Demand Response, Intelligent Energy Systems, and Smart Loads. *IEEE Transactions on Industrial Informatics*, 7(3):381–388, August 2011.

[PFM16] M. Parvizimosaed, F. Farmani, and H. Monsef. A multi-stage smart energy management system under multiple uncertainties: A data mining approach. *Renewable Energy*, 2016.

[PGJ14] Peter Kepplinger, Gerhard Huber, and Jörg Petrasch. Demand Side Management via Autonomous Control-Optimization and Unidirectional Communication with Application to Resistive Hot Water Heaters. In *e-nova 2014 Nachhaltige Gebaeude Versorgung - Nutzung - Integration*, volume 18, Pinkafeld, Austria, November 2014.

[PLC10] Liam Paull, Howard Li, and Liuchen Chang. A novel domestic electric water heater model for a multi-objective demand side management program. *Electric Power Systems Research*, 80(12):1446–1451, December 2010.

[PMFH16] Christoph Passenberg, Dominik Meyer, Johannes Feldmaier, and Hao Shen. Optimal water heater control in smart home environments. In *2016 IEEE International Energy Conference (ENERGYCON)*, pages 1–6, Leuven, Belgium, April 2016. IEEE.

[PMFS16] C. Passenberg, D. Meyer, J. Feldmaier, and Hao Shen. Optimal water heater control in smart home environments. In *2016 IEEE International Energy Conference (ENERGYCON)*, pages 1–6, April 2016.

[QZHW13] Li Ping Qian, Ying Jun Angela Zhang, Jianwei Huang, and Yuan Wu. Demand Response Management via Real-Time Electricity Price Control in Smart Grids. *IEEE Journal on Selected Areas in Communications*, 31(7):1268–1280, July 2013.

[RAB18] M. Roux, M. Apperley, and M.J. Booysen. Comfort, peak load and energy: Centralised control of water heaters for demand-driven prioritisation. *Energy for Sustainable Development*, 44:78–86, June 2018.

[RFFA12] Mohammad Rastegar, Mahmud Fotuhi-Firuzabad, and Farrokh Aminifar. Load commitment in a smart home. *Applied Energy*, 96:45 – 54, 2012. Smart Grids.

[SACQ19] Jakob Stoustrup, Anuradha Annaswamy, Aranya Chakrabortty, and Zhihua Qu, editors. *Smart Grid Control: Overview and Research Opportunities*. Power Electronics and Power Systems. Springer International Publishing, Cham, 2019.

[San14] SaniTec Produkthandel GmbH. Fach-Information Warmwassergeräte, August 2014.

[Sch09] Adolf J. Schwab. *Elektroenergiesysteme*. Springer Berlin Heidelberg, Berlin, Heidelberg, 2009.

[SE98] Y. Shi and R. Eberhart. A modified particle swarm optimizer. In *1998 IEEE International Conference on Evolutionary Computation Proceedings. IEEE World Congress on Computational Intelligence (Cat. No.98TH8360)*, pages 69–73, Anchorage, AK, USA, 1998. IEEE.

[SE18] EPEX SPOT SE. Epex spot se: Welcome. `http://www.epexspot.com/`, 2018.

[SEG17] SEG Hausgeräte GmbH. Siemens warmwasser wandspeicher. `http://www.siemens-home.bsh-group.com/de/produktliste/warmwasser/wandspeicher`, 2017. [Online; accessed 14-Dec-2017].

[SFFL14] Amir Safdarian, Mahmud Fotuhi-Firuzabad, and Matti Lehtonen. A Distributed Algorithm for Managing Residential Demand Response in Smart Grids. *IEEE Transactions on Industrial Informatics*, 10(4):2385–2393, November 2014.

[SFFL16] Amir Safdarian, Mahmud Fotuhi-Firuzabad, and Matti Lehtonen. Optimal Residential Load Management in Smart Grids: A Decentralized Framework. *IEEE Transactions on Smart Grid*, 7(4):1836–1845, July 2016.

[SH+07] Gerhard Stryi-Hipp et al. Grosol - studie zu großen solarwärmeanlagen. Survey. Bundesverband-Solarwirtschaft e.V, Berlin, Germany. `http://www.solarthermietechnologie.de/fileadmin/img/Intranet/AG2/PDF/GROSOL_Studie_BSW_final.pdf`, 2007. [Online; accessed 15-Jan-2018].

[Sia14] Pierluigi Siano. Demand response and smart grids—a survey. *Renewable and Sustainable Energy Reviews*, 30:461 – 478, 2014.

[Sio11] Fereidoon P. Sioshansi. So what's so smart about the smart grid? *The Electricity Journal*, 24(10):91 – 99, 2011.

[SLLF13] S. Salinas, M. Li, P. Li, and Y. Fu. Dynamic energy management for the smart grid with distributed energy resources. *IEEE Transactions on Smart Grid*, 4(4):2139–2151, December 2013.

[SMD+12] M. Shaad, A. Momeni, C. P. Diduch, M. Kaye, and L. Chang. Parameter identification of thermal models for domestic electric water heaters in a direct load control program. In *2012 25th IEEE Canadian Conference on Electrical and Computer Engineering (CCECE)*, pages 1–5, April 2012.

[SMRSW12] Pedram Samadi, Hamed Mohsenian-Rad, Robert Schober, and Vincent W. S. Wong. Advanced Demand Side Management for the Future Smart Grid Using Mechanism Design. *IEEE Transactions on Smart Grid*, 3(3):1170–1180, September 2012.

[SNSF16] J. J. Shah, M. C. Nielsen, T. S. Shaffer, and R. L. Fittro. Cost-Optimal Consumption-Aware Electric Water Heating Via Thermal Storage Under Time-of-Use Pricing. *IEEE Transactions on Smart Grid*, 7(2):592–599, March 2016.

[SPM+10] Arnaldo Sepulveda, Liam Paull, Walid G. Morsi, Howard Li, C. P. Diduch, and Liuchen Chang. A novel demand side management program using water heaters and particle swarm optimization. In *2010 IEEE Electrical Power & Energy Conference*, pages 1–5, Halifax, NS, Canada, August 2010. IEEE.

[SPO18] EPEX SPOT. Intraday market with delivery on the german tso zone. `http://www.epexspot.com/en/product-info/intradaycontinuous/germany`, 2018.

[SS16] Pierluigi Siano and Debora Sarno. Assessing the benefits of residential demand response in a real time distribution energy market. *Applied Energy*, 161:533–551, January 2016.

[Sta06] Ingo Stadler. *Demand response: nichtelektrische Speicher für Elektrizitätsversorgungssysteme mit hohem Anteil erneuerbarer Energien*. Habilitation. dissertation.de, Berlin, 2006.

[STI17] STIEBEL ELTRON GmbH & Co. KG. Wandspeicher 30 bis 150 l – klein-, wand- und standspeicher. `https://www.stiebel-eltron.de/de/home/produkte-loesungen/warmwasser/klein-_wand-_undstandspeicher/wandspeicher_30_bis150l.html`, 2017. [Online; accessed 14-Dec-2017].

[TC12] K. M. Tsui and S. C. Chan. Demand Response Optimization for Smart Home Scheduling Under Real-Time Pricing. *IEEE Transactions on Smart Grid*, 3(4):1812–1821, December 2012.

[Umw17] Umweltbundesamt. Endenergieverbrauch nach anwendungsbereichen in privaten haushalten 2015. `https://www.umweltbundesamt.de/sites/default/files/medien/384/bilder/dateien/3_abb_eev-nach-anwendungsbereichen-ph_2017-02-13.pdf`, 2017. [Online; accessed 15-Jan-2018].

[VDGJ12] K. Vanthournout, R. D'hulst, D. Geysen, and G. Jacobs. A smart domestic hot water buffer. *IEEE Transactions on Smart Grid*, 3(4):2121–2127, December 2012.

[VH08] András Varga and Rudolf Hornig. An overview of the omnet++ simulation environment. In *Proceedings of the 1st International Conference on Simulation Tools and Techniques for Communications, Networks and Systems & Workshops*, Simutools '08, pages 60:1–60:10, Marseille, France, ICST, Brussels, Belgium, Belgium, 2008. ICST (Institute for Computer Sciences, Social-Informatics and Telecommunications Engineering).

[VMLL14] Cynthujah Vivekananthan, Yateendra Mishra, Gerard Ledwich, and Fangxing Li. Demand Response for Residential Appliances via Customer Reward Scheme. *IEEE Transactions on Smart Grid*, 5(2):809–820, March 2014.

[VS34] Heinrich Von Stackelberg. *Marktform und Gleichgewicht*. J. springer, 1934.

[vS11] Heinrich von Stackelberg. *Market Structure and Equilibrium*. Springer Berlin Heidelberg, 2011. DOI: 10.1007/978-3-642-12586-7.

[VT15] Marcus Venzke and Volker Turau. A demand response approach locally implementable for waterbeds. In *Proceedings of 1st Workshop on Middleware for a Smarter Use of Electric Energy (MidSEE'15)*, pages 1–6, Cottbus, Germany, March 2015.

[VT16] Marcus Venzke and Volker Turau. Simulative evaluation of demand response approaches for waterbeds. In *Proceedings of the 2016 IEEE International Energy Conference (ENERGYCON)*, Leuven, Belgium, April 2016.

[VZV15] John S. Vardakas, Nizar Zorba, and Christos V. Verikoukis. A Survey on Demand Response Programs in Smart Grids: Pricing Methods and Optimization Algorithms. *IEEE Communications Surveys & Tutorials*, 17(1):152–178, 2015.

[WLM15] Wei Wei, Feng Liu, and Shengwei Mei. Energy Pricing and Dispatch for Smart Grid Retailers Under Demand Response and Market Price Uncertainty. *IEEE Transactions on Smart Grid*, 6(3):1364–1374, May 2015.

[WPSC13] Z. Wang, R. Paranjape, A. Sadanand, and Z. Chen. Residential demand response: An overview of recent simulation and modeling applications. In *Electrical and Computer Engineering (CCECE), 2013 26th Annual IEEE Canadian Conference on*, pages 1–6, May 2013.

[WSF+17] Jidong Wang, Yingchen Shi, Kaijie Fang, Yue Zhou, and Yinqi Li. A Robust Optimization Strategy for Domestic Electric Water Heater Load Scheduling under Uncertainties. *Applied Sciences*, 7(11):1136, November 2017.

[WZWP13] Chengshan Wang, Yue Zhou, Jidong Wang, and Peiyuan Peng. A novel traversal-and-pruning algorithm for household load scheduling. *Applied Energy*, 102:1430 – 1438, 2013.

[XDL+14] Zhijie Xu, Ruisheng Diao, Shuai Lu, Jianming Lian, and Yu Zhang. Modeling of Electric Water Heaters for Demand Response: A Baseline PDE Model. *IEEE Transactions on Smart Grid*, 5(5):2203–2210, September 2014.

[XOT11] Zhao Xu, Jacob Ostergaard, and Mikael Togeby. Demand as Frequency Controlled Reserve. *IEEE Transactions on Power Systems*, 26(3):1062–1071, August 2011.

[YH17] Mengmeng Yu and Seung Ho Hong. Incentive-based demand response considering hierarchical electricity market: A Stackelberg game approach. *Applied Energy*, 203:267–279, October 2017.

[YTP09] S. You, C. Træholt, and B. Poulsen. Generic virtual power plants: Management of distributed energy resources under liberalized electricity market. In *8th International Conference on Advances in Power System Control, Operation and Management (APSCOM 2009)*, 2009.

[ZMPM13] Marco Zugno, Juan Miguel Morales, Pierre Pinson, and Henrik Madsen. A bilevel model for electricity retailers' participation in a demand response market environment. *Energy Economics*, 36:182–197, March 2013.

[ZSU11] Terry L Zimmerman, Stephen F Smith, and Atikhun Unahalekhaka. Conserve: Client side intelligent power scheduling. In *Tenth international conference on autonomous agents and multiagent systems, Taipei, Taiwan*, 2011.

[ZWYK13] Zhuang Zhao, Won Cheol Lee, Yoan Shin, and Kyung-Bin Song. An Optimal Power Scheduling Method for Demand Response in Home Energy Management System. *IEEE Transactions on Smart Grid*, 4(3):1391–1400, September 2013.

List of Figures

List of Tables

List of Symbols

A_k	Coefficient matrix of upper bound constraints for LP formulation of DEWH no. k.
A	Coefficient matrix of upper bound constraints for LP formulation.
C_ρ	Specific heat capacity of water (J/kgK).
C	Heat capacity of water in DEWH (J/K).
$E_{\mathbf{loss}}$	Total daily energy lost due to heat conductivity DEWHs (J).
$E_{\mathbf{total}}$	Total daily energy demand of a DEWHs (J).
E_i	Energy consumed in slot i (J).
G	Heat conductivity of a DEWH (W/K).
H_i	Heating state of a DEWH in slot i.
M	Mean absolute percentage error.
P_G	Effective power of heat conductivity of a DEWH for mean temperature (W).
P_i	Power of heating device in slot i (W).
$P_{\mathbf{heater}}$	Rated power of heating device (W).
$P_{\mathbf{W}}$	Effective power of water draw (W).
Q	Large number for Karush-Kuhn-Tucker (KKT) complementary reduction.
T_i	Temperature in slot i (°C).
T_t	Target temperature (°C).
$T_{\infty,i}$	Asymptote of temperature change in slot i (°C).
T_∞	Asymptote of temperature change (°C).
$T_{\mathbf{cold}}$	Cold water temperature (°C).
$T_{\mathbf{env}}$	Environmental water temperature (°C).
$T_{\mathbf{max}}$	Maximum hot water temperature (°C).

$T_{\mathbf{min},i}$	Minimum hot water temperature in slot i (°C).
$T_{\mathbf{min}}$	Minimum hot water temperature (°C).
$T_{\mathbf{nom},i}$	Nominal hot water temperature in time slot i (°C).
$T_{\mathbf{nom}}$	Nominal hot water temperature (°C).
$T_{\mathbf{use}}$	Desired mix water temperature (°C).
$T_{\mathbf{cmf}}$	Minimum comfort temperature (°C).
$T_{\mathbf{cur}}$	Current actual water temperature (°C).
T	Temperature vector (°C).
V_W	Volume of hot water draw to reach T_{cmf} (l).
$V_{\mathbf{HW}}$	Volume of hot water drawn (l).
$V_{\mathbf{W}}$	Volume of water draw (l).
V	Volume of DEWH (l).
W_i	Power equivalent hot water consumption in slot i (W).
W_{HK}	Hot water consumption (W/K).
W	Power equivalent for hot water consumption (W).
ΔT_i	Required temperature difference in slot i to reach T_t later (°C).
$\Delta T_{\mathbf{min},i}$	Required temperature difference to reach $T_{\text{min},i}$ in slot i (°C).
$\Delta T_{\mathbf{nom}}$	Allowed range of hot water temperature (°C).
$\Delta\tau$	Minimum difference between two τ-values of clusters.
Δt	Duration of time slot (s).
Γ	Vector containing peak plan.
α_{PG}	Ratio of P_{heater} and P_G.
α_{PW}	Ratio of P_{heater} and P_{W}.
α_{TN}	Normalization of T_{nom} and T_{use}.
α_{TR}	Ratio of ΔT_{nom} and T_{nom}.
$\bar{T}_{\mathbf{nom}}$	Nominal hot water temperature (°C).
$\bar{T}$	Average hot water temperature (°C).
$\bar{W}$	Daily mean water consumption (l).
δ	Difference of target and actual load profile.
ϵ	Minimum difference for convergence.
γ	Exponential temperature change factor.
$\hat{P}$	Available power profile.
$\hat{\tau}$	Vector of τ-values.
$\hat{h}$	Target schedule for aggregated heating profile.
$\hat{r}$	Set of candidate price reset positions.
λ	Vector of Lagrange multipliers for KKT.

$\omega_{\mathbf{dcmf}}$	Probability of a discomfort event.
ω	PSO inertia weight.
$\overline{p_{\mathbf{ex}}}$	Maximum exchange price.
$\overline{p}$	Maximum value of price vector.
ϕ_g	PSO attraction weight of swarm.
ϕ_p	PSO attraction weight of particle.
ρ	Density of water.
τ^p	Vector of τ-values used for price.
$\tau_{\mathbf{ref}}$	Median of considered τ-values.
τ	Temperature change rate (s).
θ	Vector containing cumulative sum of peak plan.
$\tilde{\Gamma}$	Vector containing modified peak plan.
$\underline{p}$	Minimum value of price vector.
a_k	Upper bound values of constraints for LP formulation of DEWH no. k.
a	Upper bound values of constraints for LP formulation.
c_i	Probability of a water demand in time slot i.
$c_{\mathbf{eff}}$	Effective costs.
d^τ	Vector of numbers of DEWHs per cluster.
d	Number of considered DEWH clusters.
h_k	Heating profile of DEWH no. k.
h	Heating profile of a DEWH, with $0 \leq h_i \leq 1$.
i	Time slot index.
$n_{\mathbf{lowT}}$	Number of low temperature events.
n	Number of time slots.
p^ϵ	Lower bound for retail price.
p_i	Price value of slot i.
$p_{\mathbf{avg}}$	Average price.
$p_{\mathbf{eff}}$	Effective price vector.
$p_{\mathbf{ex}}$	Exchange price vector.
$p_{\mathbf{inv}}$	Inverse proportional price.
$p_{\mathbf{pty}}$	Penalty vector containing pseudo prices for temperature violation.
$p_{\mathbf{ref}}$	Reference price.
$p_{\mathbf{sort}}$	Sorted price vector.
$p_{\mathbf{th}}$	Price threshold.
$p_{\mathbf{use}}$	Average price for consumed hot water energy.
p	Retail price vector.

s	PSO swarm size.
t_h	Heating duration.
$t_{\mathbf{total}}$	Required heating time for E_{total} (s).
$t_{\mathbf{W}}$	Duration of water draw (s).
u_i	Binary heating decision in slot i, with $u_i \in \{0,1\}$.
u	Binary heating profile of a DEWH, with $u_i \in \{0,1\}$.
z	Vector of boolean decision variables for KKT complementary constraints.
$V/\bar{W}$	Ratio of tank volume and consumption.

List of Acronyms

ANT	adaptive nominal temperature.
BBT	bang-bang thermostat.
BG	balancing group.
CDF	cumulative distribution function.
CPP	critical peak pricing.
DA-RTP	day-ahead RTP.
DEWH	domestic electric water heater.
DG	distributed generator.
DLC	direct load control.
DR	demand response.
DSM	demand side management.
DSO	distribution system operator.
ELIX	European Electricity Index.
EPEX	European Power Exchange SPOT.
ESC	energy scheduling comfort.
GA	genetic algorithm.
GLPK	GNU Linear Programming Kit.
IBR	inclining block rates.
ILP	integer linear program.

KKT Karush-Kuhn-Tucker.

LP linear program.

MAPE mean absolute percentage error.
MILP mixed-integer linear program.

ODE ordinary differential equation.

PDE partial differential equation.
PDF probability distribution function.
PRC price responsive control.
PSO particle swarm optimization.
PV photovoltaic panel.

RES renewable energy sources.
RMSD root-mean-square deviation.
RNG random number generator.
RTP real-time pricing.

SA simulated annealing.

TCL thermostatically controllable load.
TOU time-of-use.
TSO transmission system operator.

VCG Vickrey-Clarke-Groves.